12-2017

Development of an Animal Model for Enterovirus for Evaluation D68 for Screening of Antiviral Therapies

W. Joseph Evans
Utah State University

DEVELOPMENT OF AN ANIMAL MODEL FOR ENTEROVIRUS D68 FOR EVALUATION OF ANTIVIRAL THERAPIES

by

W. Joseph Evans

A thesis submitted in partial fulfillment
of the requirements for the degree

of

MASTER OF SCIENCE

in

Animal, Dairy and Veterinary Science

Approved:

_____	_____
E. Bart Tarbet Ph.D. Major Professor	Craig W. Day Ph.D. Committee Member
_____	_____
Kerry A. Rood M.S., DVM Committee Member	Mark R. McLellan, Ph.D. Vice President for Research and Dean of the School of Graduate Studies

UTAH STATE UNIVERSITY
Logan, Utah

2017

ABSTRACT

Development and Validation of an Animal Model for Enterovirus D68 for Screening of Antiviral Therapies

by

W. Joseph Evans, Master of Science

Utah State University, 2017

Major Professor: Dr. E. Bart Tarbet
Department: Animal, Dairy and Veterinary Science

Enterovirus D68 (EV-D68) is one of many non-polio enteroviruses, although it is unique in that it shares epidemiologic and biologic features with human rhinoviruses. In 2014 a mutated strain emerged in the U.S. belonging to the B1 clade and has only six coding differences from previous strains commonly found in the U.S. However, of the six genetic polymorphisms in the EV-D68 polyprotein, five are present in neuropathogenic poliovirus. In 2015, development of a model for EV-D68 infection in AG129 mice started by serially-passaging virus in 4-week-old mice. For each passage mice were infected intranasally and virus was recovered from lung tissue three days post-infection (p.i.). Despite a lack of weight loss, virus titer increased in the lung from $10^{6.5}$ to $10^{7.5}$ $CCID_{50}$/mL by 8 hours p.i., and to $10^{8.5}$ $CCID_{50}$/mL by 24 hours p.i. In addition, histological changes and an increase in the pro-inflammatory cytokines were observed in lung tissues as the virus adapted to mice. Histological lesions observed on days 2-6 with a peak on days 3-4 included interstitial inflammation and alveolar wall injury. MCP-1

exhibited a 15-fold increase while RANTES exhibited a 2.5-fold increase compared to uninfected mice as mouse passage increases.

A time course of infection study determined that virus spread from the lungs to the blood, liver, kidney, and spleen, with clearance of virus by day 9 p.i. Viremia peaked at day 1 p.i. and cleared by day 5 p.i. This is the first report of a respiratory disease model for EV-D68 infection in mice, and has potential use for evaluation of experimental therapeutics. When treated with 200mg/kg/day guanidine simultaneous with infection, mice exhibited a 320-fold reduction of virus titers in lungs compared to placebo and undetectable levels of virus in whole blood.

PUBLIC ABSTRACT

Development and Validation of an Animal Model for Enterovirus D68 for Screening of Antiviral Therapies

W. Joseph Evans

Enterovirus D68 (EV-D68) virus has become more prevalent over the last 15 to 20 years. EV-D68 attacks the respiratory system and can cause severe disease in individuals who have underlying respiratory problems. There have also been reports of individuals with EV-D68 showing signs of neurological system problems and acute flaccid paralysis. Because of the increase in patients with EV-D68 and also the potential for neurological disease, an animal model is needed to study the disease and to evaluate experimental therapies for EV-D68 infection.

To develop the animal model, 4-week old AG129 mice that lack alpha and beta interferon receptors, making them immunosuppressed, were used. The mice were infected with EV-D68 by the intranasal route to allow infection of the lungs. On day-3 post-infection the mice were euthanized and lungs were removed and homogenized for collection of virus. The newly collected virus was then used to infect another set of mice. This procedure was repeated 30 times. As passage number increased so did the amount of virus that was collected from the lungs of mice. The virus titer increased 320-fold between mouse passage 0 to 30.

At the end of the thirtieth passage, multiple tissues (lungs, liver, kidney, spleen, blood, brain, spinal cord and leg muscle) were collected from infected mice over several days and titered to demonstrate how quickly the virus spread to various tissues within the mouse. The virus replicated most rapidly in the lungs and remained in the lungs longer than the other tissues evaluated. However, large quantities of virus were found in all tissues evaluated.

Finally, several experimental antiviral compounds were evaluated: rupintrivir, pleconaril, ribavirin, enviroxime and guanidine, all of which showed therapeutic potential in cell culture. In the animal model rupintrivir, pleconaril, ribavirin and enviroxime did not show any therapeutic effect. Only guanidine reduced the amount of virus that was found in the lungs as well as in whole blood.

ACKNOWLEDGMENTS

I would like to thank Dr. Bart Tarbet for his help and mentoring throughout the project. I would especially like to thank my committee members, Drs. Craig W. Day and Kerry A. Rood, for their support and assistance throughout this process. I would also like to thank the Institute for Antiviral Research (IAR) at Utah State University for the use of their labs and facilities including all the technicians that work for the IAR. A lot of work went into running the animal experiments, taking care of the animals, collecting tissues, and running *in vitro* studies.

I give special thanks to my family, friends, and colleagues for their encouragement, moral support, and patience as I worked through this project. I would especially like to thank my wife Liz Evans for her patience with the early mornings, long hours, late nights and weekends spent working on this project.

W. Joseph Evans

CONTENTS

Page

LIST OF TABLES

LIST OF FIGURES

CHAPTER I

INTRODUCTION

Since the 1960's enteroviruses have been increasing in prevalence throughout the world (1). Enteroviruses are members of the enterovirus genus, in the picornavirus family (2). Picornaviruses are small, non-enveloped, positive sense, RNA viruses (3). Enterovirus D68 (EV-D68) was first isolated from four pediatric patients that had pneumonia in 1962 in California (2). Between 1962 and 2009, cases of EV-D68 have been rare. However, between 2009 and 2013 there were 79 cases reported through the United States National Enterovirus Surveillance System (4). In 2014, the United States and Canada had the largest outbreak of EV-D68 that has been reported so far. Between August 2014 and January 2015 there were about 1,100 cases of EV-D68 reported in the U.S. (5). In addition, EV-D68 has been reported across the world with cases from Asia to Europe (6, 7).

Since EV-D68 was first isolated it has been well known as a respiratory virus (8). Most severe cases of EV-D68 are in young children (9, 10). Individuals with underlying respiratory problems seem to be the most at risk for a severe infection. Like with rhinovirus infections, individuals with EV-D68 have exhibited asthma-like exacerbations (10). During the 2014 outbreak many patients with EV-D68 needed more intensive care than patients that had other underlying respiratory disease (4). However, EV-D68 does not only cause respiratory disease. During the 2014 outbreak, and ever since then, neurological disease has been observed in a number of patients that were positive for EV-

D68. This disease is described as acute flaccid paralysis or myelitis (11, 12). Even though patients that develop acute flaccid paralysis are rare, the increase in prevalence and the severity of the respiratory infections make EV-D68 an important emerging disease.

EV-D68 has been the subject of numerous studies including development of better detection assays (13), study of mechanisms for infection (14), and evaluating antiviral therapies in cell culture (15). The current problem we face is that there is not an approved therapy for EV-D68 infection. This is due largely to the fact that up until recently, there was not a good animal model for evaluation of experimental antiviral therapies identified in vitro (15).

Recently, two animal models for EV-D68 have been described. M. C. Patel, et al. (16) developed a model in adult cotton rats. This model gives insight into the respiratory side of the disease and the speed at which EV-D68 replicates. The second model published was developed in two-day-old Swiss Webster mouse pups by A. M. Hixon, et al. (17). This model provided evidence that EV-D68 is a causative agent of acute flaccid paralysis as observed in some of the EV-D68 patients infected in 2014. Cotton rats are large and harder to handle than mice. It is also difficult to get reagents for testing samples from adult cotton rats. Two-day old mice are difficult to work with because you have to keep the pups with the mother. Also, neither of the above-mentioned models has been used to evaluate the efficacy of antiviral therapies. The initial goal of our project was to adapt EV-D68 to AG129 mice. AG129 mice are immune suppressed, which makes the mouse more susceptible to infection by viruses. We adapted EV-D68 to cause disease signs after 30 serial passages in four-week-old mice. The next goal was to

characterize the pathogenicity of EV-D68 in the mouse. This included determining the time course for infection in the lung, liver, kidney, spleen, blood, leg muscle, spinal cord and brain. An optimum infectious dose was determined by infecting various dilutions of the virus in mice and determining the amount of recovered virus in these tissues. Finally, we evaluated the antiviral efficacy of five antiviral compounds in our model to demonstrate the applicability of this model for evaluation of experimental therapies.

CHAPTER II

LITERATURE REVIEW

Enterovirus D68 Background

Enteroviruses are classified into different phylogenetic groups, or clades A, B, C, D and E. Enterovirus D68 (EV-D68) is a small, non-enveloped, positive sense, RNA virus in the picornaviridae family (3, 18, 19). EV-D68 has a genome of approximately 7,500 nucleotides long (19). EV-D68 was first isolated in 1962 from four patients in California (2). EV-D68 is a member of the genus enterovirus that is part of the picornaviridae family (2). Also included in the picornaviridae family are echoviruses, rhinoviruses (non-polio enterovirus) and poliovirus (3, 20). According to the CDC, there are approximately 15 million cases of enterovirus a year in the U.S. (21). Enteroviruses, which typically infect the alimentary tract, have also been reported to have a neurological disease associated with the infection (22). Enteroviruses are also known to cause myocarditis, aseptic meningitis, hand-foot and mouth disease, and upper and lower respiratory tract disease (23). EV-D68 is a known respiratory virus that usually causes upper respiratory tract infections. After the discovery of EV-D68, initial cases of virus infection were rare. However, in the early 2000's the number of cases worldwide started to increase (10). According to N. Khetsuriani, et al. (1), enteroviruses in general have been increasing in prevalence since the 1960's. Between 2009 and 2013 there were 79 cases of EV-D68 reported through the United States National Enterovirus Surveillance System, almost double the amount of cases of EV-D68 reported over the three decades

earlier (4). T. Imamura and H. Oshitani (10) suggested that the increase in prevalence was not because of improved detection methods but because there is actually more people getting sick from enteroviruses.

In 2014, the United States experienced an outbreak of EV-D68 that centered in the Midwest (24). By January 2015, 49 states in the U.S. reported cases of EV-D68, which numbered around 1,100 (5, 25, 26). However, EV-D68 is not just localized to the United States, many other countries have reported cases of EV-D68 since the virus was first isolated in 1962. Between 2008 and 2011 the Philippines, Japan, and the Netherlands all reported an increase in the number of cases of EV-D68 (6, 7). Italy initially reported cases of EV-D68 in 2008. Since that time numerous cases were reported in Italy between 2010 and 2012 (27). In Beijing, China between 2006 to 2010, EV-D68 was detected frequently among adults that were exhibiting acute respiratory tract infections (8). During the 2014 outbreak in the U.S., Canada also reported 221 cases in nine provinces (4, 28). Not only have the numbers of reported cases increased, but also there have been at least 14 fatal cases since the 2014 outbreak (5, 23, 29-32). The increase in disease incidence and the number of fatalities associated with infection by EV-D68 have made this virus a public health concern.

The original patients in 1962 from which the virus was isolated were all young children that presented with pneumonia (3, 10). The virus has primarily affected infants to teenagers (9, 10). However, EV-D68 has been identified as the causative agent of disease in adults as well (23, 29, 33, 34). Specifically, in Beijing, China, EV-D68 was detected in adults with respiratory tract infections (8).

EV-D68 is a respiratory virus. This is due to the types of cellular receptors utilized by EV-D68 to gain entrance into the host cells. Individuals with underlying respiratory diseases such as asthma, reactive airway disease or chronic obstructive pulmonary disease (COPD) are more at risk for severe complications (7, 9, 10, 26, 29). Included in these complications are lower respiratory tract infections. In fact EV-D68 has a higher detection rate in patients with lower respiratory tract infections than in those with upper respiratory tract infections (10, 23, 35). One reason for this observation is that EV-D68 is known to exacerbate asthma, which might cause an enhancement of the immune response in the lower respiratory tract. The enhanced immune response in the respiratory tract might be causing the more severe respiratory illness that has been observed (10).

Typical symptoms of an EV-D68 infection include coughing, labored breathing, wheezing, and fever (5, 25, 36). In at least one case of a four-year old girl with interstitial pneumonia, complications became severe within 17 hours of the first sign of illness (36). This suggests that the virus replicates quickly in the host. Originally EV-D68 was isolated from samples obtained from four young patients that presented with pneumonia. EV-D68 infection has been associated with neurological disease as well. In fact, of all the viruses that cause infections of the central nervous system (CNS), enteroviruses are among the most common (37). The neurological symptoms associated with EV-D68 are described as acute flaccid paralysis (36, 38). During the 2014 outbreak, cases of acute flaccid paralysis associated with EV-D68 infection were seen in Colorado and California (38). However, between August and December 2014, 33 states reported having cases of acute flaccid paralysis associated with EV-D68 infection (31, 39). At

least one child with acute flaccid paralysis also exhibited a viremia (38). However, it appears that the majority of symptoms associated with EV-D68 are respiratory. M. Matsumoto, et al. (36) suggest that only 48% of patients will present with a fever. Even fewer patients have presented with neurological disease as these symptoms have only been observed in rare cases (3, 25, 36). According to the CDC, the neurological disease of acute flaccid myelitis occurs in less than one in a million cases (12). Some reports suggest this is higher among enterovirus infected patients.

Since the 2014 outbreak of EV-D68, prevalence of EV-D68 in the United States has been fairly low. In 2015, the CDC reported none of the 700 samples received from patients tested positive for EV-D68. However, in 2016 sporadic cases of EV-D68 were detected throughout the U.S. although, not as many cases as the outbreak in 2014 (5). Although, during this same time period there was a rise in acute flaccid myelitis (AFM) or neurological disease that is often associated with EV-D68 (12). Thus far in 2017, it was reported that 136 patients from 37 states were confirmed to have AFM (12).

In 2016, the Netherlands reported having an upsurge of EV-D68 cases. M. Knoester, et al. (11) reported that EV-D68 infections in 2015 were low in numbers or were minimal. However in 2016, the medical center in this study reported 25 cases of EV-D68. Out of those patients, 17 were children with "life-threatening respiratory distress" (11). There were 13 pediatric patients that required admission to the ICU. M. Knoester, et al. (11) also reported that one child, a 4-year old boy was admitted for "clinical characteristics of AFM". Along with the paralysis that he was experiencing, the patient had to be placed on ventilation for breathing support due to respiratory distress. EV-D68 was the only virus that was detected from bodily fluids collected from this

patient. Cerebral spinal fluid was collected and was tested for a variety of other viruses with negative results. Adult patients in the Netherlands with respiratory difficulties also tested positive for EV-D68, six of them were transplant recipients (11). These observations suggests that EV-D68 targets or at least causes more severe disease in individuals that have underlying medical conditions or pre-existing health problems, and that neurological disease or AFM is a rare symptom associated with EV-D68 infection.

Characteristics of EV-D68

When EV-D68 was first characterized in 1962, there were four isolates or strains of virus, one from each patient: Fermon, Franklin, Robinson and Rhyne named after the patients from whom they were isolated. Because all the strains had similar properties, Fermon was chosen as the representative strain (2, 10). EV-D68 was classified as an enterovirus because it shared characteristics with other known enteroviruses such as acid stability (2). Enteroviruses are sub-categorized into four sub-species A through D (3, 20). After the original classification of the virus, EV-D68 was further classified into the sub-species of D enterovirus (10). Currently there are only five enteroviruses in the D sub-set: EV-D68, EV-D70, EV-D94, EV-D111, and EV-D120 (10, 40). Though they are classified as D enteroviruses, they each have their own disease profile. EV-D68 is a respiratory virus that has been shown to have some neurological affinities (3, 10, 36, 38). Enterovirus D70 has been identified as a causative agent for hemorrhagic conjunctivitis (40, 41) and enterovirus D94 has been identified as a causative agent for acute flaccid

paralysis (42). Enteroviruses D111 and D120 were both identified in non-human primates (10).

EV-D68 was originally classified as an enterovirus on the basis of acid stability and pathogenesis in EV-D68 in suckling mice (2, 18, 43). The original study showed that the Fermon strain did not replicate in suckling mice but the Rhyne strain did, just not in the respiratory tract (2). EV-D68 has been further classified as an enterovirus based on antigenicity toward neutralizing antibody tests (2). Serological studies have also shown that the original EV-D68 Fermon strain differs from the strains of EV-D68 currently circulating (40, 44).

EV-D68 shares a number of similar characteristics with human rhinoviruses. Human rhinoviruses (HRV) are a common cause of upper and lower respiratory tract infections, and are a frequent cause of the common cold (45, 46). D. Mertz, et al. (47) described HRVs as the leading cause of diseases of the respiratory tract. EV-D68 has been shown to be similar to HRVs in cell culture, in that it grows better at 33°C than at 37°C and is acid sensitive (15, 48). This is a characteristic of a virus that typically causes upper respiratory tract infections. Enteroviruses typically grow better at 37°C and are acid stable, as is EV-D68 (20, 22). Oberste et al. and Blomqvist et al. independently showed that two sub-lines of the Fermon strain were actually acid sensitive (20, 22). In addition, Oberste et al. showed acid sensitivity of multiple isolates of EV-D68 from 1989 to 2002 (22). These studies also showed that EV-D68 replicates to higher virus titers at 33°C than at 37°C (20, 22).

S. Blomqvist, et al. (20) suggests that a sub-type of human rhinovirus, HRV-87, is actually a serotype of EV-D68. Interestingly HRV-87 was first isolated in 1963 in the

same lab as the EV-D68 isolate (22). HRV-87 and EV-D68 have been compared in multiple studies to determine if they have been misclassified as either rhinovirus or enterovirus. S. Blomqvist, et al. (20) suggests that the dividing line between EV-D68 and rhinoviruses is possibly more blurred than what was originally held to be true. S. Blomqvist, et al. (20) determined that HRV-87 is more closely related to EV-D68 and other enteroviruses than to rhinoviruses. H. Ishiko, et al. (49) compared the sequence of the VP4 gene of HRV-87 to that of EV-D68 and other rhinoviruses. They found that HRV-87 had more than 97% nucleotide identity with EV-D68. The next closest homology was 76.8% with EV-D70. In their study, H. Ishiko, et al. (49) compared 66 enteroviruses and 12 rhinoviruses. They therefore concluded that HRV-87 is actually a strain of EV-D68 (20, 22, 49). A. C. Palmenberg and J. E. Gern (50) reclassified HRV-87 in 2015 as an EV-D68.

Genome Description and EV-D68 Classification/Identification

Picornavirus RNA gives rise to the four structural proteins, VP1, VP2, VP3 and VP4 (10, 18). There are 60 copies each of the VP1, VP2 and VP3 viral proteins within the icosahedral shell. The VP4 protein, creates a network on the interior of the capsid (51). The VP1 sequence is most often used for picornavirus classification based on RNA sequence, since it is the most variable region of the picornavirus genome, and more specifically the enterovirus genome (10, 18, 33, 43, 52). EV-D68 has been classified into three clades A, B and C (30). Clades A and C differentiated between 1995 and 2001. Clade B came about around the year 2007 (30). Because of the ability to use the VP1

segment of the genome for identification of EV-D68 and its characterization into three subclades, B1, B2 and B3, these clades have been used to identify isolates from patients around the world. These results give evidence that the EV-D68 isolates are not geographically isolated or independent (10, 53). Evaluation of samples from the 2014 outbreak by W. Huang, et al. (54) revealed that the majority of these samples belonged to a novel clade of EV-D68 called the B1 clade (19). As W. Huang, et al. (54) compared the 2014 strains to those from previous years; they identified two locations with significant differences; T860N and S1108G. According to W. Huang, et al. (54) these two variable locations are related to "protease cleavage activity" and "peptide maturation" respectively. They suggest that this variability could be the cause of the increase in prevalence of EV-D68 and increase in disease severity (54). In addition, the B1 clade of EV-D68 appears to be associated with the occurrence of acute flaccid myelitis (38).

During the 2014 outbreak of EV-D68, the CDC released an emergency use RT-PCR assay to help identify EV-D68 among patients (55). Since then others have either modified the CDC Protocol, or developed their own RT-PCR assay, specifically targeting the VP1 gene to increase the sensitivity of detection towards EV-D68 infections in patients (13). The VP1 gene is valuable for identifying the phylogenetic relatives and clades of EV-D68, as well as identifying EV-D68 as the cause of disease in patients. Targeting the VP1 gene has shown that different clades of EV-D68 seem to be the main cause of the outbreaks observed around the world (27, 33, 56).

EV-D68 Infection of Host Cells

Many enteroviruses use an immunoglobulin-like receptor to bind to and release their genomic RNA into the host cell, which is the method of replication used by polioviruses and rhinoviruses (51, 57, 58). However, EV-D70, which is a close relative of EV-D68, has been described as using sialic acid as a receptor (59, 60). Hemorrhagic conjunctivitis is associated with EV-D70. Since sialic acid is known to be present in at least two forms in the human respiratory tract, these receptors were suspect receptors for cell entry (61). EV-D68 was shown by Y. Liu, et al. (51) to use sialic acid as a cellular receptor to gain entry into the host cell (51). EV-D68 was shown to have a high affinity for the α2-6 sialic acid receptor, which is more abundant in the upper respiratory tract in humans (62). Even though EV-D68 has a higher affinity for α2-6 sialic acid receptors, EV-D68 had a higher detection rate in patients with lower respiratory tract infections, which are also more severe infections. The type of sialic acid that is more abundant in the lower respiratory tract is the α2-3 receptor. EV-D68 shows little to no affinity for the α2-3 receptor. This could suggest that there is another mechanism that plays a role in lower respiratory tract infections (3).

Clinical Case Presentation of EV-D68 Infections

There is not currently an approved therapy or vaccine available for EV-D68. Patients are treated by managing symptoms (4). When children infected withy EV-D68 visited the emergency room at the British Colombia Children's Hospital (BCCH), physicians treated them by following an asthma protocol, which entailed administering

oral dexamethasone and three rounds of salbutamol and ipratropium (4). They also used a pediatric respiratory assessment measure or PRAM score to evaluate the severity of the breathing difficulties that were associated with these patients. Chest X-rays revealed that in some of the patients there was a peribronchial thickening and hyperinflation of the lungs. Also noted was evidence of airspace disease in the form of minor and major patchy changes (4). Along with these clinical evaluations, some of the most severe cases required admission to the ICU, where the children were placed on ventilators for intensive respiratory support (4). There were similar observations noted in a review of case studies completed in Kansas City, Missouri and Alberta Canada (47, 63).

J. E. Schuster, et al. (63) reviewed the data from Children's Mercy Hospital (CMH) in Kansas City Missouri, for patients admitted to the hospital with respiratory difficulties during the 2014 outbreak of EV-D68 in the U.S. The pediatric patients, between 0 and 17 years old, that were admitted to the hospital and were positive for enterovirus had high neutrophil counts and abnormal radiographic findings. They also noted that these patients did not test positive for other secondary infections. In this study ventilation was not required, however several patients required admission to the intensive care unit for management of breathing difficulties (63) and they used albuterol and intramuscular epinephrine at higher amounts for children that tested positive for EV-D68 than children that tested negative for EV-D68.

In blinded studies, D. Mertz, et al. (47) noted that patients who tested positive for EV-D68 required more intensive care than others with similar histories and respiratory presentations (4, 47, 63). Of the types of infection involved in these studies, whether rhinovirus, influenza or a bacterial infection, patients with EV-D68 required more

intensive care. These studies identified EV-D68 as a more severe respiratory disease than other types of respiratory infections among children. However, these studies were biased toward younger aged patients 0-18 because they were conducted at three children's hospitals (4, 47, 63).

In a study conducted by M. Knoester, et al. (11), a 4-year old patient was diagnosed with AFM along with EV-D68 being the only causative agent that was reported. Along with his influenza-like respiratory signs that lasted at least a week, he had "rapidly progressing asymmetric facial paralysis", along with "asymmetric weakness of arms and legs". This 4-year old also showed bulbar paralysis, which involves functions such as swallowing, speaking and chewing. Upon analysis of cerebrospinal fluid, no abnormalities were found. "Hyperintense nonenhancing gray matter lesions" were found in the brainstem and in the spinal cord upon an MRI. Hyperintense nonenhancing gray matter lesions are bright spots on MRI scans. M. Knoester, et al. (11) completed an electromyography that revealed injury to the motor axon and the anterior horn of the spinal cord.

There are two important conclusions that can be drawn from these EV-D68 case presentations. The first is that there is a need to quickly and effectively identify patients that are EV-D68 positive. The second is the need for an antiviral therapy to treat patients, and the development of vaccines for use as a preventative measure.

Rapid detection of EV-D68 infections have been addressed by several different groups. The first is the Center for Disease Control, which developed an RT-PCR protocol to help with the outbreak. Another group, T. N. Wylie, et al. (13) then took the CDC protocol and modified it to make it more sensitive to more strains of EV-D68. This

protocol was used in our studies to verify the strains of EV-D68. Other reports have identified new developments in RT-PCR (54).

Antiviral Evaluation of EV-D68 Infections In Vitro

There is an immediate need for an antiviral therapy, in addition to vaccines to help in treatment and prevention of EV-D68 infections. Currently, there are not any approved antiviral therapies or vaccines for EV-D68. This is not because there have not been any positive results in finding antiviral drugs that show efficacy *in vitro*. The antivirals were evaluated and EC_{50}'s and EC_{90}'s were reported. The EC_{50} is the concentration of drug that yields 50% protection against the virus or the 50% effective concentration. The EC_{90} is the concentration of drug that yields 90% protection against the virus in cell culture. Following is a summary of *in vitro* evaluations of antiviral compounds against EV-D68.

Rupintrivir or AG7088 is a 3C protease inhibitor (64). Viral 3C protease is needed to process precursor proteins into functional proteins necessary for RNA replication in picornaviruses (65, 66). Rupintrivir binds to the 3C protease, which then inhibits the virus from replicating (64). D. A. Matthews, et al. (65) and A. K. Patick, et al. (66) also showed that rupintrivir is an effective treatment for different rhinovirus strains *in vitro.* These values, shown in Table 1 were based on the activity of rupintrivir against 48 different strains of rhinovirus. D. A. Matthews, et al. (65) reported that rupintrivir was specially formulated for intranasal treatment and was soon evaluated in clinical trials but proved non-effective. Since the original tests of rupintrivir against

rhinoviruses, a number of labs have tested the efficacy of the compound against EV-D68. L. Sun, et al. (67) tested the efficacy of rupintrivir against ten isolates of EV-D68 on Hela Rh cells. E. Rhoden, et al. (68) tested rupintrivir against three representative strains or isolates of EV-D68 from the 2014 outbreak results shown in Table 1. An additional study reported high activity for rupintrivir against EV-D68, *in vitro* using RD cells with an EC_{50}, similar to that reported by E. Rhoden, et al. (68).

Table 1 Antiviral efficacy (EC_{50} values) of rupintrivir evaluated against multiple strains of EV-D68 *in vitro*.

EC_{50} (μM)	CC_{50} (μM)	Strains	Author
0.023	>1000M	48 Strains or Rhinovirus	D. A. Matthews, et al. (65)
0.082	>1000	EV-D68	D. A. Matthews, et al. (65)
0.0018 and 0.003	NT	Ten Isolates	L. Sun, et al. (67)
0.0046 ± 0.0016	NT	Three Representative Strains	E. Rhoden, et al. (68)
0.0046 ± 0.0027	134 ± 21	US/KY/14-18593	D. F. Smee, et al. (15)

Pleconaril is a picornavirus capsid binding inhibitor (69). Capsid inhibitors prevent virus attachment and/or the virus from uncoating (15, 70, 71). L. Sun, et al. (67) and D. F. Smee, et al. (15) demonstrated pleconaril to be active against EV-D68 (see Table 2). D. F. Smee, et al. (15) pleconaril was also shown to be slightly less active against HRV-87 than EV-D68. D. F. Smee, et al. (15) also showed that pleconaril is not

active against EV71. Y. Liu, et al. (14) describes that the VP1 protein for most enteroviruses contain a pocket factor, or the VP1 binding pocket (72-74). The VP1 protein is responsible for the binding in EV-D68, which is then responsible for the un-coating of the virus (14, 75). Y. Liu, et al. (14) describes that pleconaril binds to this pocket factor which then inhibits EV-D68 and rhinoviruses from binding to host cells and infecting cells.

In 2012 G. Zhang, et al. (76) assessed the efficacy of pleconaril in treating EV71 in neonatal mice. When 1-day old mouse pups were infected with EV71 then treated with 80mg/kg/day of pleconaril, their survival rate was about 80 percent. Also reported by G. Zhang, et al. (76) was that when pleconaril was tested against EV71 in RD cells, the EC_{50} was from 0.13 to 0.54μg/mL. This is significant because Y. Liu, et al. (14) and D. F. Smee, et al. (15), reported pleconaril to be inactive against EV71 and yet showed high activity against EV-D68 and rhinoviruses. This data suggests that pleconaril might have a good potential to prove effective in treating EV-D68 infections. Pleconaril is also in phase II clinical trials with healthy human volunteers that were then infected with rhinovirus in the form of two 200mg tablets for five days. Pleconaril can be orally absorbed by the patient (77).

Enviroxime also showed efficacy against EV-D68. D. F. Smee, et al. (15) reported enviroxime to exhibited activity against two strains of EV-D68, RV-87 and EV71. L. Sun, et al. (67) tested enviroxime against ten strains of EV-D68 grown in Hela Rh cells. Results are shown in Table 3. The mechanism of action isn't well understood. There were reports that enviroxime worked against the 3A(B) protein of rhinovirus (79,

80). However, others reported that enviroxime did not disrupt the binding of 3A(B) proteins to bind to RNA (81).

Table 2 Antiviral efficacy (EC_{50} values) of pleconaril evaluated against multiple strains of EV-D68 *in vitro*.

EC_{50} (μM)	CC_{50}	Strains	Author
0.6 ± 0.14	Not Shown	One strain	Y. Kim, et al. (78)
0.08 to 0.8	Not shown	10 Strains	L. Sun, et al. (67)
0.13 ± 0.09	11.3 ± 0.03	Two Strains	D. F. Smee, et al. (15)
4.44 to 6.11	Not Shown	Three Strains	E. Rhoden, et al. (68)
0.38 ± 0.01	Not Shown	Fermon	E. Rhoden, et al. (68)
0.43 ± 0.02	Not Shown	One Strain	Y. Liu, et al. (14)

Enviroxime also showed efficacy against EV-D68. D. F. Smee, et al. (15) reported enviroxime to exhibited activity against two strains of EV-D68, RV-87 and EV71. L. Sun, et al. (67) tested enviroxime against ten strains of EV-D68 grown in Hela Rh cells. Results are shown in Table 3. The mechanism of action isn't well understood. There were reports that enviroxime worked against the 3A(B) protein of rhinovirus (79, 80). However, others reported that enviroxime did not disrupt the binding of 3A(B) proteins to bind to RNA (81).

Table 3 Antiviral efficacy (EC_{50} values) of enviroxime evaluated against multiple strains of EV-D68 *in vitro*.

EC_{50} (μM)	CC_{50}	Strains	Author
0.19 to 0.45	Not shown	10 Strains	L. Sun, et al. (67)
0.27 to 0.31	95 ± 27	Two Strains	D. F. Smee, et al. (15)
0.19 ± 0.11	Not Shown	Human Rhinovirus	D. F. Smee, et al. (15)
1.0 ± 1.1	Not Shown	Enterovirus 71	D. F. Smee, et al. (15)

Guanidine HCl (guanidine) is an enterovirus replication inhibitor. In negative stranded RNA, the function of viral protein 2C is inhibited by guanidine interaction (82). B. Loddo, et al. (83) tested guanidine in vitro on Hela cells and MS cells and showed good activity against poliovirus. More recently guanidine was also reported to be an effective treatment for EV-D68, HRV-87 and EV71 *in vitro* by D. F. Smee, et al. (15). Guanidine was shown to be less effective against EV71 than EV-D68 (15). These results are shown in Table 4.

Table 4 Antiviral efficacy (EC_{50} values) of guanidine evaluated against multiple strains of EV-D68 *in vitro* Reported by D. F. Smee, et al. (15).

EC_{50} (μM)	SI	Strains
80 ± 21	46	US/KY/14-18953
91 ± 11	40	Fermon
91 ± 10	40	Human Rhinovirus
305 ± 5	12	Enterovirus 71

SI = Selectivity Index=(CC_{50}/EC_{50})

EC50 = 50% Effective Concentration

Guanidine was also tested in suckling (newborn) mice as a possible treatment for echovirus-9 and coxsackiesvirus A9 (84). Both of these viruses belong to the picornavirus family. Guanidine was tested in conjunction with 2-α-Hydroxybenzyl-benzimidazole (HBB). Neither compound alone was protective against either virus. However when administered together, the suckling mice were protected against mortality (84). E. C. Herrmann, Jr., et al. (85) reported that when infant mice were infected with coxsackiesvirus A16, guanidine treated with two injections per day with 97 mg/kg per injection and combined with HBB, the death rate was significantly reduced. They also report tremors at 145 mg/kg per injection and also 97 mg/kg per injection. Because of this there is some promise for the efficacy of guanidine against EV-D68.

Animal Models

Mice provide a good model for studying many virus infections. Mice can be inexpensive and easy to handle and many strains of mice are available. However for many human viruses including EV-D68, mice are not the natural host, so the virus must be adapted to infect the animal. Influenza is an example of a virus that does not naturally infect mice. To produce disease in the mouse, the virus must first be adapted to mice by serial passage through the lungs of mice (86). Furthermore, for the purpose of evaluating antiviral therapies, passaging the virus in mice to make it lethal to the mouse may be required and is difficult to achieve.

Three EV-D68 animal models have been developed since the beginning of this project. One in cotton rats, one in two-day old Swiss Webster mice and ferrets. The first

model takes advantage of the affinity of EV-D68 to bind to sialic acid receptors in adult cotton rats. Cotton rats have been shown to have high numbers of α2,6-linked sialic acid receptors (87). M. C. Patel, et al. (16) used three different strains of EV-D68: Fermon, VANBT/1, and MO/14/49 (16) representing clades A and B that are relevant to the United States. They determined that the VANBT/1 strain replicated more than the other two strains in cotton rats. Using VANBT/1, these authors determined that EV-D68 replicates quickly in the nasal tissues as well as in the lungs, similar to what is observed in humans (16). M. C. Patel, et al. (16) infected animals with EV-D68, then euthanized and collected nasal and lung tissues at 0.5, 2, 4, 6, 8, 10, 24, 48 and 96 hours. In cotton rats, virus measured in tissues (tissue titers) were detected in nasal tissue collected at 0.5 hours post infection. The tissue titers then dropped at the 2 to 4 hour time points p.i. and then increased and peaked at 10 hours p.i. (16). Virus was cleared in the nose by 48 hours p.i. A similar pattern was observed in the lung tissues. Differences between male and female cotton rats were negligible.

Pro-inflammatory cytokines were evaluated at the same time points. Monocyte chemo-attractant protein-1 (MCP-1) and neutrophil chemo-attractant chemokine (GRO) levels peaked at 4-hour p.i. and then decreased (16). Other cytokines that showed significant difference between uninfected and infected rats at the specified time points were IP-10, RANTES, Interferon-β, Mx-1, Mx-2, IL-6 and Interferon-γ. M. C. Patel, et al. (16) also showed lung pathology in infected mice. The severity of the pathology peaked at 48 hours p.i., with moderate signs of disease noted.

This study evaluated the ability of vaccination to protect from EV-D68 infection. Three strains of EV-D68, both live and inactivated by ultraviolet light, were used to

inoculate cotton rats. Cotton rats were then infected with EV-D68 intranasally after one-week post vaccination. M. C. Patel, et al. (16) showed that immunized animals showed no clinical signs of disease. The vaccinated animals were also able to clear virus from their tissues faster than the unimmunized rats.

The second animal model developed was in two day-old Swiss Webster mice using seven strains of EV-D68. Five strains from the 2014 U.S. outbreak: US/KY/14-18953 (clade A), IL/14-18952 and CA/14-4231 (both clade B), MO/14-18947 and CA/14-4232 (both clade B1) (17) as well as two of the original strains of EV-D68, Fermon and Rhyne, were evaluated.. The virus was inoculated into mice by intracerebral injection with as much virus as possible. By doing this, they were able to induce acute flaccid myelitis (AFM). Acute flaccid paralysis and acute flaccid myelitis are used interchangeably in the literature (88). These results gave laboratory confirmation that AFM can be caused by an EV-D68 infection. Of the five 2014 strains that were evaluated, four caused AFM and even mortality in mice. Of the strains of virus originally isolated in 1962, only Rhyne induced some mild limb weakness (2).

After intracerebral injection, the infected mice exhibited limb weakness and paralysis in the front limbs, although some limb weakness and paralysis were observed in both the front and rear limbs. When spinal cord samples were taken on day 0 p.i. just after infection, viral titers were undetectable. However, samples collected on day 2 to 4 had increased titers (17). Virus titers in the brain collected at the same time points had a reverse pattern; the virus had high titers in the brain 1 hour p.i. and then by day 2 to 4 p.i. viral titers were undetectable. They were also able to show that the motor neurons of the anterior horn in paralyzed limbs were severely injured or dead.

Alternate routes of infection were evaluated using the two-day old Swiss Webster mouse pups and the MO/14-18947 strain of EV-D68 (17). Following intramuscular injection paralysis was observed in all mice. However, paralysis was only observed in 2 out 73 mice following intranasal infection, and took 8 and 10 days p.i. for signs to develop. Similar results were seen in mice infected by intraperitoneal injection, where only 1 out of 22 mice showed paralysis, and paralysis did not occur until day 5 p.i..

A. M. Hixon, et al. (17) showed the protective affect of EV-D68 antibodies to prevent paralysis and death. They injected 1 day-old pups with pooled immune sera against [EV-D68] MO/14-18947 and a control serum. The mice were then challenged with EV-D68 24 hours later. The control group, had 57% of the mice develop paralysis with 18% mortality. Comparatively, in the mice treated with the "pooled immune sera", only 4.5% of mice showed paralysis and no mortality (17). This neonate model was used to show that EV-D68 can cause AFM and also that there is a possibility of treating EV-D68 with IVIGs.

The third animal model was developed in ferrets. The ferrets were infected intranasally with $10^{4.5}$ $CCID_{50}$ with EV-D68 Fermon. Body weight, temperatures, respiration, sneezing and nasal discharge were measured. Animal feces, nasal washes, throat swabs, and organs were harvested. Four of the 15 ferrets had respiratory illness, including cough, nasal discharge and dry nose. No change was observed in body temperature, although mock-infected ferrets gained more weight than EV-D68 infected ferrets suggesting that mock-infected ferrets were healthier than infected ferrets. Virus load was determined by qPCR and was observed on multiple days p.i. in feces, nasal washes, blood, lymph nodes and lungs. Histopathological manifestations were present in

the lungs yet not in the trachea. These 3 animal models all have serious limitations in the lab. Cotton rats are expensive and hard to work with. 2-day old mice are difficult to work with and intracerebral injection is difficult and variable. Ferrets are costly. So a better model was needed.

AG129 Mice

AG129 mice are a valuable because they are immune compromised. Both A129 and G129 mice were genetically altered using embryonic stem cell gene targeting intercrossed to generate the AG129 mice (89). The A129 mice are deficient in INF-α/β receptors, while G129 mice are deficient in the INF-γ receptor (89, 90). IFNs provide an innate response to infection by foreign pathogens (91). According to C. A. Biron (92) the interferons that take a lead role in the early stages of infection are INF-α/β. For example C. A. Biron (92) showed that IFN-β activates proteins that then inhibit later steps in the life cycle of the virus (91). A. G. Goodman, et al. (91) described the activation and recruitment of T-cells and natural killer cells by INF-α/β (93). These T-cells and natural killer cells then secrete INF-γ (91, 93). Due to the lack of interferon receptors, AG129 mice are immune compromised.

Since AG129 mice are immune deficient, they are more susceptible to viruses that would not normally infect mice. Therefore, AG129 mice are a valuable tool for studying human viruses. For example, AG129 mice have been used to study influenza and more recently the newly emerged Zika virus outbreak (94). Other viruses have been tested including Enterovirus 71, at least two strains of coxsackiesvirus, dengue virus, yellow

fever virus, Japanese encephalitis virus, and Chikungunya virus; some even without adaptation (95-100). Because of the success observed with AG129 mice as models for other viruses, AG129 mice were selected for use in model development for EV-D68 infection.

CHAPTER III

ENTEROVIRUS D68 ADAPTATION TO 4-WEEK-OLD AG129 MICE

In Vitro Evaluation of EV-D68 Isolates

One approach to developing an animal model for EV-D68 was to initially adapt the EV-D68 virus to replicate in mouse cells in culture. Four strains of EV-D68 were obtained from the American Type Cell Culture (ATCC) along with several different strains of mouse cells to grow in cell culture. The four strains of EV-D68 were US/IL/14-18982, US/KY/14-18953, US/MO/14-18949 and US/MO/14-18947, all of which were isolated during the 2014 EV-D68 outbreak. These viruses were passaged in RAW mouse macrophage cells, and 3T3 mouse embryo fibroblast cells. Cells were seeded into T-25 flasks 24 hours prior to infection. After 24 hours, the cells were infected with EV-D68, one flask per strain, and incubated at 33°C and 5% CO_2. The cells were then observed for up to three days post-virus exposure. Once the cells within the flask reached 80-100% cytopathic effect (CPE), the flasks were frozen at -80°C to rupture cells and release virus. After freezing, the cells were thawed and homogenate containing the virus was aliquoted into cryovials. The same procedure was used for all viruses evaluated.

The homogenate from each passage was titered using a standard endpoint dilution assay on 96-well plates seeded with human rhabdomyosarcoma (RD) cells. Micro-plates were seeded 24 hours prior to virus-exposure and incubated at 37°C and 5% CO_2 to ensure a cell confluence of 100% (15). After addition of virus the micro-plates were

incubated 6 days at 33°C and 5% CO_2 then examined for CPE. The 50% cell culture infectious doses ($CCID_{50}$) were then calculated using the Reed and Munech endpoint dilution (101). Hereafter, each mouse passage will be referred to as MP0, MP1, etc.

Each of the five strains of EV-D68 was serially passaged four times in both of the cell lines. Three of the four strains, US/IL/14-18982, US/KY/14-18953, and US/MO/14-18949 started with viral titers between $10^{3.5}$ to $10^{5.5}$ $CCID_{50}$/mL on the first passage in mouse tissues. The second passage resulted in 10 to 100-fold reduction for most strains of EV-D68 in both cell lines. By the third and fourth passages, virus titers were undetectable (Table 5). This suggests that these strains of EV-D68 (US/IL/14-18982, US/KY/14-18953 and US/MO/14-18947) were not adapting to the mouse cells. One strain of EV-D68, US/MO/14-18949 did increase in virus titer with sequential culturing in mouse cells. The titer after the first passage of virus was 10^6 $CCID_{50}$/mL, which then was slightly lower after passage two. After the fourth passage in both murine cell lines, the virus titers increased by 10-fold. Based on this information, EV-D68 US/MO/14-18949 was selected for adaptation in the mouse.

Table 5 Virus Titers During Adaptation of EV-D68 in Two Mouse Cell Lines.

Cell Lines	EV-D68 US/IL/14-18952				EV-D68 US/KY/14-18953			
	Passage 1	**Passage 2**	**Passage 3**	**Passage 4**	**Passage 1**	**Passage 2**	**Passage 3**	**Passage 4**
Raw	4.67	3.00	1.00	1.00	2.50	0.67	<0.67	<0.67
3T3	3.33	0.67	<0.67	<0.67	3.50	1.50	<0.67	<0.67
Cell Lines	**EV-D68 US/MO/14-18949**				**EV-D68 US/MO/14-18947**			
	Passage 1	**Passage 2**	**Passage 3**	**Passage 4**	**Passage 1**	**Passage 2**	**Passage 3**	**Passage 4**
Raw	3.00	3.67	3.50	4.33	3.33	2.33	0.67	<0.67
3T3	5.00	4.67	5.00	6.00	3.33	<0.67	<0.67	<0.67

Values listed in the table are log $CCID_{50}$/mL.

Development of a Mouse Model

Because EV-D68 does not naturally cause disease in mice, an immune suppressed mouse strain was selected for development of the animal model. AG129 [129/Sv] mice are deficient in both alpha/beta (IFN-α/β) and gamma (IFN-γ) interferon receptors. It may be that the presence of interferon or pathways influenced by interferon in a normal mouse could impede the ability of EV-D68 to replicate sufficiently to yield any pronounced lung disease in a normal mouse. Because AG129 mice lacked these receptors, EV-D68 would have a better chance of adapting to the mice.

EV-D68 virus was serially passaged 30 times in 4-week old AG129 mice of both genders. The AG129 mice came from a germ free breeding colony at Utah State University. Each passage was completed by inoculating a group of 6 mice, 3 males and 3 females, with 90 μL of virus intranasally (i.n.). Mice were then observed for three days p.i. On day 3 p.i., 2 male and 2 female mice were euthanized and their lungs were collected. Virus was recovered from the homogenized lung tissue and then used to infect a subsequent set of mice. A sample of lung homogenate was also used to determine a virus titer following the procedure described previously. The two remaining mice were observed for 21 days p.i. for signs of disease such as weight loss and mortality.

Over the 30 serial passages, no weight loss or mortality was observed. However, as the passage number increased, the viral titer increased as well (Figure 1). The virus titer of EV-D68 at passage 1 was 10^5 $CCID_{50}$/mL and by passage 15 it had increased to $10^{8.8}$ $CCID_{50}$/mL in lungs. The initial aim of the project was to create a lethal model for EV-D68 in AG129 mice. Therefore, subsequent passaging of adapted virus was continued. From mouse passage 15 to 30 virus titers in the lungs varied between $10^{7.6}$

and $10^{8.8}$ $CCID_{50}$/mL, but clinical signs were not observed in the infected mice at any passage number.

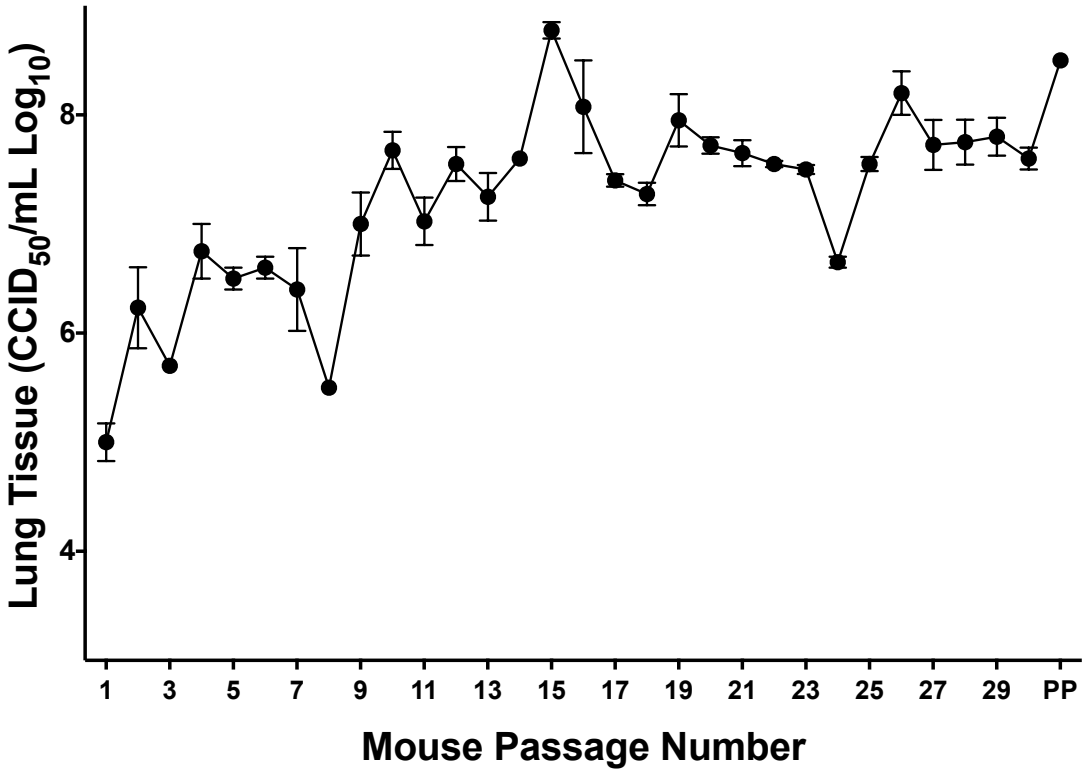

Figure 1 Virus titers in lungs after serial passage of EV-D68-US/MO/14-18949 in AG129 mice. Virus titers in the lungs collected from mice during virus passage show an increase in titer of more than 1000-fold between passage 1 to 15. Between passages 12 to 30 and plaque purified (PP) the virus titers plateau around $10^{7.5}$ $CCID_{50}$/mL.

Because of the lack of clinical signs of disease other than virus titers, other markers of disease were evaluated to verify that the virus was adapting to the mouse. Pro-inflammatory cytokine levels were evaluated for this purpose. Two cytokines showed an increase in concentration as mouse passage increased, MCP-1 and RANTES (Figure 2). MCP-1 is involved in regulating migration and infiltration of monocytes

and/or macrophages (102). RANTES also aids in the regulation of macrophage migration and plays a role in the progression of inflammation from acute to chronic (103). Both MCP-1 and RANTES increased significantly between MP1 and MP15. MCP-1 increased significantly ($P = <0.05$) by MP11 compared to MP1, then remained fairly constant between MP15 and MP30. RANTES did not increase significantly from MP1 to MP25, but did show a significant increase from MP25 to MP30.

In addition to lung virus titers and cytokine levels, we evaluated lung tissues from different mouse passages for histological lesions. We tested four mice infected with MP-0 and MP-19 and compared lung injury to the lungs from uninfected mice. A lung injury scoring system was used to differentiate the amount of observable lung lesions. A lung score of "-", or 0 equals no damage, "1+" equals minimal damage, "2+" equals mild damage, "3+" equals moderate damage and "4+" equals severe damage (Table 6). The six categories of observations made for each lung sample were: 1) bronchial epithelium injury, 2) bronchiolar epithelium injury, 3) alveolar wall injury, 4) lymphocyte around bronchioles, 5) interstitial inflammation (perivascular and alveolar) and 6) pulmonary edema. For each of these observations, group 1 (MP0 infected) did not show any lesions, meaning that MP0 did not cause any observable lung injury. However, group 2 (MP19 infected) showed alveolar wall injury scores of 1+ to 2+. The scores for lymphocytes around bronchioles for three mice were 2+ and for one mouse 2+ to 3+. For interstitial inflammation, the MP19-infected mice had a scores of 2+ to 3+. Finally, three of the group 2 mice exhibited a pulmonary edema score of 1+ and one with a score of 2+. Group 3, which was the uninfected vehicle control group, had lung scores of 0 for all groups. Because we observed increased lung pathology scores from MP0 to MP19, more

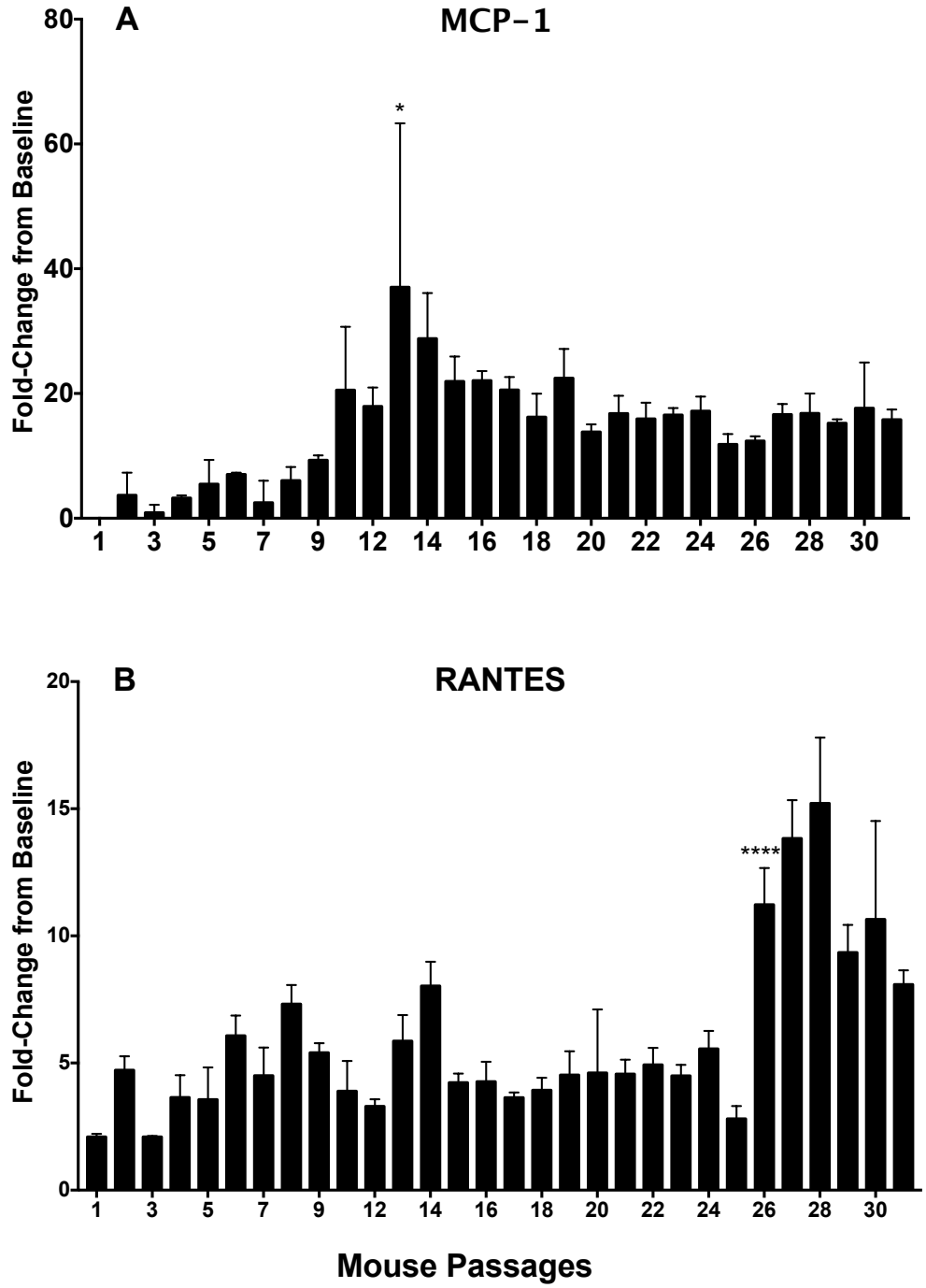

Figure 2 Pro-inflammatory cytokines MCP-1 and RANTES levels during mouse adaptation of EV-D68 –US/MO/ 2014. Fold changes compared to baseline in levels of MCP-1 and RANTES as mouse passage increased. Baseline is determined from uninfected control mice and is set to equal a value of 1. Both MCP-1 and RANTES exhibited significant increases as mouse passage increased. Average of 4 samples, 2 male, 2 female. Stats were compared to the mouse passage previous. *P <0.05, **P <0.01, ***P <0.001, ****P<0.0001.

passages of EV-D68 were completed in mice.

Determining *de novo* Virus Replication Following Infection of Mice

To verify that EV-D68 was truly adapting to AG129 mice and replicating in the lung and that we were not simply recovering input virus, we determined *de novo* virus replication in the lung. Poliovirus grown in the presence of neutral red becomes light sensitive as the dye becomes incorporated into the virion. When the neutral-red-bound virus is then exposed to visible light, the virus is rendered inactive (104). We used this principle to demonstrate *de novo* virus replication in the lungs of infected mice. Mouse passage 16 of EV-D68 was grown in in cell culture media containing 10 μg/mL neutral red (Sigma-Aldrich, St. Louis MO). RD cells were seeded into a T-150 flask 24 then infected with a 1:1000 dilution of EV-D68 MP16. The flasks were then incubated in the dark at 33°C with 5% CO_2 for two days until 100% CPE was reached. The virus was then harvested, aliquoted and frozen for later use.

Three mice were inoculated intranasally with the light sensitive EV-D68, and then euthanized three-days post-virus exposure. Lungs were collected and homogenized in the dark. Lung homogenate samples were then split in half. Half the sample was exposed to 10 minutes of fluorescent light and the other half was kept in the dark. Viral titers were determined for the original light sensitive virus along with the lung homogenates, with light sensitive virus treated identically to virus from infected lungs. Virus titers from lung homogenates exposed to light and unexposed to light were compared. Lung homogenates from mice infected with light sensitive EV-D68 showed similar titers

Table 6 Lung Histological Lesion Score Comparison of MP0 and MP19 for Lung Observations.

Group #	Bronchial epithelium injury	Bronchiolar epithelium injury	Alveolar wall injury	Lymphocyte around bronchioles	Interstitial inflammation (perivascular and alveolar)	Pulmonary edema
MP0 Infected	-	-	-	-	-	-
	-	-	-	-	-	-
	-	-	-	-	-	-
	-	-	-	-	-	-
MP19 Infected	-	-	++	++ to +++	++ to +++	+
	-	-	+	++	++	+
	-	-	++	++	++ to +++	++
	-	-	++	++	++ to +++	+
Uninfected control	-	-	-	-	-	-
	-	-	-	-	-	-

Lung injury score from 0 to 4 with - being no damage, + is minimal, ++ is mild, +++ is moderate and ++++ is sever.

regardless of light exposure. The light sensitive virus had a titer of $10^{7.2}$ $CCID_{50}$/mL before exposure to light, and a titer of $10^{3.0}$ $CCID_{50}$/mL after exposure to light. Lung titers for samples not exposed to light averaged $10^{7.55}$ $CCID_{50}$/mL, while titers for lung samples exposed to light averaged $10^{7.5}$ $CCID_{50}$/mL (Figure 3). This clearly shows that EV-D68 is in fact replicating in the lungs of mice after challenge infection since the virus replicating in mouse tissues was not light sensitive.

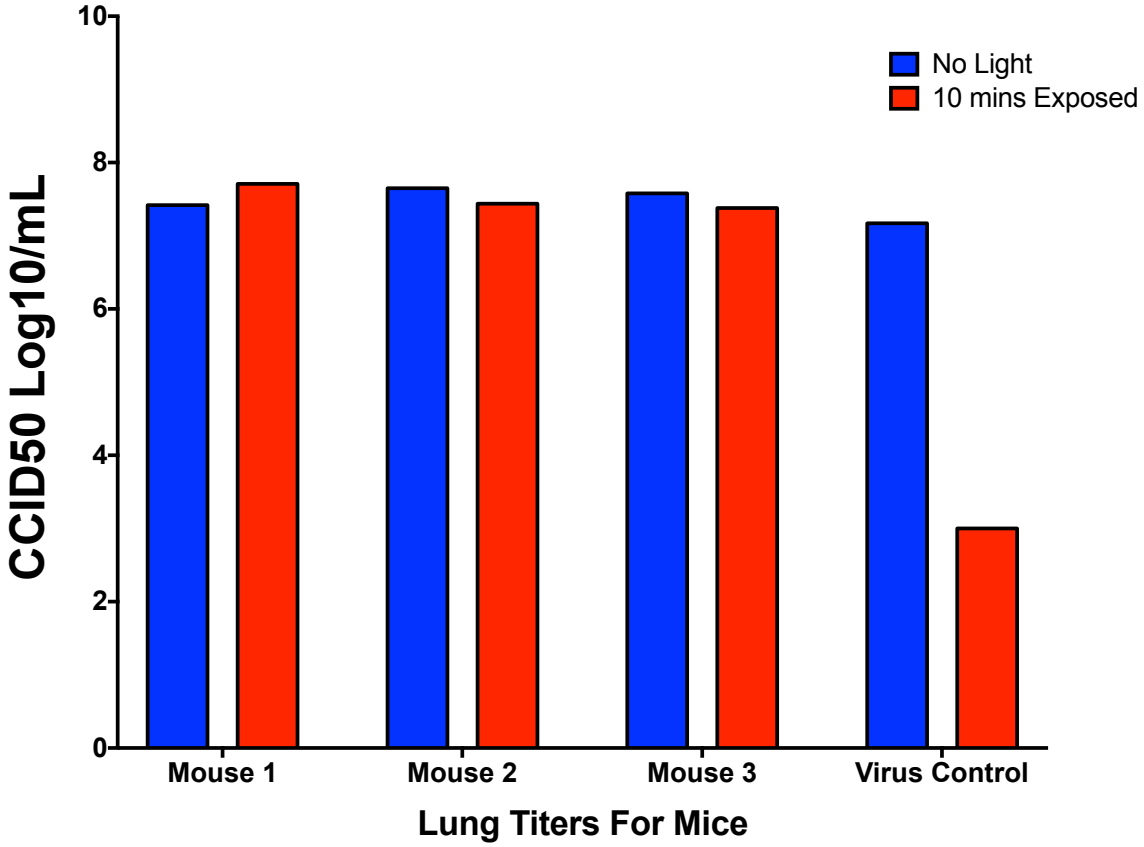

Figure 3 Light Sensitive EV-D68 Infection in Mice. Lung homogenates from mice infected with light sensitive EV-D68 before and after exposure to 10 minutes of fluorescent light. Virus samples from mouse lungs had similar titers before and after light exposure. However, light sensitive virus that was not passaged through mice, showed a 10,000-fold difference when virus was exposed to 10 minutes of fluorescent light compared to virus handled in the dark.

Evaluation of Alternative Adaptation Strategies

D. F. Smee and D. L. Barnard (86) described using mannan as a way to aid the adaptation of influenza viruses to mice. Mannan is a plant polysaccharide that binds host cell collectins that can inhibit influenza virus (86). Six passages of EV-D68 in mice were completed using mannan in the infection medium. The first passage from mannan-infected mice had an average titer of $10^{7.6}$ $CCID_{50}$/mL, whereas by the last passage virus titers decreased 3.2-fold to an average of $10^{7.1}$ $CCID_{50}$/mL. Fucoidan, another additive, was also evaluated in two passages of EV-D68, as done with mannan. After the second passage in mice, the virus titer had decreased 3.2-fold from an average of $10^{8.0}$ $CCID_{50}$/mL to $10^{7.5}$ $CCID_{50}$/mL. Infection with these additives did not cause the mice to exhibit any signs of disease. Therefore mannan and fucoidan were not used for further passaging.

Another adaptation method included passage of virus through younger mice. The idea was that younger mice would not have a fully developed immune response, giving the virus a better chance for replication and survival. For this process virus was passaged in two-week old AG129 mice starting with MP22. After the first passage virus titers averaged $10^{8.2}$ $CCID_{50}$/mL. Through the five passages, no clinical signs were observed and virus titers decreased steadily throughout passaging. At the end of five passages the virus titers averaged $10^{7.5}$ $CCID_{50}$/mL, which was a 3.2-fold decrease (Table 7). Obviously, the AG129 mouse immune response is suppressed, but not absent.

Table 7 Lung Virus Titers from 2-Week Old AG129 Pups Infected with EV-D68.

Mouse Passage	Lung Virus Titers ($CCID_{50}$/mL Log_{10})				
	Mouse 1	**Mouse 2**	**Mouse 3**	**Mouse 4**	**Mouse 5**
1	8.0	8.5	8.0	-	-
2	8.3	8.8	7.5	7.6	7.6
3	7.4	7.5	-	-	-
4	7.5	7.6	7.6	-	-
5	7.4	7.5	7.6	-	-

Passages were completed in groups of 2 to 5 mice depending on availability.

Evaluation of Alternative Routes of Infection

Different routes of infection were evaluated to identify the optimum route for use in the mouse model. The routes initially evaluated included: intranasal (i.n.), intra-thecal (i.t.), retro-orbital (r.o.), intra-venous (i.v.) and intra-peritoneal (i.p.). Four mice were used to test each route of infection. Two mice from each group were euthanized day 3 post infection and multiple tissues (kidney, brain, lungs, spleen and liver) were collected for virus titer. Viral titers in tissues were highest in all 5 tissues for mice infected via the intranasal route. Other routes of infection resulted in virus spreading to various tissues, however no clinical signs were observed (Table 8). From these studies, intranasal infection was identified as the best route of infection for EV-D68.

Table 8 EV-D68 virus titers in various tissues following different Routes of Infection in 4-week-old AG129 Mice.

Route of infection	Kidney	Brain	Lung	Spleen	Liver
i.t.	0.67	0.67	0.67	0.67	0.67
	3.25	0.67	0.67	0.67	4.50
r.o.	4.50	0.67	0.67	0.67	4.25
	4.25	0.67	0.67	0.67	1.25
i.v.	0.67	0.67	5.75	0.67	0.67
	0.67	0.67	5.50	0.67	0.67
i.p.	0.67	0.67	0.67	2.50	4.25
	0.67	0.67	1.67	0.67	4.75
i.n.	4.75	2.67	8.00	4.00	5.00
	5.00	2.67	8.00	5.00	4.50

Limit of virus detection is 0.67.
Values expressed in Log_{10} $CCID_{50}$/mL.

Evaluation of Alternative Strains of EV-D68

The strain of EV-D68 used for the adaptation process was the US/MO/14-18949 strain. However, other strains of EV-D68 were passaged in mice to confirm that the Missouri isolate was the best candidate for adaptation. One representative strain of EV-D68 that did not passage *in vitro*, US/KY/14-18953, was passaged four times in four-week-old mice.

This study also confirmed that virus strains that did not replicate in mouse cells *in vitro*, would not replicate *in vivo* in mice. Virus was inoculated into mice via intranasal infection, and then recovered three days post-virus exposure, and virus titers determined in the lungs. Between the first and second mouse passage, virus titers were $10^{4.3}$

$CCID_{50}$/mL (Figure 4). After the third passage virus titers decreased about 100-fold. By the fourth passage the lung virus titers were undetectable.

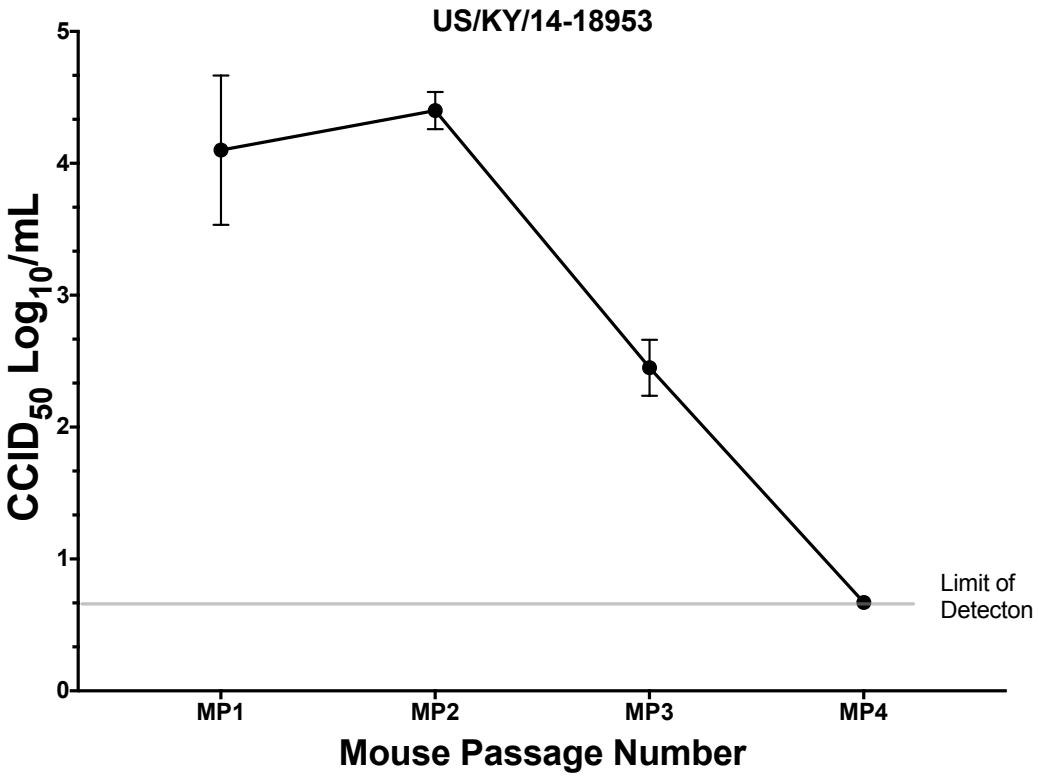

Figure 4 EV-D68 isolate US/KY/14-18953 titers from lungs after passages in AG129 mice.

CHAPTER IV

EVALUATION OF MOUSE MODEL

Development of a Respiratory Disease Model for Enterovirus D68 in 4-Week Old Mice for Evaluation of Antiviral Therapies and Vaccines

W. Joseph Evans, Brett L. Hurst, Donald F. Smee, Arnaud Van Wettere, E. Bart Tarbet

Institute for Antiviral Research, Utah State University, Logan, UT; Department of Animal, Dairy and Veterinary Sciences, Utah State University, Logan, Utah

Corresponding Author: E. Bart Tarbet, Utah State University, Logan, Utah, 84322-5600

E-mail: bart.tarbet@usu.edu

Tel: 1 (435) 797-3954

Running title: Development of Respiratory Disease Model for Enterovirus D68 in 4-Week Old Mice

Abstract

Enterovirus D68 (EV-D68) is a non-polio enterovirus that affects the respiratory system and can cause serious complications, especially in children and older people with weakened immune systems. As an emerging virus, there are no current antiviral therapies or vaccines available. The goal of this project was to develop a mouse model of human EV-D68 infection that mimicked the disease observed in humans. This model could be valuable in evaluating experimental therapies and vaccines. We initially adapted the virus by serial passage in AG129 mice, which are deficient in IFN- α/β and –γ receptors. For each passage, mice were infected via the intranasal route. After three days the virus was recovered by homogenization of lung tissues, followed by titration in human rhabdomyosarcoma (RD) cells.

Despite a lack of observable clinical signs in the mice, virus titer increased 320-fold, and the pro-inflammatory cytokines MCP-1 and RANTES increased 15-fold and 2-fold, respectively, over 30 passages in mice. Extensive passaging of the virus caused increased inflammation of lung tissue, as determined by evaluation of histological lesions. In addition, a time course of EV-D68 infection was determined in lung, blood, liver, kidney, spleen, spinal cord and brain samples taken on multiple days after infection. Lung pathology and selected cytokines in lungs and blood were also measured over time. This is an effective mouse model for EV68 disease using virus titers, lung pathology and cytokine markers, and it will be useful in evaluating infection and antiviral compounds in the future.

Introduction

Enterovirus D68 (EV-D68) was first isolated in 1962 in California from four patients with respiratory illness (2). EV-D68 is a member of the Enterovirus genus in the Picornaviridae family (105). Viruses of the picornaviridae are small, single stranded, non-enveloped viruses containing positive sense RNA (8). EV-D68 shares some characteristics with rhinoviruses. Like rhinoviruses, EV-D68 is a respiratory virus (3, 10). Most enteroviruses are known for being stable in acid. When EV-D68 was first isolated in 1962, the studies concluded that EV-D68 was acid-stable (2). However, later studies have concluded that EV-D68 is actually acid-sensitive (20, 22). M. S. Oberste, et al. (22) showed that two sub-strains of Fermon (the originally isolated strain (2)) along with multiple other newer isolates of EV-D68 were also acid-labile (22). Rhinoviruses are known to be acid-labile and to replicate at lower temperatures than most animal viruses in cell culture (43). These characteristics are also exhibited by EV-D68. A recent change in taxonomy has classified rhinovirus-87 as a strain of EV-D68 (50).

According to the Centers for Disease Control and Prevention (CDC), enteroviruses cause about 15 million infections annually in the United States. Most people infected with enterovirus are asymptomatic or have only mild illness (26). However individuals with asthma or reactive airway disease (25, 26), infants and/or individuals with weakened immune systems can have serious complications when infected with EV-D68 (15). EV-D68 infections were rarely reported after their initial discovery in 1962 (10). However, since the 2000's EV-D68 has been increasing in prevalence and is becoming recognized as a cause of respiratory illness. The Philippines experienced a small outbreak of EV-D68 in 2008 through 2009 (6). In 2009, the

Netherlands and the United States also reported cases of EV-D68. In 2010, Japan reported more than 120 cases of EV-D68 (6, 7). China, Italy and Canada have also reported small outbreaks or clusters of EV-D68 infections in recent years as well (4, 8, 27).

In 2014, the United States experienced an outbreak of Enterovirus D68 with over 1,100 cases reported (68). The cases were mostly children with severe respiratory illness (10). Enterovirus D68 patients presented with shortness of breath, cough, and nasal congestion. Patients also showed decreased air entry or wheezing, and severe to moderate respiratory distress, and evidence of airspace disease showing minor and major patchy changes within the lungs. During this outbreak, some patients required respiratory support (4). In addition, some individuals who tested positive for EV-D68 exhibited neurological disease. During the 2014 U.S. outbreak two states, Colorado and California originally reported these cases of acute flaccid paralysis. However, by mid December at least 33 states in the U.S. reported children with acute flaccid paralysis who were positive for EV-D68 (31, 36, 38, 39). Other enteroviruses have also been known to be neurotropic as well (22).

Since EV-D68 has been increasing in prevalence over the last few years, it is important to find treatment strategies against infection. To date there are no approved treatments for EV-D68, although there are many compounds that have shown efficacy against EV-D68 *in vitro*, including Rupintrivir, Enviroxime and Pleconaril (15, 67, 68). One reasons treatments have not been approved is that until recently, there has not been an animal model available for study of experimental therapeutics against EV-D68. A cotton rat infection model was recently reported using non-adapted EV-D68 (16). In

addition, a model was recently developed showing the neurotropic effects of EV-D68 in neonatal Swiss Webster mouse pups (17). Unlike these models, we developed an EV-D68 model in AG129 mice by serial passaging the virus. Herein we demonstrate that EV-D68 increased its ability to replicate and to cause lung pathology with increasing mouse passages. We also describe the pathogenesis of the virus over time in different mouse tissues. Finally, we compared the mouse-adapted EV-D68 to rhinoviruses and show that both can be treated by similar antiviral compounds *in vitro*. This comparison demonstrates that the mouse model developed in 4-week-old AG129 mice can be used as a model for evaluating antivirals against both EV-D68 and rhinoviruses.

Materials and Methods

Viruses and Cell Lines. The following viruses were obtained from the American Type Culture Collection (ATCC, Manassas, VA): enterovirus D68 (US/MO/14-18949), enterovirus D68 (US/MO/14-18947) enterovirus D68 (US/KY/14-18953), enterovirus D68 (US/IL/14-18982) and human rhinovirus type 14. Human rhabdomyosarcoma (CCL-136) cells (RD), A549, 3T3 and RAW 264.7 cells were also obtained from ATCC. HeLa-Ohio-1 (human cervical epithelioid carcinoma) cells were obtained from Dr. Frederick Hayden (University of Virginia, Charlottesville, VA).

Cell Culture Media. Cells lines were grown in minimum essential media (MEM) (GE Healthcare Hyclone, Logan, UT USA) with 5% fetal bovine serum (FBS). Media used for EV-D68 cell culture infection included 2% FBS and 25 mM $MgCl_2$ in

MEM + 50 μg/ml of gentamicin. Tissues harvested from mice were homogenized in MEM. In addition, MEM served as the infection vehicle for infections of mice.

Passage of virus in mice. Four strains of EV-D68 were passaged three times on mouse 3T3 and RAW cells and EV-D68 (US/MO/14-18949) was the only strain that continued to replicate in consecutive passages. Therefore, Enterovirus D68 (US/MO/14-18949) was selected for adaptation in mice. Male and female AG129 mice were obtained from a germ free breeding colony at Utah State University. AG129 mice are deficient in IFN- α/β and –γ receptors (90, 106). Four-week old, male and female mice were used to serially-passage EV-D68 in mice (86). For each passage the animals were infected intranasally with the virus. After three days lungs were from the mice and homogenized in blender bags containing 1 mL of MEM. Part of the recovered virus was titrated on human rhabdomyosarcoma cells. Part of the lung homogenate sample was pooled and used to re-infect the next group of mice. This was repeated for 30 passages. A modified CDC RT-PCR protocol was used to verify that samples from the mouse passages contained EV-D68 (13). Each mouse-passaged virus was labeled sequentially as MP1, MP2, etc.

Plaque Purification of Mouse Passage 30 (MP30pp). RD cells were seeded into 12-well microplates 24 hours prior to infection. EV-D68 MP30 was serially diluted and plated onto the 12-well microplates. The virus was incubated with cells for 1-hour p.i. The growth medium was removed and replaced with 0.6% sea plaque agarose (FMC Bioproducts, Rockland, ME USA), 2% FBS and 25mM $MgCl_2$. Cells were observed visually for plaques for 3 days p.i. Individual plaques were then picked at random and inoculated into T-25 flasks containing RD cells and growth media. Cells in T-25 flasks

were observed 2 to 3 days post plaque harvesting for CPE. The virus from the T-25 flasks showing 100% CPE was then used to repeat the plaque purification procedure three times. The resulting virus stock was labeled as MP30pp.

Mouse Passage Comparison. To show how the virus adapted to growth in the mouse over the 30 passages, five groups of mice were infected with the following mouse passages; MP0, MP10, MP20, MP30, and MP30pp along with an uninfected control group. There were 4 mice per group. Multiple tissues (lungs, liver, kidneys, spleen and whole blood) were harvested from the mice on day three p.i. and virus titers determined on RD cells (Figure 5).

Virus Titration Assay. Virus titers were determined on RD cells in 96-well microplates. Plates were seeded with cells 24 hours prior to infection and incubated at 37°C and 5% CO_2. Samples collected from mouse tissues or cell culture were serially diluted, and each 10-fold dilution added to four wells. Microplates were then incubated for 6 days at 33°C with 5% CO_2(15). Six days p.i., cells were examined visually for viral cytopathic effect. The 50% cell culture infectious doses ($CCID_{50}$) were calculated using an endpoint dilution method (101) and virus titers were expressed per mL.

Histopathology. Tissues collected from mice were sent to the Utah Veterinary Diagnostic Laboratory for evaluation by Dr. Arnaud Van Wetter, a board certified Veterinary Pathologist. For histological analyses, the left lobe of the lung, liver, and kidney were always submitted for consistency. The top half of each spleen was submitted for histological evaluation. These analyses were completed for the mouse passage comparison as well as the natural history studies.

Lung Cytokine/Chemokine Evaluations. A sample (200 µl) from each lung homogenate was tested for cytokines and chemokines using a chemiluminescent ELISA-based assay according to the manufacturer's instructions (Quansys Biosciences Q-Plex™ Array, Logan, UT). The Quansys multiplex ELISA is a quantitative test in which 16 distinct capture antibodies have been applied to each well of a 96-well plate in a defined array. Each sample supernatant was tested at 2 dilutions for the following: IL-1α, IL-1β, IL-2, IL-3, IL-4, IL-5, IL-6, IL-10, IL-12p70, IL-17, MCP-1, IFN-γ, TNFα, MIP-1α, GM-CSF, and RANTES.

Definition of abbreviations are: IL - interleukin; MCP - monocyte chemoattractant protein; IFN - interferon; TNF - tumor necrosis factor, MIP – macrophage inflammatory protein; GM-CSF - granulocyte/ macrophage colony stimulating factor; and RANTES - regulated upon activation, normal T cell expressed and secreted.

Cytokine and chemokine levels are reported in fold changes compared to levels in from uninfected control mice.

Virus Growth Curve Evaluations. The viral growth curve for EV-D68 MP0 and MP30pp was obtained on three human cell lines, RD, Hela-Ohio and A549. Multiple time points were evaluated from 6 to 72 hours p.i. at 6 hour intervals. Samples from all three cell lines were evaluated in triplicate at each time point on RD cells.

Antiviral Compounds. Enviroxime was obtained from the U.S. Army Medical Research Institute of Infectious Diseases (USAMRIID), Ft. Detrick, Frederick, MD through the NIAID antiviral screening program. Pirodavir was purchased from AdooQ Bioscience, (Irvine, CA). Pleconaril was obtained from the former Biota Pharmaceuticals

(Notting Hill, Victoria, Australia). Rupintrivir and Guanidine HCl were purchased from Sigma Aldrich (St. Louis, MO).

Ethical Treatment of Animals. This study was completed under the approval of the Institutional Animal Care and Use Committee of Utah State University. The work was performed in the AAALAC-accredited Laboratory Animal Research Center of Utah State University in accordance to the National Institutes of Health Guide for the Care and Use of Laboratory Animals (107).

Statistical Analysis. Statistical Analysis was completed using Prism 7, Graph Pad Software (San Diego, CA). For comparison of virus titers in different tissues, a one-way analysis of variance (ANOVA) was completed followed by Tukey's multiple comparison, and by two-way ANOVA for effects based on the day p.i. using Prism 7.0d. Cytokines and chemokine levels were compared by ANOVA assuming equal variance and normal distribution.

Results

Mouse Passaged Virus Comparison. A mouse passaged virus comparison was completed to determine which virus produced the highest infection and greatest disease signs for the model (Figure 5). From MP0 to MP10, there was an increase in virus recovered from the mouse lungs from $10^{5.8}$ to $10^{7.0}$ $CCID_{50}$ per mL. Between MP10 to MP30 there was smaller increase in lung virus titers to $10^{7.2}$ $CCID_{50}$ per mL. Virus titers for MP0 in liver samples were undetectable, while MP30 and MP30PP were 10 to 100-fold higher ($10^{5.5}$ and $10^{4.8}$ $CCID_{50}$ per mL) than MP10 and MP20 ($10^{3.0}$ and $10^{3.5}$ $CCID_{50}$

per mL). Kidney and spleen showed a similar increase in virus titer for higher mouse passaged virus. Virus titers in whole blood were undetectable in MP0, then increased from MP10 to MP30 from $10^{1.33}$ to $10^{2.5}$ $CCID_{50}$ per mL of virus. Viremia has also been shown in clinical patients with EV-D68 (38). This was consistent with observations of histological lesions from infected lungs showing interstitial pneumonia of various severity, suggesting exposure occurred through the blood rather than through airways. These observations are highly suggestive that blood is the route by which the virus is spreading.

Lung samples from mice infected with MP0, MP10, MP20, MP30, and MP30pp were evaluated using a panel of 16 pro-inflammatory cytokines and chemokines. Mice infected with MP0 showed similar levels of cytokines to those of the uninfected control mice. However, the pro-inflammatory cytokines MCP-1 and RANTES showed significant increases compared to uninfected mice in the groups infected with MP10, MP20, MP30 and MP30pp as virus passages continued. The mice infected with MP30 showed the highest levels of MCP-1 and RANTES. The mice infected with MP30pp also showed significantly higher levels of MCP-1 than the mice infected with MP0, MP10, and MP20. However, RANTES levels decreased with the plaque purified strain of virus compared to MP30 (see Figure 6). Pro-inflammatory cytokines from other tissues were evaluated as well, although significant differences compared to control mice were not observed.

A comparison of the histological lesions demonstrated an increase in injury to lung tissues as the virus passage number increased (Table 9). A lung injury scoring system of 1+ to 4+ was used for evaluation (“-”, or 0 = no damage, 1+ = minimal

damage, 2+ = mild damage, 3+ = moderate damage and 4+ = severe damage). All tissue samples were compared to uninfected control mice. Interstitial pneumonia in the lungs increased from MP0 to MP30. Mice infected with MP30 had interstitial pneumonia that was mild to moderate with lung scores from 2+ to 3+.

This histological lesion data show that lung injury caused by EV-D68 increased as virus was passaged and that infection with MP30 caused greater lung injury than MP10 or MP20. Even though lung virus titers, RANTES levels, and histological lesions scores appeared to be slightly lower after plaque purification of MP30, we selected MP30pp as the virus isolate for use in additional pathogenesis studies of EV-D68 in AG129 mice.

Natural History. A time course of infection for EV-D68 in AG129 mice was evaluated in lungs, liver, kidney, spleen, whole blood, leg muscle, spinal cord and brain tissues using EV-D68 MP30pp. Tissues were harvested at 8 hours and day 1, 3, 5, 7, 9 p.i. We also evaluated different infectious doses by comparing our undiluted challenge stock, $10^{6.5}$ $CCID_{50}$/mouse (group 1) to a $10^{5.5}$ $CCID_{50}$/mouse (group 2) and $10^{4.5}$ $CCID_{50}$/mouse (group 3) along with uninfected controls (group 4). Each of the different test groups included 28 mice. At each time point, four mice per group were euthanized and the tissues collected for virus titers, histological analyses and a measure of pro-inflammatory cytokines. Lungs from four mice in group 1 were euthanized at 4 hours p.i. and recovered 10^{6} $CCID_{50}$ virus per mL. By 8-hours p.i. the lung virus titers increased to $10^{7.7}$ $CCID_{50}$/mL and by 24 hours (day 1) post-virus to its peak titer at $10^{8.3}$ $CCID_{50}$/mL. The titer remained high through day 3 p.i., then started to decrease on day 5 and by day 9 were undetectable. Groups 2 and 3 showed similar virus titers to group 1, only with 10-fold less virus detected for each time point until day 3 p.i. By day 3, groups 2 and 3 had

similar lung virus titers to group 1, 10^8 $CCID_{50}$/mL and $10^{7.7}$ $CCID_{50}$/mL, respectively. After day 3, virus titers in lungs declined through day 7 and day 9 p.i. Liver, kidney, and spleen samples had titers between 10^4 to 10^5 $CCID_{50}$/mL on day 3 p.i. Virus titers in these tissues then decreased on day 5 p.i. and by day 7 p.i. viral titers were undetectable (Figure 7).

Whole blood, leg muscle, spinal cord and brain tissue was only collected from mice infected with $10^{6.5}$ $CCID_{50}$, $10^{4.5}$ $CCID_{50}$ and uninfected control mice. Virus titers in whole blood, increased rapidly and peaked on day 1, after which time the whole blood titers decreased and by day 5 were undetectable (Figure 8). In addition, virus increased rapidly in the CNS (spinal cord and brain tissues) in mice infected with $10^{6.5}$ $CCID_{50}$. Figure 8 shows the time course of infection for both challenge doses in the CNS. Virus titers in the spinal cord showed 10^3 $CCID_{50}$/mL by day 1 p.i. and maintained that level through day 5 p.i. in mice infected with $10^{6.5}$ $CCID_{50}$. Virus titers in spinal cord from mice infected with $10^{4.5}$ $CCID_{50}$ mice were undetectable on day 1 p.i., but by day 3 reached $10^{2.5}$ $CCID_{50}$/mL and peaked on day 5 p.i. at $10^{2.67}$ $CCID_{50}$/mL. Virus titers in brain tissue peaked on day 1 p.i. in mice infected with $10^{6.5}$ $CCID_{50}$ at $10^{3.5}$ $CCID_{50}$/mL and they decreased 10-fold by day 3 p.i. Titers in brain tissue from mice infected with $10^{4.5}$ $CCID_{50}$ did not peak until day 3 p.i. Both groups of infected mice had titers were almost undetectable by day 5 p.i. Figure 8 also shows virus titers from leg muscle after intranasal infection, indicating that EV-D68 infection ion the mouse becomes systemic and replicates at multiple sites. Virus titers in the blood are lower than in the other tissues evaluated and clears more rapidly, suggesting that the virus is replicating in those tissues and that the titer is not coming from any remaining blood in the tissues. In

addition, we wanted to evaluate whether the virus was gaining access to the CNS by retrograde axonal transport from peripheral nerves in the leg, so determination of virus in leg muscle was considered important to ascertain the potential of EV-D68 to cause neurological infection and lesions by this route.

Table 10 lists the histological injuries observed in lung tissues from groups 1-4, after challenge infection. Six categories of histological injury were evaluated; bronchial epithelium injury, bronchiolar epithelium injury, Alveolar wall injury, Lymphocytes around bronchioles, interstitial inflammation (perivascular and alveolar), and pulmonary edema. Alveolar wall injury and interstitial inflammation or pneumonia, are the only observations that showed any signs of injury or damage in the lungs.

On day 1 p.i., group 4 mice had an average lung score for alveolar injury of 0 to 1+ and an interstitial inflammation of 1+. Group 1 mice on day 1 p.i. had a lung score for alveolar injury of 1+ to 2+ and an interstitial inflammation score from one mouse of 2+ to 4+. These observations were consistent with the viral titer results. Both alveolar injury and interstitial inflammation reached a peak by day three p.i. for groups 1-3. The alveolar injury amongst groups 1-3 peaked between 2+ and 3+. In addition, groups 1-3 all had interstitial pneumonia scores of 2+ to 3+. Similar results were observed on day 5 p.i. for interstitial inflammation, whereas alveolar injury started to resolve. By day 7 p.i., histological lesions for both categories for all three groups began to resolve and by day 9, all lesions had resolved. The lung scores for mice in group 4 had all resolved by day 3 p.i. for all categories. When compared against sham-infected mice (group 4), there was more severe injury in mice that were infected with EV-D68. In summary, pathology was seen in lungs and was similar across the different virus inoculums.

Samples from liver, kidney and spleen were also evaluated, but histological lesions were not observed (data not shown). The entire spinal cord, brain and leg muscle tissue sample from groups 1 and 3 were used to obtain virus titers, therefore these samples were not evaluated by histology.

Pro-inflammatory cytokines were determined in lung samples after infection. MCP-1 and RANTES (a chemokine) had significant increases on day 3 p.i. compared with uninfected control (Figure 10), similar to observations in the mouse passage study (Figure 6). However, the largest increase in cytokine levels was observed on day 1 p.i. This rapid response is characteristic of EV-D68 infections and has also been described by M. C. Patel, et al. (16). On day 1 p.i., MCP-1 from group 1 mice increased about 50-fold compared to the vehicle control mice (Figure 10). RANTES from group 1 mice also showed a 9-fold increase on day 1, 3 and 5 p.i. compared to controls. Other pro-inflammatory cytokines also had significant increases on day 1. IL-6 had the most significant response, with a 150-fold increase compared to controls. In addition, IL-1α, Il-1β, IL-5, and TNFα had 10 to 20-fold increases compared to the control group (Figure 9). Other cytokines that showed a significant increase on day 1 included: IL-2, IL-3, Il-4, IL-10, IL-12p70, IFNγ, and GM-CSF (see supplemental information). Some of these (IL-2, IL-4 and GM-CSF) showed significant increases on day 5 p.i. as well. MIP-1α showed significant increase at eight hours p.i. and day 3 p.i. (Figure 10).

Comparison of *In Vitro* Viral Replication Curves. An *in vitro* replication curve of EV-D68 MP0, MP30 and MP30PP was completed on three cell lines: RD, Hela-Ohio, and A549 cells. After infection, samples were collected from each culture at 6, 12, 18, 24, 30, 36, 42, 48, 54, 60, 66 and 72 hours and are shown in Figure 11. Growth curves

were done in triplicate. In all three-cell lines MP30 and MP30pp started to replicate sooner, as determined by the earlier increase in virus titer than did MP0. The virus titers were also higher in MP30pp than in MP0 in the Hela-Ohio and A549 cells at each time point. After 54 hours, RD cells infected with MP30 and MP30pp showed declines in virus titer. RD cells infected with MP30 and MP30pp reached 100 percent cytopathic effect (CPE) by 72 hours p.i., and represent the last time point taken for RD cells. Because of this, Figure 11 shows MP0 titers reaching the same point as those for MP30 and MP30pp by 72 hours. The passaging of EV-D68 in mice appears to have improved the ability of the virus to replicate in cell culture, especially in RD cells.

Comparison of Routes of Infection. Multiple routes of infection were evaluated for efficacy in AG129 mouse infection; intrathecal (i.t.), intravenous (i.v.), intraperitoneal (i.p.), retro orbital (r.o.), intramuscular (i.m.), intracranial (i.c.) and intrasiatic notch (i.s.). Samples from multiple tissues were collected during mouse passaging of the virus and titers were evaluated. Most of the alternative routes of infection did not show any viral titer in the lungs or other tissues. Infection by the r.o. and i.v. routes showed minimal amounts of virus in lungs, kidney and liver tissue (data not shown). This verified that the intranasal route of infection provided the optimum route for a disease model. This is also the most clinically relevant route to EV-D68 infections in humans leading to a respiratory tract infection.

RT-PCR Verification of Mouse Passaged Virus. Viral RNA from mouse lungs infected with EV-D68 was extracted using the Qiagen AMP Viral RNA mini kit. RNA samples (60μL) from each of the EV-D68 mouse passages, MP0, MP10, MP20, MP30 and MP30pp were evaluated. The RT-PCR protocol, primers, probe and cycle

parameters used for analyses were adapted from T. N. Wylie, et al. (13). Primers and probes are specific for EV-D68, therefore, enterovirus 71 (EV-71) RNA was used as a negative control. Alternatively, RNA samples were evaluated using a protocol for identification of EV-71 from the Center for Disease Control with primers and probe specific for EV71(107). Using the EV-D68 protocol, all five mouse passage variants of EV-D68 were confirmed as EV-D68 and the EV-71 RNA was negative. Primers used were; CACTGAACCAGAAGAAGCCA (forward), CCAAAGCTGCTCTACT-GAGAAA (reverse) and TCGCACAGTGATAAATCAGCACGG (probe).

***In Vitro* Antiviral Comparison.** The in vitro comparison of EV-D68 MP0, MP30PP and rhinovirus 14 (RV-14) was completed to show that the mouse model developed for EV-D68 may also be applicable for rhinoviruses. This study evaluated multiple compounds that are known inhibitors of EV-D68 (15). Table 11 shows the antiviral comparison in vitro. Rupintrivir showed the most activity against all 3 virus strains. Enviroxime and pleconaril also showed high activity against these viruses. Guanidine, a known inhibitor of poliovirus (83), was tested previously by D. F. Smee, et al. (15) against EV-D68. It exhibited activity with a 50% effective concentration (EC_{50}) of 44.7 ± 11.9 and 61.0 ± 10.5 with an SI of 31.7 and 23.2 against EV-D68 MP0 and MP30pp. Against rhinovirus-14, guanidine had an EC_{50} of 80.7 ± 16.2 and an SI of 37.6. From these results, it appears that compounds active against rhinovirus are also active against EV-D68, lending credence to the hypothesis that this mouse model could be used to evaluate antiviral compounds against rhinoviruses using this EV-D68 mouse model.

Discussion

Because of the recent increase in clinical cases of EV-D68 infection, along with the neurological disease and fatalities, the significance of this virus has increased. Many studies have evaluated the efficacy of antiviral therapies such as rupintrivir, ribavirin, pleconaril and others *in vitro* (15, 37, 67). However as of yet, the only treatments available are supportive. During the 2014 outbreak of EV-D68 most of the patients presented with severe asthma-like symptoms. In at least two locations these patients were given albuterol and other bronchodilators to help with breathing, and in both locations, there were smaller numbers of patients that required ventilation and intensive care management (4, 63). However, these treatment regimens are for the respiratory symptoms of EV-D68 disease and have no effect on acute flaccid paralysis. Therefore, there is need for development of antiviral therapy that can prevent both the respiratory and neurological disease signs associated with EV-D68.

To aid in the development of antiviral therapies and vaccines for EV-D68, development of an animal model is critical. Recently, three animal models have been developed. The first model in adult cotton rats (16) takes advantage of the abundance of α2,6 linked sialic acid receptors in the cotton rats respiratory system. In this model, using non-adapted EV-D68, M. C. Patel, et al. (16) showed a "mild cumulative pathology" in the lungs (16). In addition, MCP-1 peaks at 4-hours post-virus exposure of the VANBT/1 strain of EV-D68 (16). After this initial peak, the cytokine levels decreased rapidly. Other cytokines were also shown to rise to a peak and then fall off rapidly at different time points.

A second model has been developed in neonatal Swiss-Webster mice (17). In this model, the authors were able to induce limb paralysis and death in two day-old mouse pups by intracerebral injection of virus using 5 different strains of EV-D68. This model provided evidence that EV-D68 does cause neurological disease. In addition, A. M. Hixon, et al. (17) demonstrated that serum containing EV-D68 antibodies was able to confer immunity to mice when the mice were treated with the antibody serum 1 day prior to infection (17).

The third model, developed in ferrets, evaluated the Fermon strain of EV-D68 in feces, nasal washes, throat swabs, blood, lymph node and lungs. Detectable levels of EV-D68 were observed in all of these tissues (108). The ferrets were infected via intranasal infection and virus was quantified in tissues by qPCR. These authors demonstrated that EV-D68 causes a lower respiratory infection by histological analysis, in which no pathological changes were observed in the trachea while "remarkable pathogenesis" was seen in the lower respiratory tract (121).

In our model, we demonstrate an increased ability of mouse-adapted virus to infect 4-week old (juvenile) AG129 mice. By using juvenile mice, this model replicates more closely what is seen in the human population since the majority of cases are in patients that are young children to teenagers (4, 10, 29, 63, 109, 110). Yet this median age is also beneficial because EV-D68 has also been shown to cause disease and even fatalities in adults (32-34). This model shows how rapidly the virus can cause injury in mouse lungs, along with the rapid spread of virus from lungs to the blood and then to other tissues in the mouse. These results are consistent with reports that most patients were sick 1.5 to 2 days before being taken to the hospital and or treatment clinic (4, 36,

63). Also of note, the longest average stay for patients in the hospital was 4.75 days (62). This suggests that an uncomplicated EV-D68 infection replicates and spreads rapidly, and then resolves in about one week. However, it is not known how long neurological signs take to resolve in patients with neurological disease.

This model is also more convenient than previously described models, since one model requires of cotton rats which are hard to work with as well as a lack of reagents compared to mice, another model is in neonatal mice which is not convenient, and the ferret model is costly and not available in many labs.

The data in this study shows that virus from a respiratory tract infection can leave the lungs and enter the bloodstream. Then resulting viremia then spreads the virus to other tissues in the mouse, including the CNS, suggesting that EV-D68 is capable of causing neurological disease along with the respiratory disease.

Conclusion

This model of EV-D68 infection in 4-week-old AG129 mice has the potential for use in evaluating experimental therapies and vaccines. In addition, this model has well-established viral endpoints and a clinical profile that can be used to evaluate amelioration of clinical disease parameters. Antivirals can also be assessed on their ability to protect the CNS from virus spread, thus possibly providing therapies to prevent and protect against both EV-D68 respiratory and neurological disease.

Acknowledgments

This work was completed at the Institute for Antiviral Research at Utah State University. A special thanks to Craig W. Day Ph.D. for his efforts in editing and review of the manuscript. Funding for the project was provided by contract number HHSN2722010000391 from the Virology Branch, DMID, NIAID, NIH.

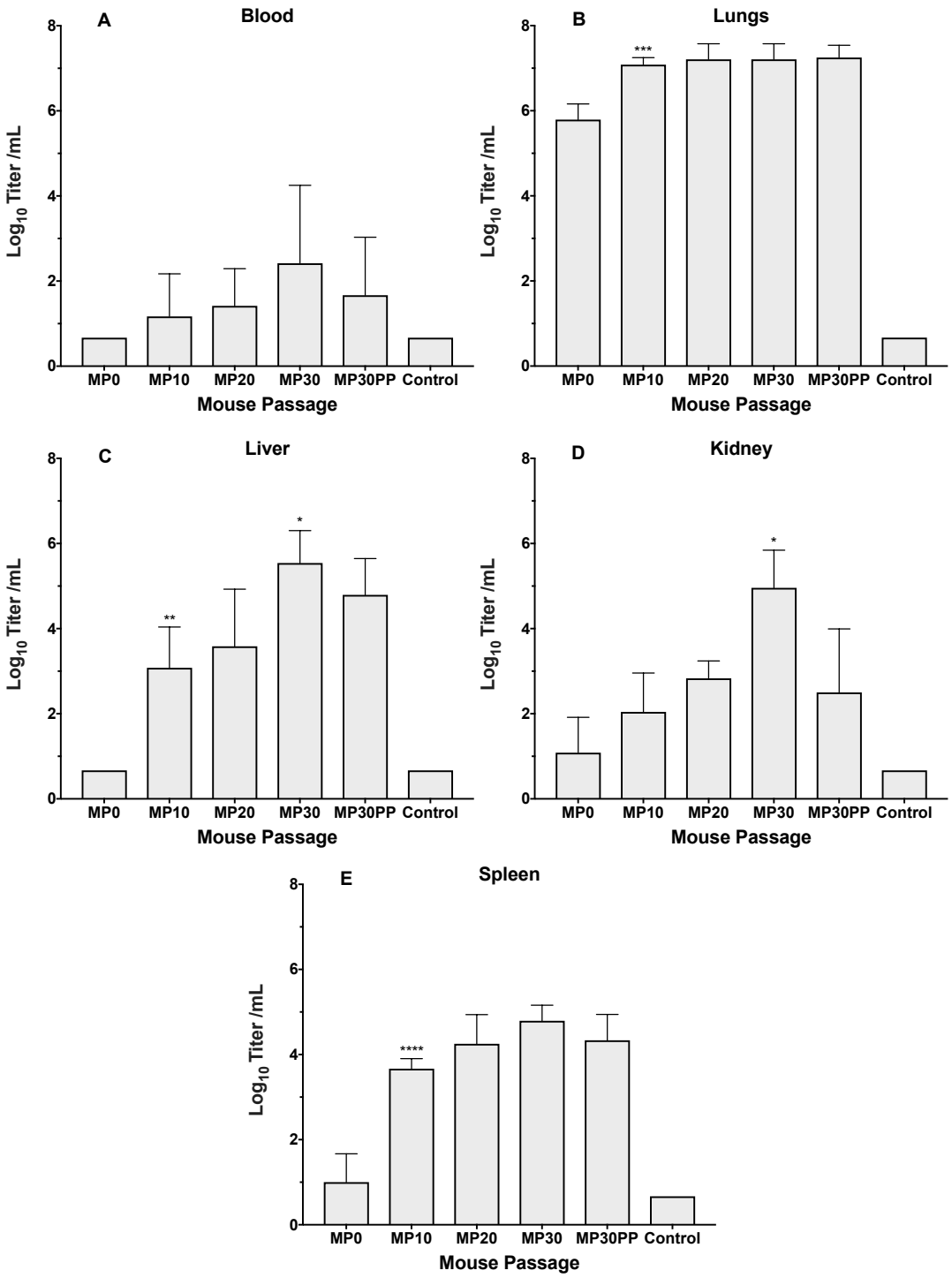

Figure 5 EV-D68 Virus titers in blood, lungs, liver, kidney and spleen after various passages through Ag129 mice. Significance is shown by comparison against the previous passage. MP30 showed similar significance against MP20 and MP30pp in kidney tissue. *P <0.05, **P <0.01, ***P <0.001, ****P<0.0001.

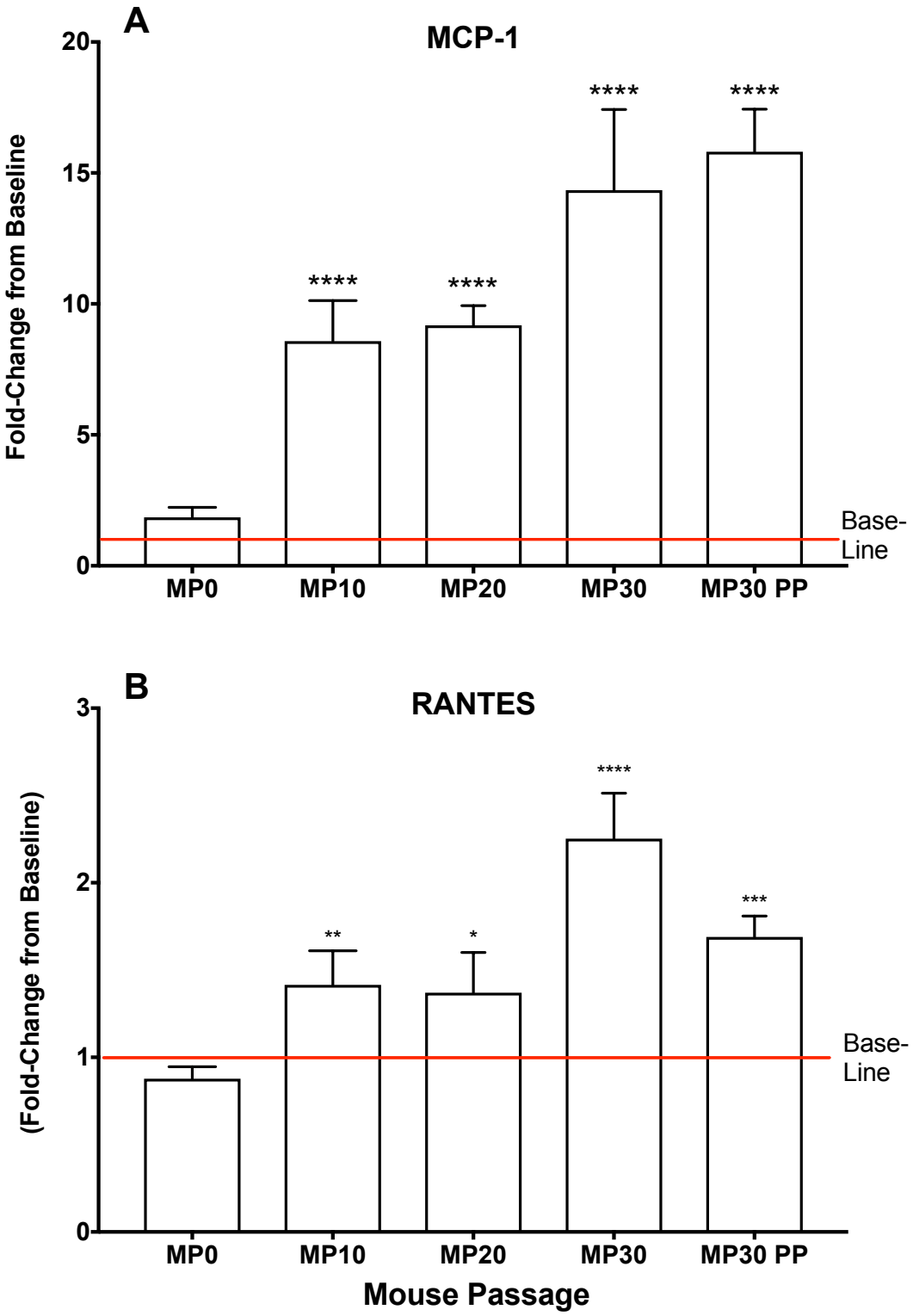

Figure 6 MCP-1 and RANTES in lung samples after infection with mouse-adapted EV-D68. MCP-1 showed the greatest change compared to the uninfected mice as virus-adaptation increased. The lung samples were collected from mice on day 3 post-virus exposure. *P <0.05, **P <0.01, ***P <0.001, ****P<0.0001.

Table 9 Comparison of histological injury in lungs after infection with different virus passages of mouse-adapted EV-D68.

EVD68 Mouse Passage	Bronchial Epithelium Injury	Bronchiolar Epithelium Injury	Interstitial Inflammation (Perivascular and Alveolar)
MP0	-	-	-
	-	-	++
	-	-	+
	-	-	+
MP10	-	-	++
	-	-	++
	-	-	++
	-	-	++
MP20	-	-	++ to +++
	-	-	++ to +++
	-	-	++ to +++
	-	-	++ to +++
MP30	-	-	+++
	-	-	++
	-	-	+++
	-	-	+++
MP30pp	-	-	++ to +++
	-	-	++ to +++
	-	-	++
	-	-	++
Uninfected	-	-	-
	-	-	-
	-	-	-

An injury scoring system of 0 (-) to 4 (++++) was used for evaluation. A score of - = no damage, + = minimal damage, ++ = mild damage, +++ = moderate damage and ++++ = severe damage. All samples were compared to uninfected control mice for each day.

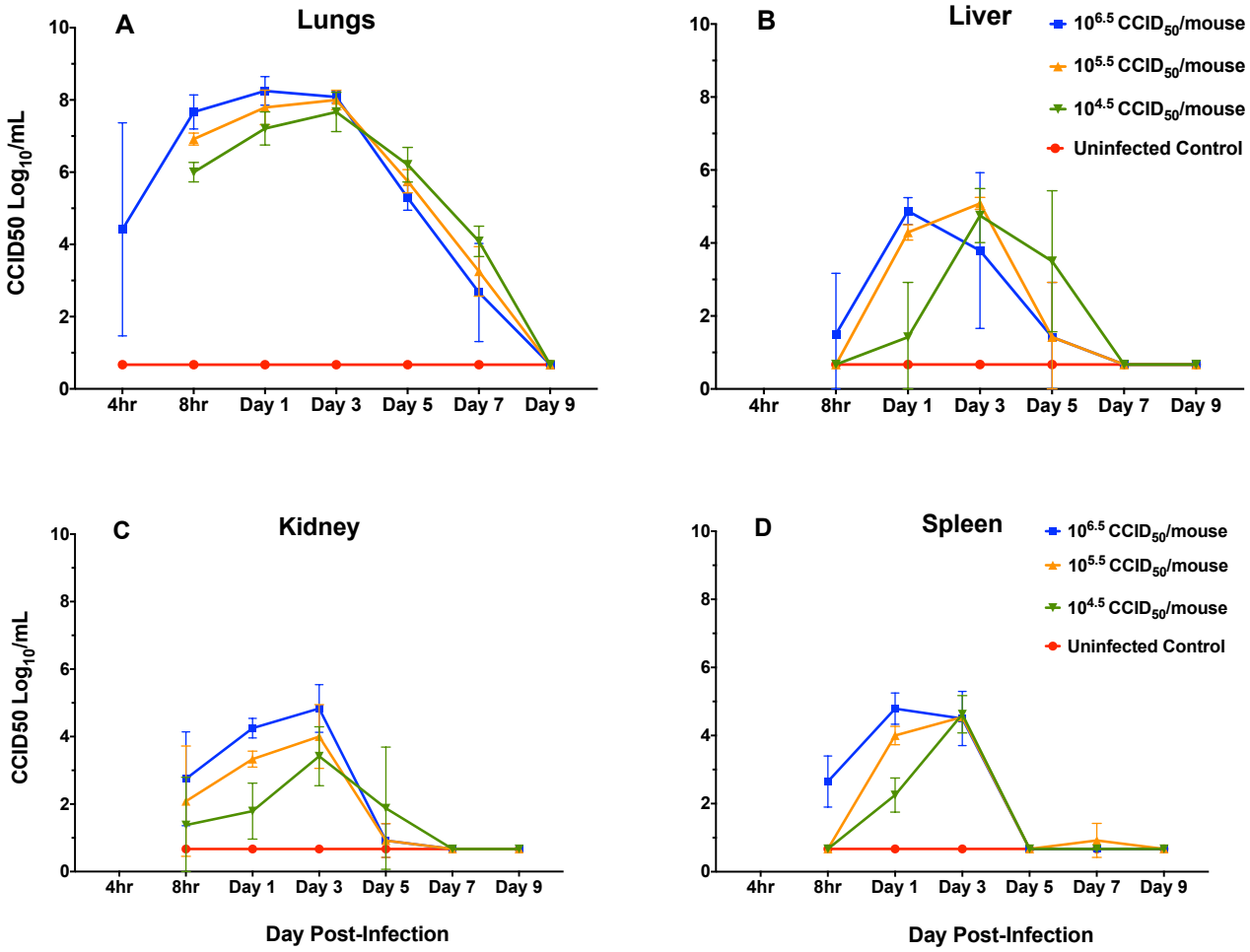

Figure 7 Time course of infection for EV-D68 MP30pp in lungs, liver, kidney and spleen. Three infectious doses and one group of infection medium were evaluated at six time points.

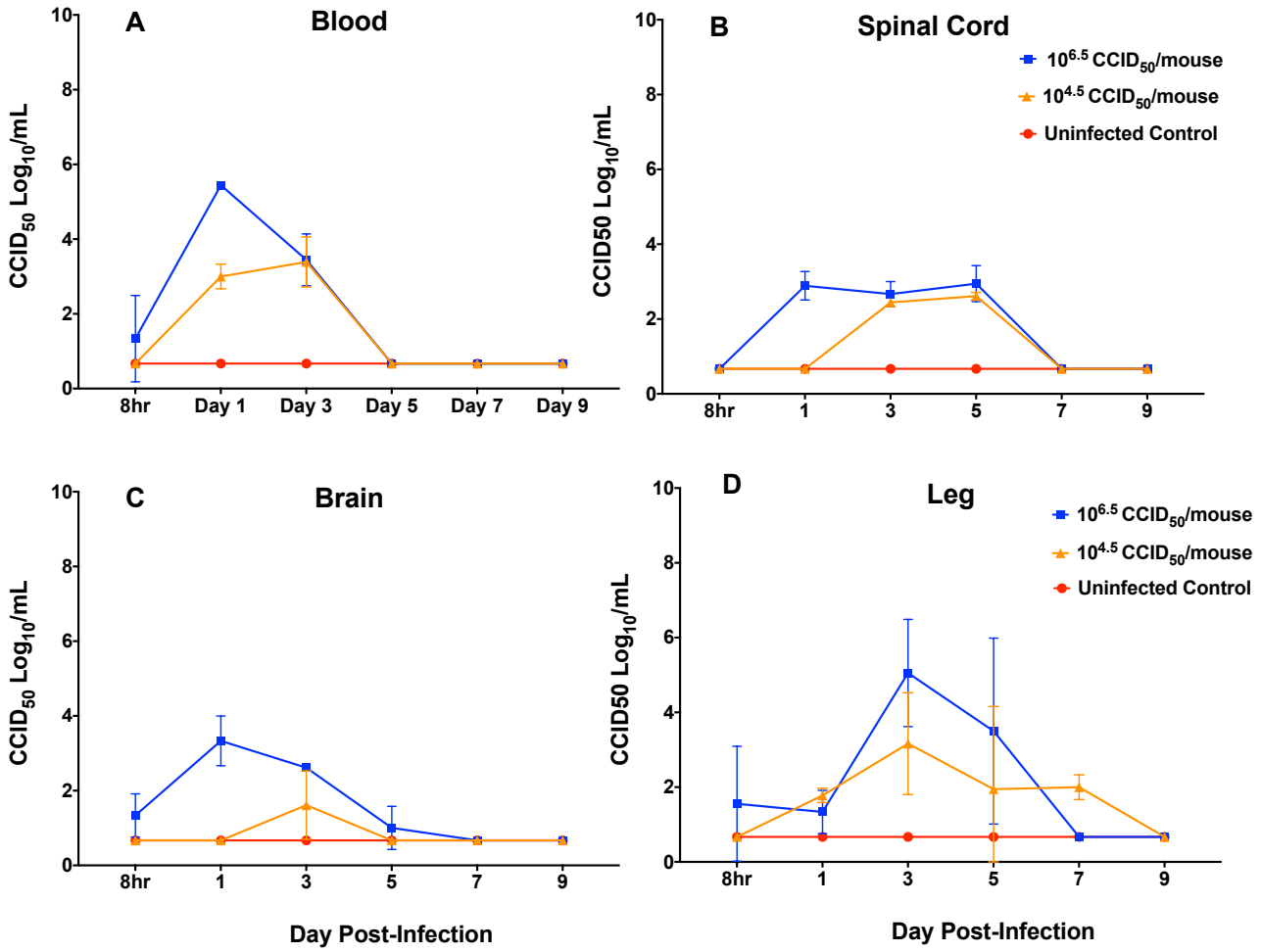

Figure 8 Time course of infection for EV-D68 MP30pp in blood, spinal cord, brain and leg muscle. Two infectious doses and one group of infection medium were evaluated at six time points.

Table 10 Time course of histological lesions in lungs after infection with various inoculum levels of EV-D68 MP30 virus.

EV-D68 INOCULUM PER MOUSE	Day of Harvest	Bronchial & Bronchiolar epithelium injury	Alveolar wall injury	Lymphocyte around bronchioles	Interstitial inflammation (perivascular and alveolar)	Pulmonary edema
$10^{6.5}$	Day 1	-	++	-	+++	-
		-	+	-	++	-
		-	++	-	+++/++++	-
Vehicle Control	Day 1	-	+	-	+	-
		-	-	-	+	-
		-	+	-	+	-
		-	-	-	+	-
$10^{6.5}$	Day 3	-	++	-	+++	-
		-	++	-	+++	-
		-	++	-	++/+++	-
		-	++	-	++/+++	-
$10^{5.5}$	Day 3	-	++/+++	-	++/+++	-
		-	++	-	++/+++	-
		-	++	-	++/+++	-
		-	++	-	++/+++	-
$10^{4.5}$	Day 3	-	++	-	++/+++	-
		-	++	-	++/+++	-
		-	++	-	++/+++	-
		-	++	-	+++	-
$10^{6.5}$	Day 5	-	+	-	++	-
		-	++	-	++/+++	-
		-	++	-	++/+++	-
		-	+	-	++	-
$10^{5.5}$	Day 5	-	+	-	++	-
		-	++	-	++/+++	-
		-	++	-	++/+++	-
		-	++	-	++/+++	-
$10^{4.5}$	Day 5	-	++	-	++	-
		-	+	-	++	-
		-	+	-	++	-
		-	++	-	+++	-
$10^{6.5}$	Day 7	-	-	-	-	-
		-	+++	-	+++/++++	-
		-	+	-	++	-
		-	+	-	++	-
$10^{5.5}$	Day 7	-	+	-	++/+++	-
		-	+	-	++	-
		-	+	-	++/+++	-
		-	+	-	++	-
$10^{4.5}$	Day 7	-	+	-	++/+++	-
		-	+	-	++	-
		-	+	-	++/+++	-
		-	+	-	++	-
$10^{6.5}$	Day 9	-	+	-	++	-
		-	-	-	+	-
		-	+	-	++	-
		-	-	-	+	-
$10^{5.5}$	Day 9	-	-	-	+	-
		-	-	-	+	-
		-	-	-	+	-
		-	-	-	+	-
$10^{4.5}$	Day 9	-	+	-	++	-
		-	+	-	++	-
		-	-	-	+	-
		-	+	-	++	-

Note: vehicle control had not pathology after day-1.

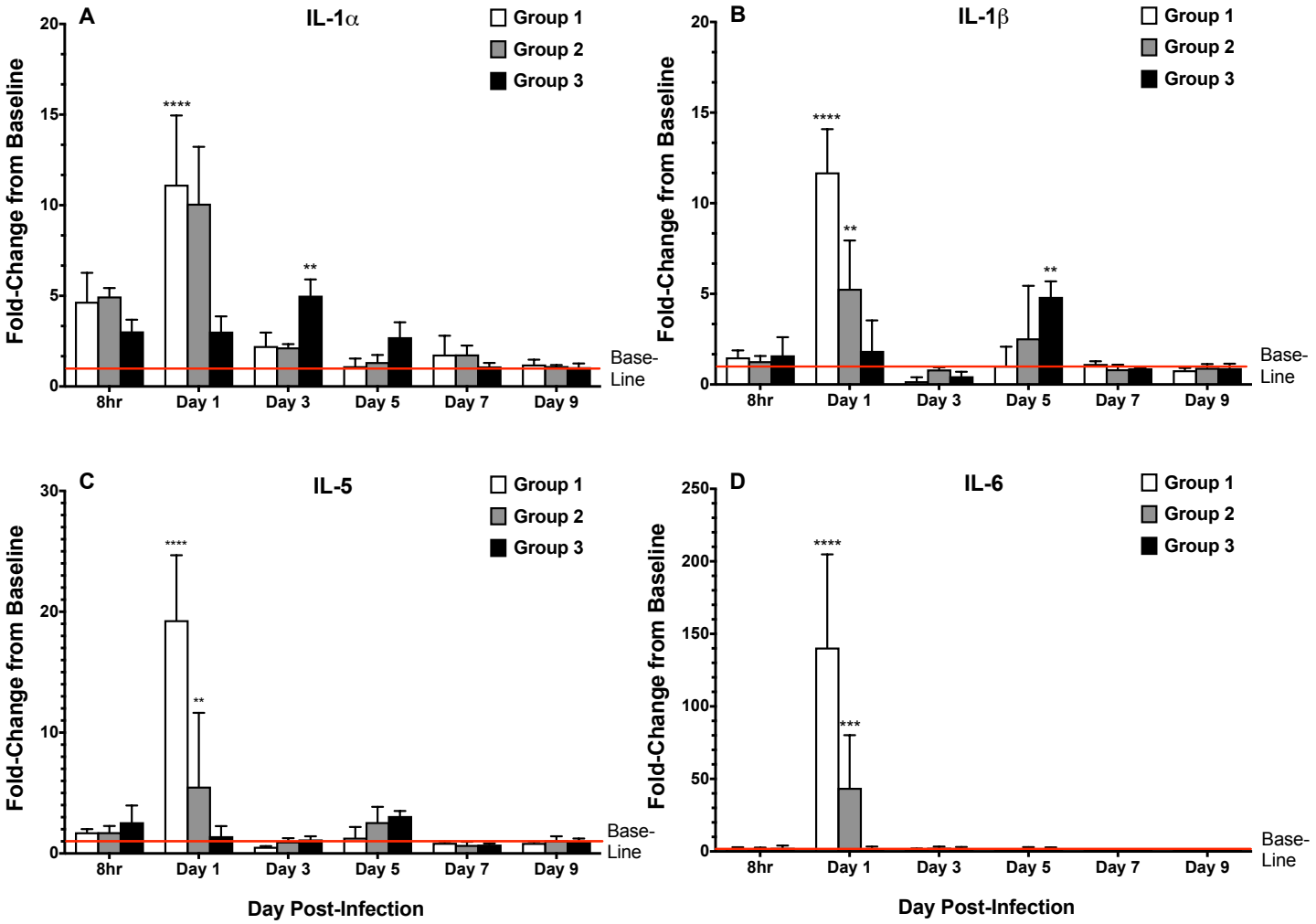

Figure 9 Time Course of IL-1α, IL-1β, IL-5, IL-6 in Lungs. Pro-Inflammatory cytokines from lung samples taken from EV-D68-infected mice harvested on multiple days p.i. were compared to uninfected control mice. Group 1 =$10^{6.5}$ $CCID_{50}$/mouse, group 2 = $10^{4.5}$ $CCID_{50}$/mouse and group 3 = infection medium control. *P <0.05, **P <0.01, ***P <0.001, ****P<0.0001.

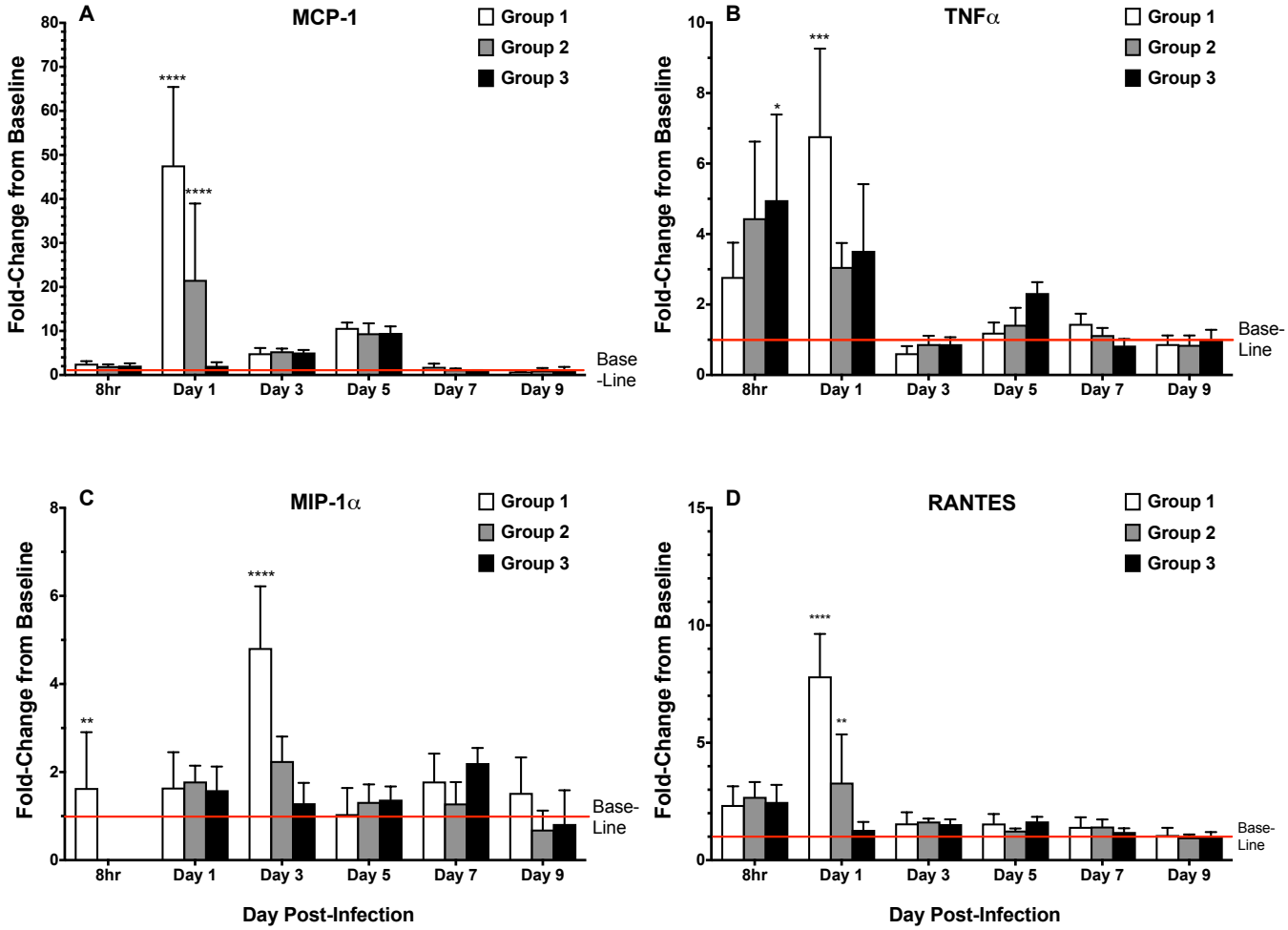

Figure 10 Time course of MCP-1, TNFα, MIP-1α, RANTES in Lungs. Pro-Inflammatory cytokines and chemokines from lung samples taken from mice infected with EV-D68 on multiple days p.i. were compared to uninfected control mice. Pro-inflammatory chemokines, RANTES, showed a significant difference compared to the control through day 7 p.i.. *P <0.05, **P <0.01, ***P <0.001, ****P<0.0001. Group 1 =$10^{6.5}$ $CCID_{50}$/mouse, group 2 = $10^{4.5}$ $CCID_{50}$/mouse and group 3 = infection medium control.

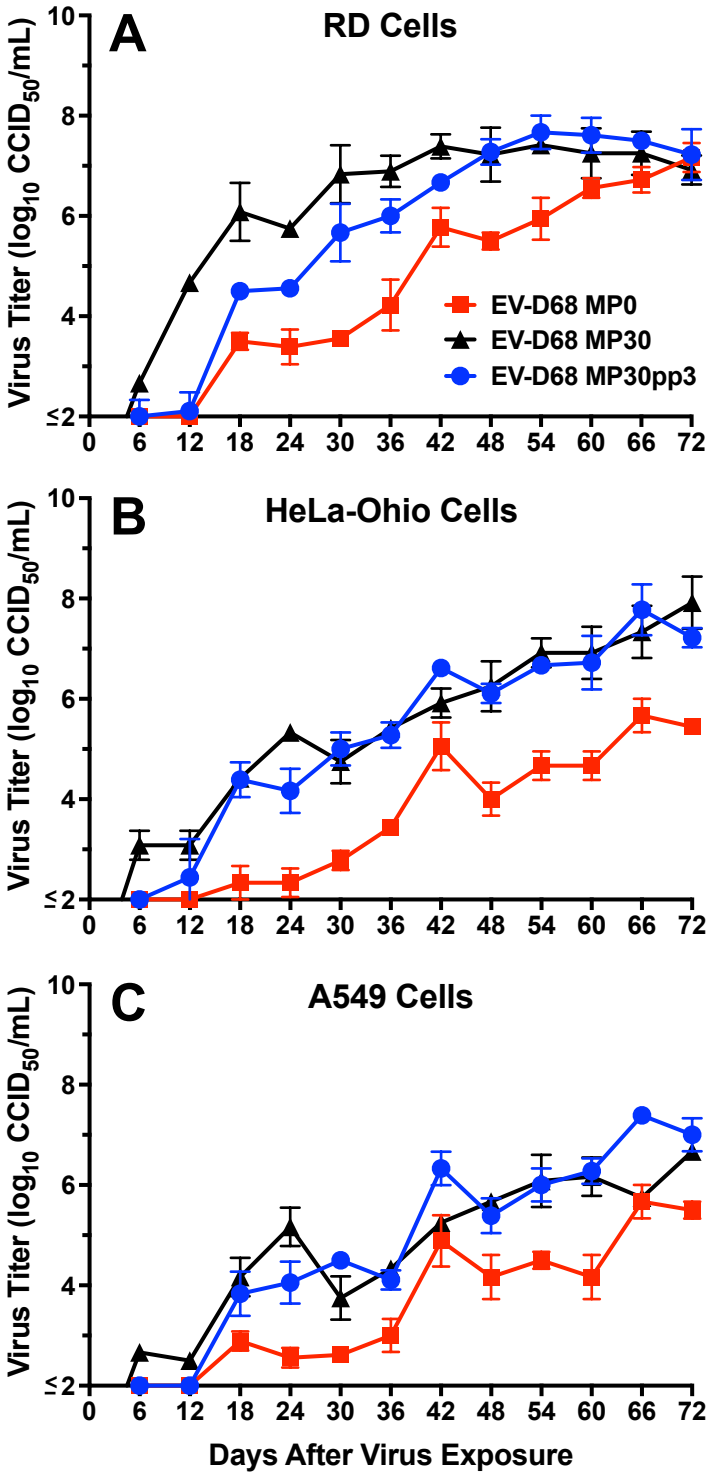

Figure 11 Viral Replication Curve *In Vitro*. Comparison between enterovirus D68 MP0, MP30, and MP30pp on 3 different cell lines; RD, Hela-Ohio and A549. Each time point represents the average of 3 independent experiments.

Table 11 In Vitro Antiviral Comparison of EV-D68 MP0, MP30pp and rhinovirus-14.

Compound	CC_{50}[a]		EV-D68/Missouri (MP0)		EV-D68/Missouri (MP30PP)		Rhinovirus-14	
	RD	Hela-Ohio	EC_{50}[b]	SI[c]	EC_{50}[b]	SI[c]	EC_{50}[b]	SI[c]
Enviroxime	14.1 ± 4.8	22.3 ± 9.7	0.03 ± 0.0	469	0.07 ± 0.03	201	0.13 ± 0.1	108
Pleconaril	10.5 ± 3.5	4.7 ± 2.3	0.08 ± 0.0	131	0.08 ± 0.00	131	0.08 ± 0.0	59.1
Guanidine HCl	1420 ± 315	3030 ± 577	44.7 ± 11.9	31.7	61.0 ± 10.5	23.3	80.7 ± 16.2	37.6
Rupintrivir	>1.0 ± 0.0	>1.0 ± 0.0	0.0003±0.0	>3333	0.0004 ± 0.0001	>2500	0.003 ± 0.0004	>333

Units are μM

[a]50% cytotoxic concentration (CC_{50}) ± standard deviation from 3 independent determinations.

[b]50% effective virus-inhibitory concentration ± standard deviation from 3 independent determinations.

[c]SI-Selectivity Index = CC_{50} / EC_{50} using the CC50 in RD cells.

Enterovirus D68 tested on RD cells, Rhinovirus-14 tested on Hela-Ohio cells.

Supplemental Information

Comparison of Pro-Inflammatory Cytokines and Chemokines. IL-1α, IL-1β, IL-2, IL-3, IL-4, IL-5, IL-6, IL-10, IL-12p70, IL-17, IFNγ, TNFα, MIP-1α and GM-CSF were evaluated by Quansys 16-plex array (Logan, Utah). IL-1α, IL-1β, IL-6, MIP-1α and GM-CSF did not show an increase as the mouse passage number increased (see Figure 12-15).

Time Course for Pro-Inflammatory Cytokines and Chemokines after infection. Pro-inflammatory cytokines IL-2, IL-3, IL-4, IL-10, IL-12p70, IFNγ and GM-CSF all showed between a 2 to 5-fold increase in cytokine levels during day 1 p.i. in group 1. It is characteristic of the virus to show a rapid time course of infection. After day 1 p.i., most of these cytokines decreased to levels similar to the uninfected control group with few exceptions (IL-2, IL-4 and GM-CSF) that showed significance on day 5 as well (see Figure 16-17).

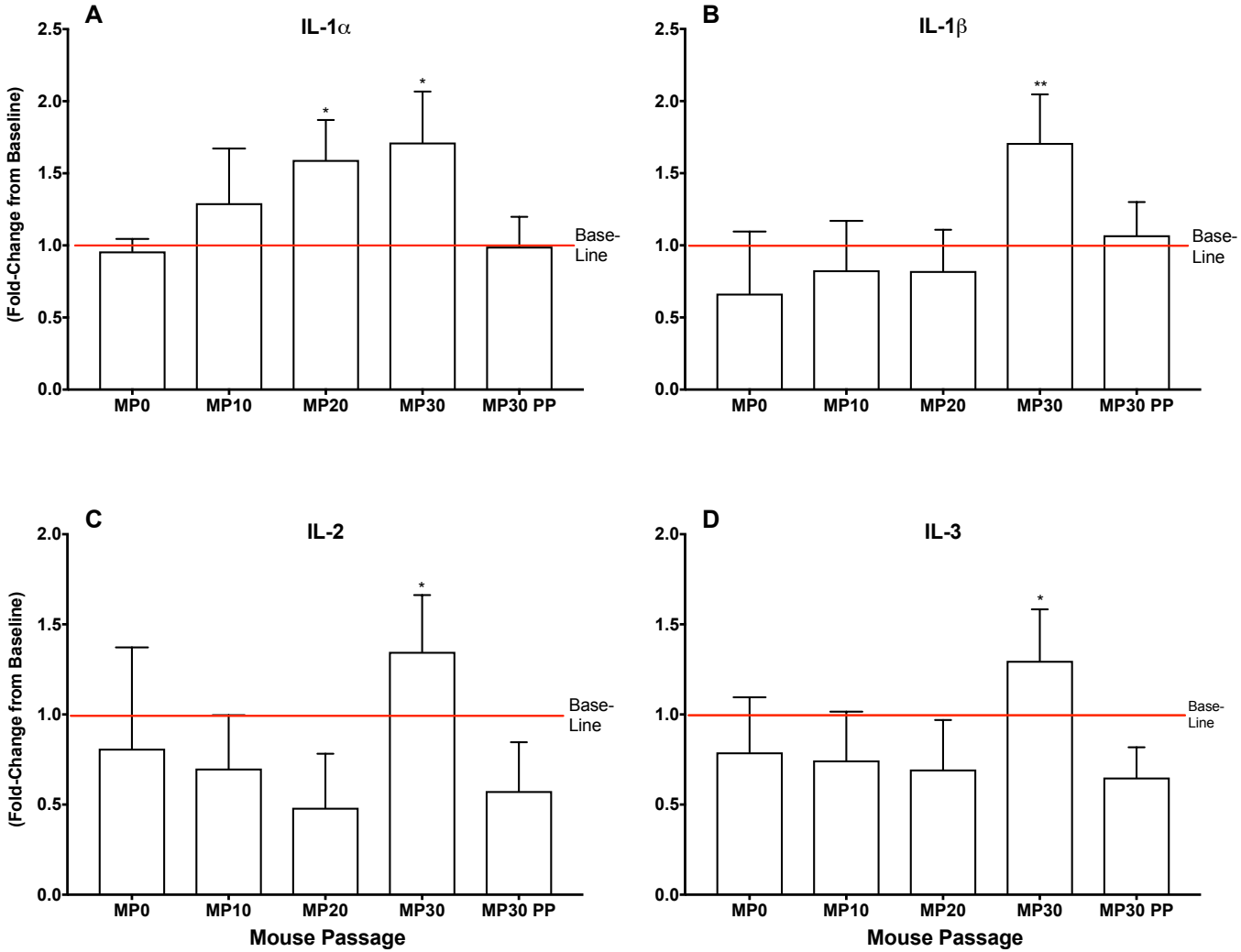

Figure 12 IL-1a, IL-1β, IL-2, IL-3 in lung samples after infection with various passages of mouse-adapted EV-D68. The statistics shown are all compared to the baseline. *P <0.05, **P <0.01, ***P <0.001, ****P<0.0001.

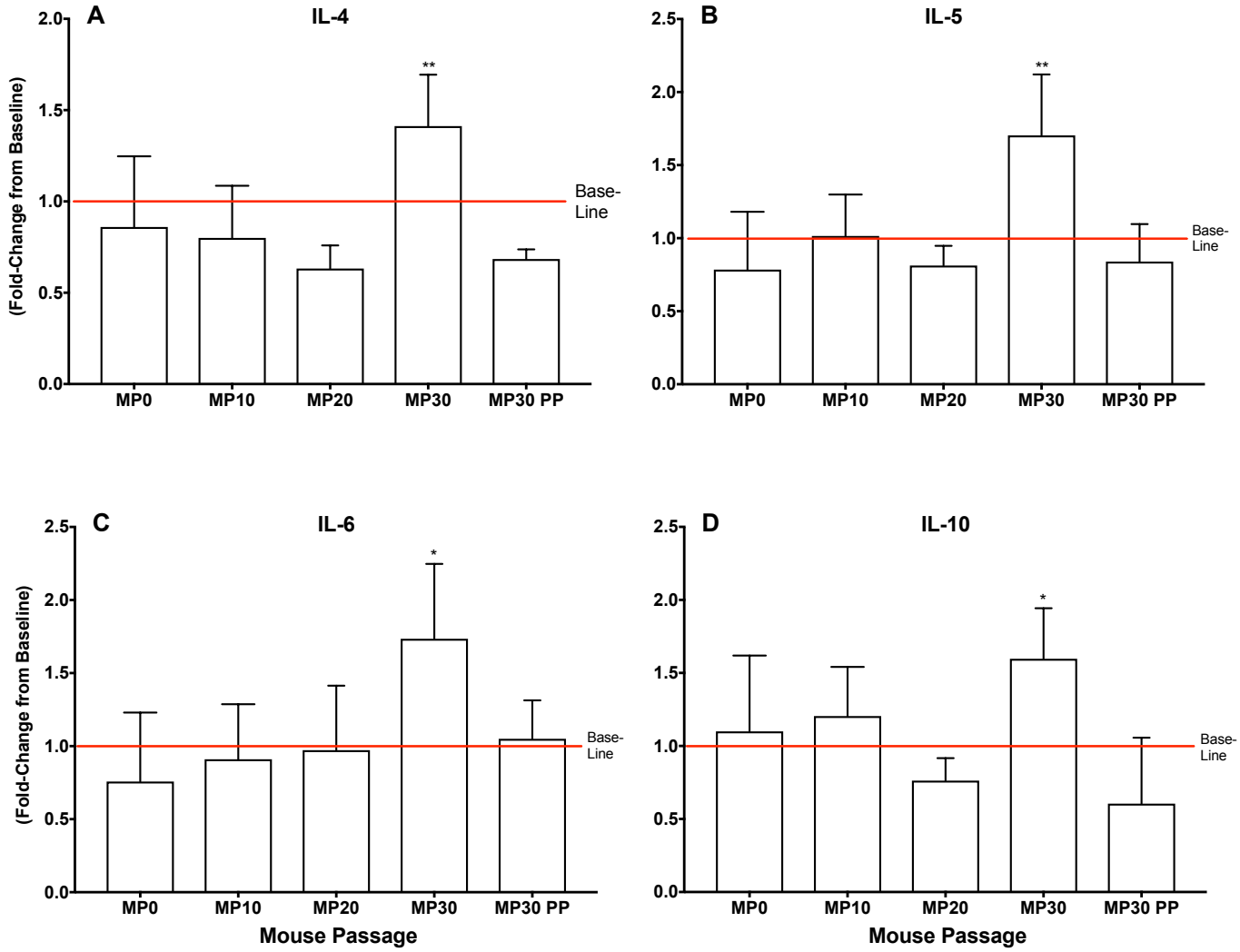

Figure 13 IL-4, IL-5, IL-6, IL-10 in lung samples after infection with various passages of mouse-adapted EV-D68. The statistics shown are all compared to the Base Line. *P <0.05, **P <0.01, ***P <0.001, ****P<0.0001.

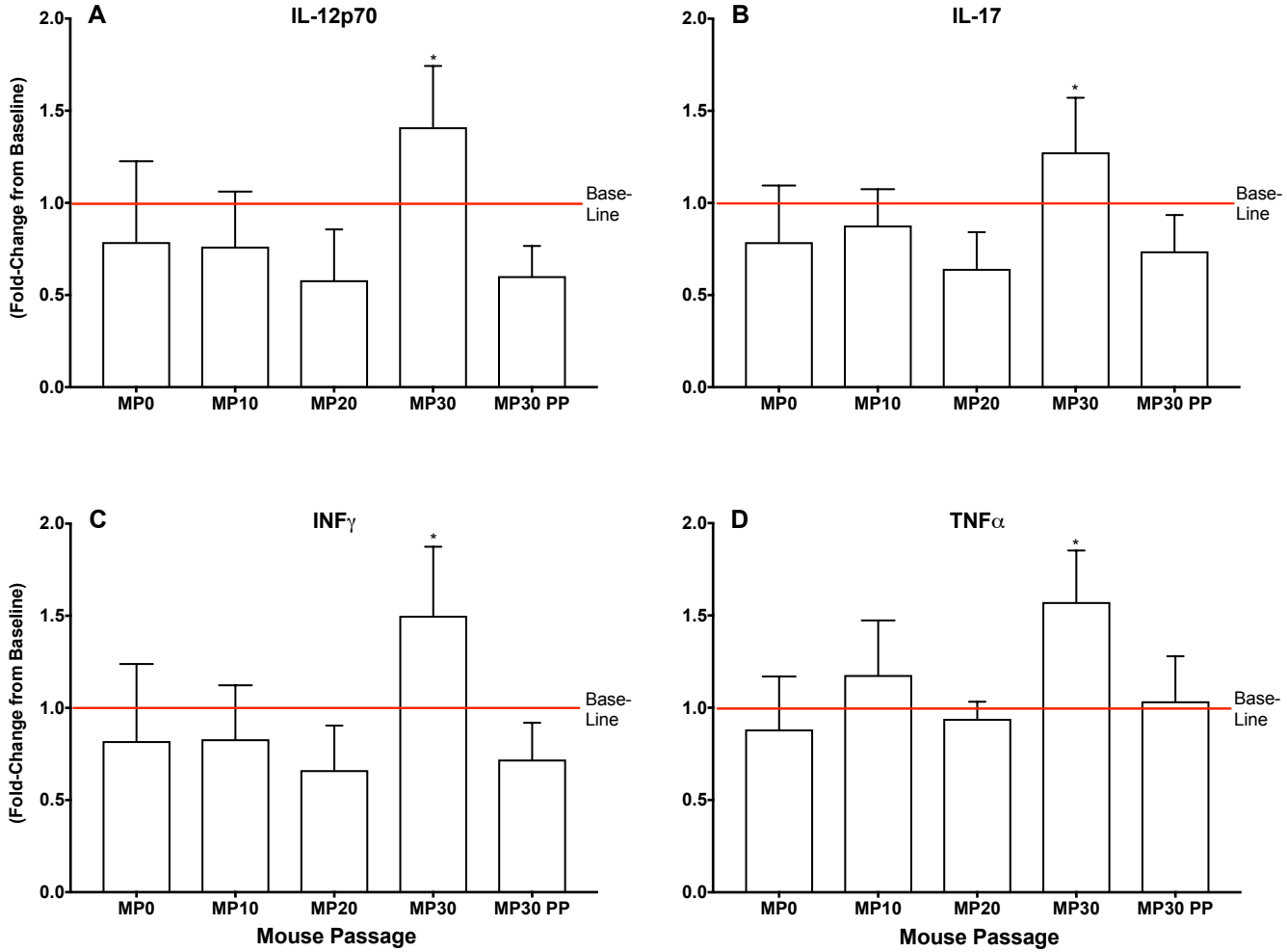

Figure 14 IL-12p70, IL-17, INF, IL-10 in lung samples after infection with various passages of mouse-adapted EV-D68. The statistics shown are all compared to the Base Line. *P <0.05, **P <0.01, ***P <0.001, ****P<0.0001.

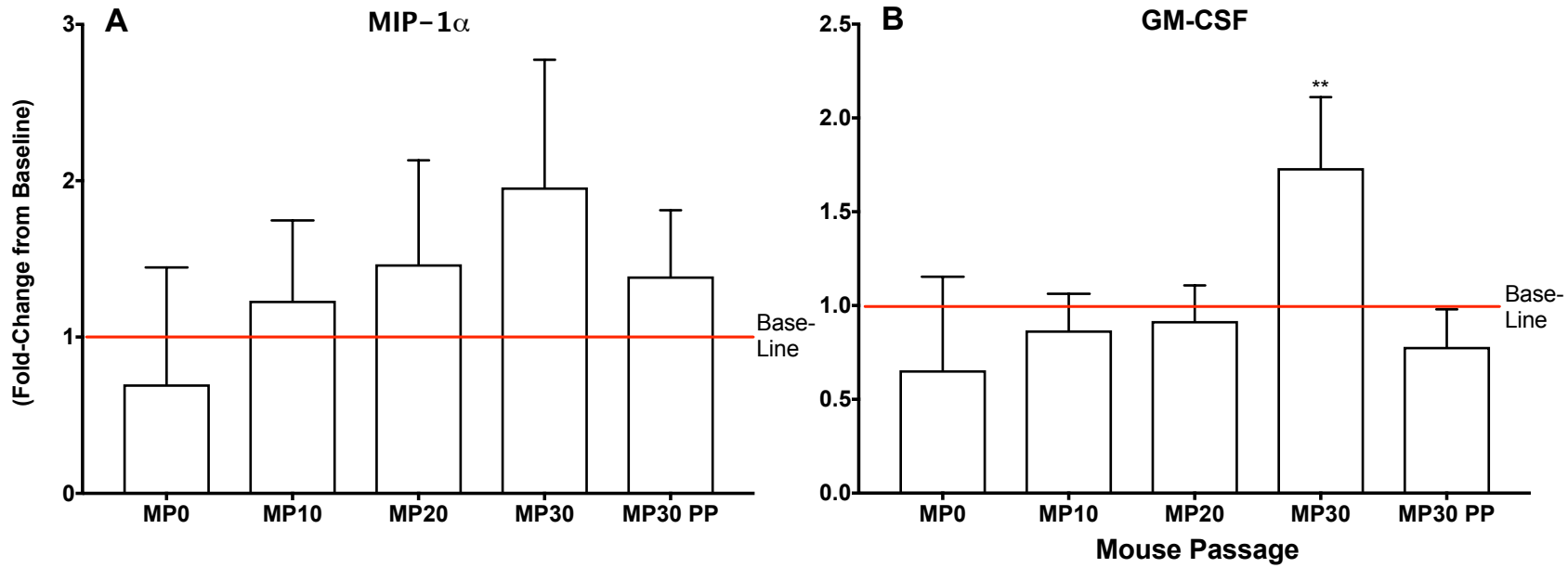

Figure 15 MIP-1α and GM-CSF in lung samples after infection with various passages of mouse-adapted EV-D68. The statistics shown are all compared to the Base Line. *P <0.05, **P <0.01, ***P <0.001, ****P<0.0001.

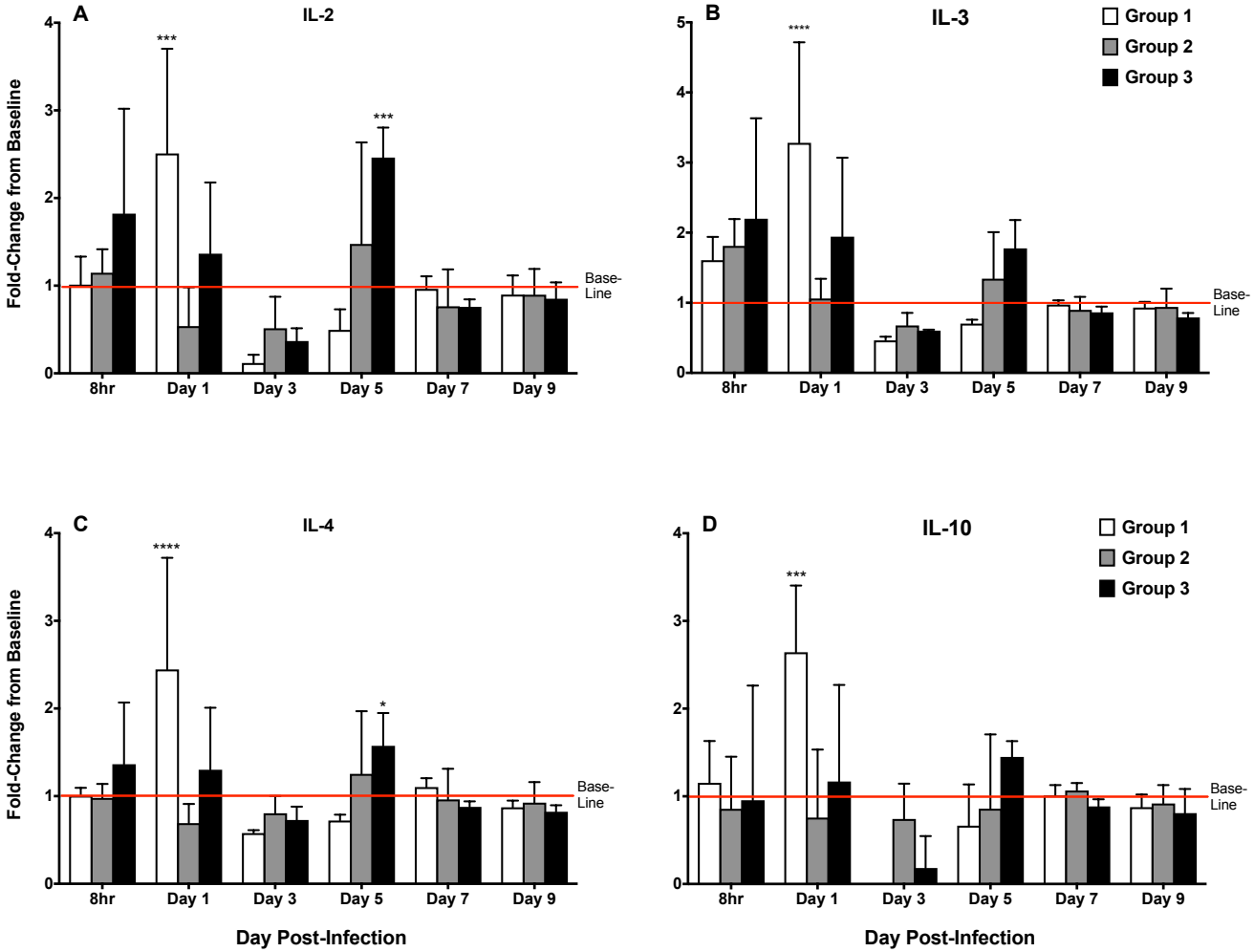

Figure 16 IL-2, IL-3, IL-4, IL-10 levels in lung samples after infection with MP30pp mouse-adapted EV-D68. All cytokines showed significant increases on day 1 p.i. compared to baseline. *P <0.05, **P <0.01, ***P <0.001, ****P<0.0001.

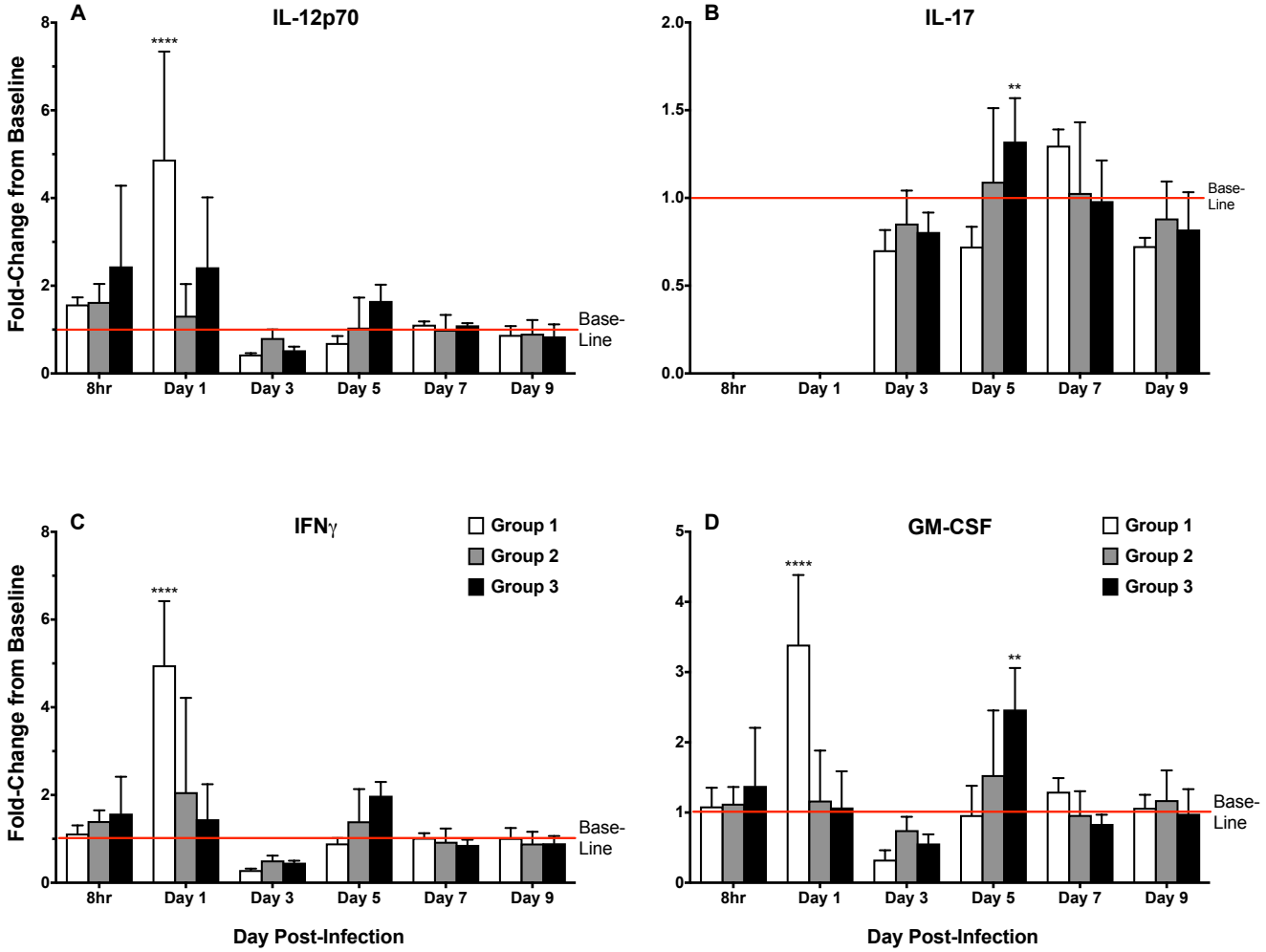

Figure 17 IL-12p70, IL-17, INFα, GM-CSF levels in lung samples after infection with MP30pp mouse-adapted EV-D68. All cytokines showed significant increases on day 1 p.i. compared to baseline. *P <0.05, **P <0.01, ***P <0.001, ****P<0.0001.

CHAPTER V

PLETHYSMOGRAPHY EVALUATION

Plethysmography Evaluation of EV-D68 MP30 Infected Mice

To further evaluate the affects/signs/severity of disease, the respiratory function of mice was evaluated by plethysmography. Mice were put into a sealed chamber and respiratory function was measured under two conditions, the first was room air and the second was a challenge of 7% CO_2, 50% O_2 and balanced with N_3, which is referred to as the CO_2 challenge. The parameters evaluated were; inspiratory time, expiratory time, peak inspiratory flow, peak expiratory flow, tidal volume, expired volume, relaxation time, minute volume, frequency, end inspiratory pause, end expiratory pause, enhanced pause, and mid-expiratory flow.

The first evaluation of plethysmography was completed using EV-D68 MP30 with four infectious doses; $10^{6.5}$ $CCID_{50}$/mL (group 1), $10^{6.0}$ $CCID_{50}$/mL (group 2), $10^{5.5}$ $CCID_{50}$/mL (group 3), $10^{5.0}$ $CCID_{50}$/mL (group 4) and a mock infected group (group 5). Each group had four 4-week-old mice. Room air was the first parameter measured. Each mouse was allowed to acclimate in the chamber for five minutes. After acclimation, the parameters were measured for five minutes. This same procedure was done for the CO_2 challenge. Lung function recordings were taken just prior to infection and then every day for seven days. Time parameters were measured in msec, and volume parameters were measured in mL and reported as a percent of the control group.

When respiratory function was measured under room air conditions, the results were highly variable (see Appendix). When mice were challenged with CO_2 there was a more notable difference between groups. The only parameter that showed significance was enhanced pause. Enhanced pause is scaled to the strength of the inhale and exhale which is calculated by (PEF/PIF) x pause. PEF is the peak expiratory flow, PIF is the peak inspiratory flow while the pause takes place between the expiratory cycle(111). By day 6 group 1 mice showed significant differences in enhanced pause compared to uninfected control mice. Day 7 also showed significant increase in enhanced pause of group 1 compared to group 5 (Figure 18).

Plethysmography Evaluation of Mouse Passaged Virus

To qualify plethysmography as a viable means to evaluate morbidity following EV-D68 infection, a mouse passage comparison study was conducted. The study design was similar to that of the virus passage comparison described in Chapter IV. Six groups of four mice per group were used. The EV-D68 virus passages used included: MP0, MP10, MP20, MP30, MP30pp and a mock-infected control group. Mice from each group were evaluated prior to infection and then every other day for 15 days starting on day 1.

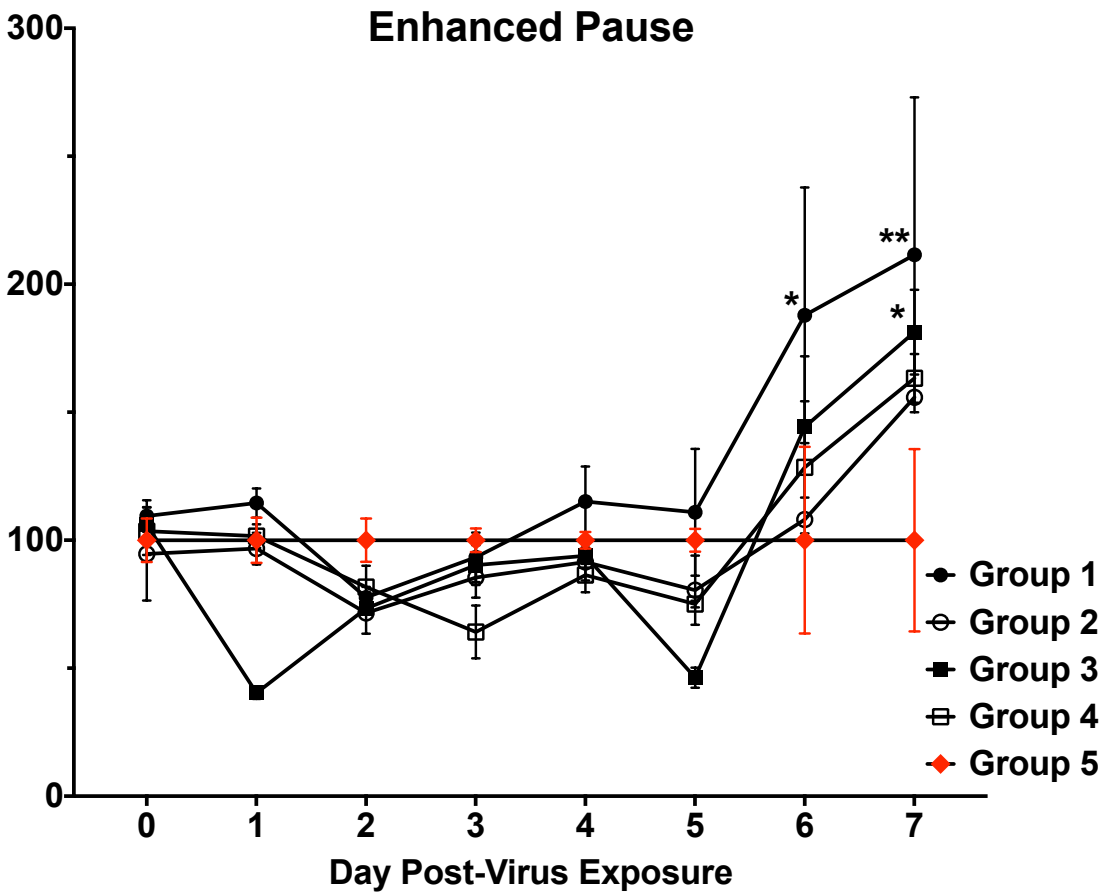

Figure 18 Plethysmography (CO_2): Evaluation of lung function in EV-D68 MP30 infected mice compared to uninfected mice. Parameters of infected mice were compared to uninfected controls and are reported as percentages, 100% being the baseline. *P <0.05, **P <0.01, ***P <0.001, ****P<0.0001.

Mice were evaluated under two conditions; room air and under CO_2 stress. The CO_2 stress helps the mice take normal breaths consistently. However, unlike the initial study where enhanced pause in the CO_2 stressed mice showed significant differences between EV-D68 infected mice and uninfected mice on day 5 and 7, this study did not show any statistical difference after CO_2 stress (Figure 19). There was a significant difference between mice infected with EV-D68 MP30 and MP30pp in the enhanced

pause (Penh) evaluation under room air on day 5 p.i. However, this was the only significant difference observed (Figure 20).

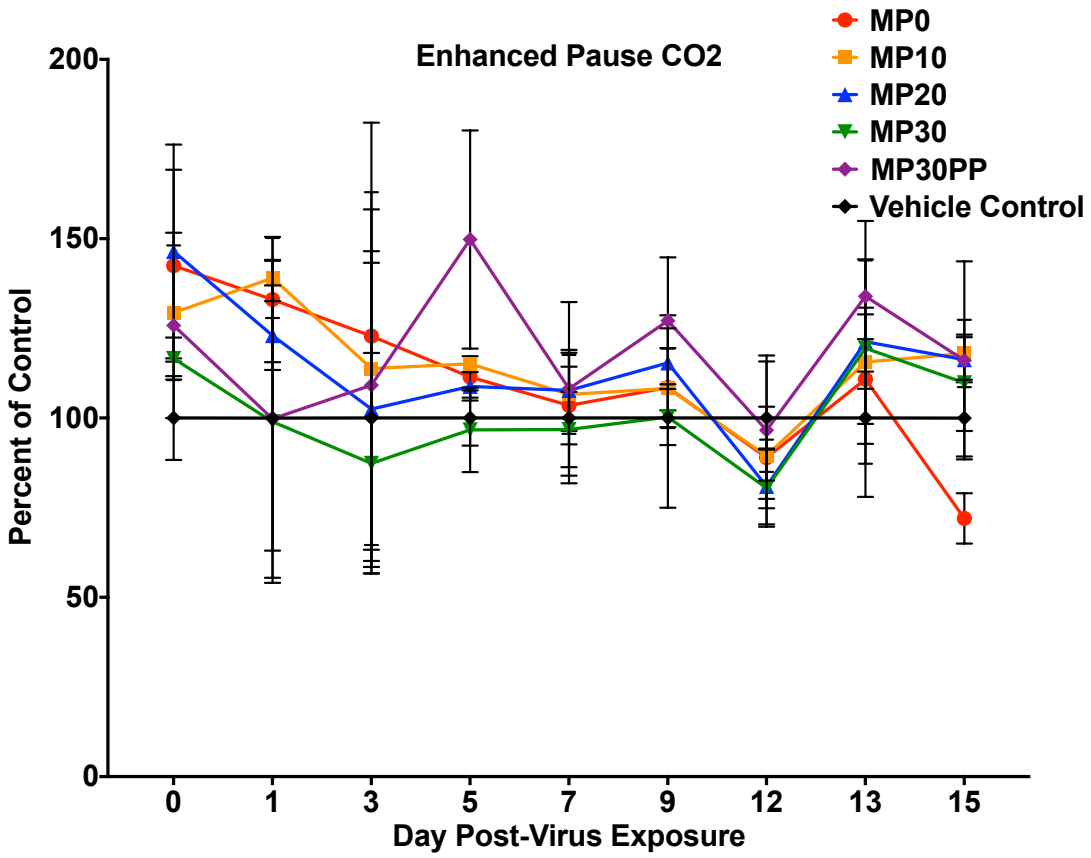

Figure 19 Comparison of Mice Infected with Different Virus Passages of EV-D68 Under CO_2 Stress. No statistical difference was observed in mice that were infected with EV-D68 and uninfected mice. Data is reported as a percentage of uninfected control mice.

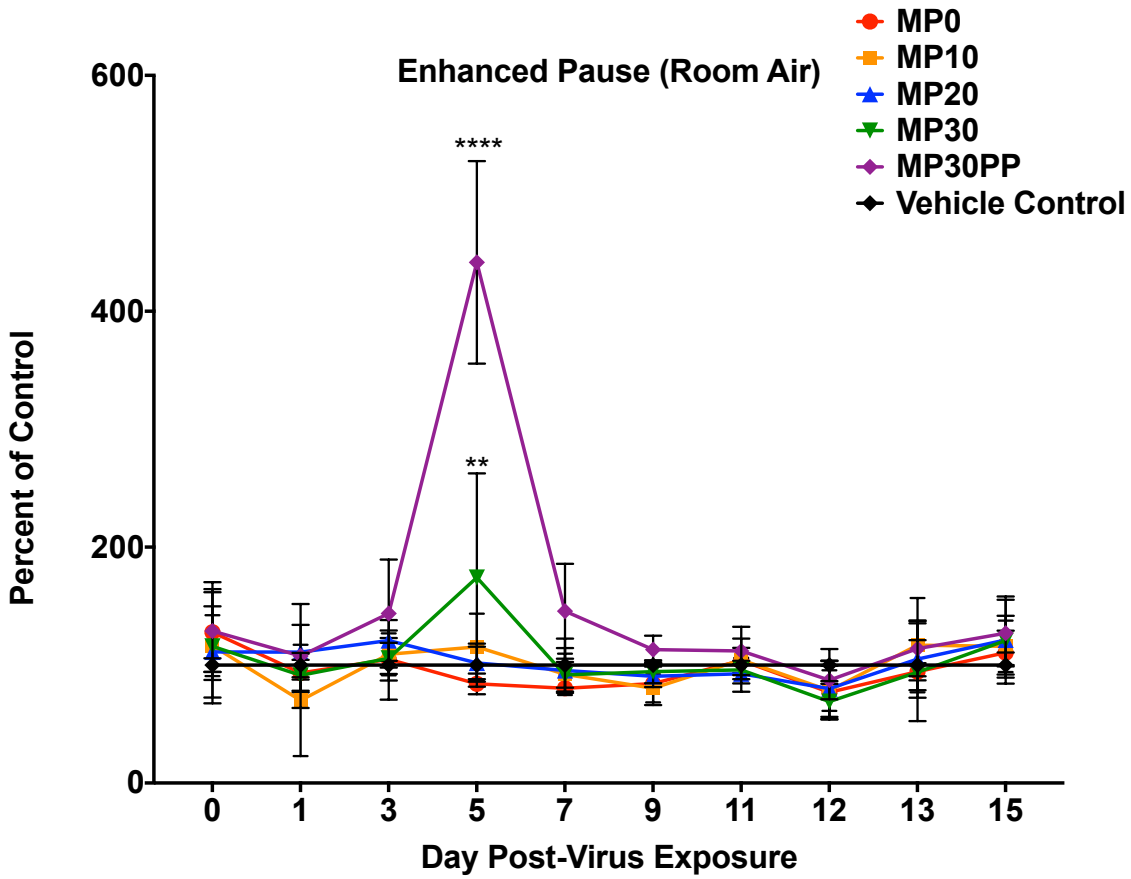

Figure 20 Comparison of Mice Infected with Different Virus Passages of EV-D68 Under Room Air. A significant difference was observed in mice that were infected with EV-D68 MP30, MP30pp and uninfected mice on day 5 p.i. Data shown is a comparison to the control mice and reported as a percentage. *P <0.05, **P <0.01, ***P <0.001, ****P<0.0001.

Evaluation of Infectious Doses of EV-D68

Along with a comparison of EV-D68 mouse passages, a comparison was done of EV-D68 MP30pp at different infectious doses: $10^{6.5}$ $CCID_{50}$/mL, $10^{5.5}$ $CCID_{50}$/mL, $10^{4.5}$ $CCID_{50}$/mL and mock infected mice. There were four mice per infectious dose. Lung function for each mouse was evaluated just prior to infection and then every other day after that for 15 days.

The enhanced pause (Penh) measured in room air with mice infected with EV-D68 MP30pp $10^{6.5}$ $CCID_{50}$/mouse showed the most significant increase on day 5 compared to control (Figure 21). Mice infected with EV-D68 MP30pp at $10^{5.5}$ $CCID_{50}$/mouse also showed a significant increase compared to control.

We evaluated Penh under CO_2 stress and under room air after EV-D68 MP30pp challenge at different doses. Even though the CO_2 challenge did not produce as high of a change between infected and uninfected mice as did the room air measurement, it did show that there is a consistent difference between EV-D68 infected mice and uninfected mice. Figure 21 shows that infection with EV-D68 MP30pp produced a dose responsive effect in Penh under room air. Figure 22 shows the dose response of EV-D68 infection under CO_2 challenge.

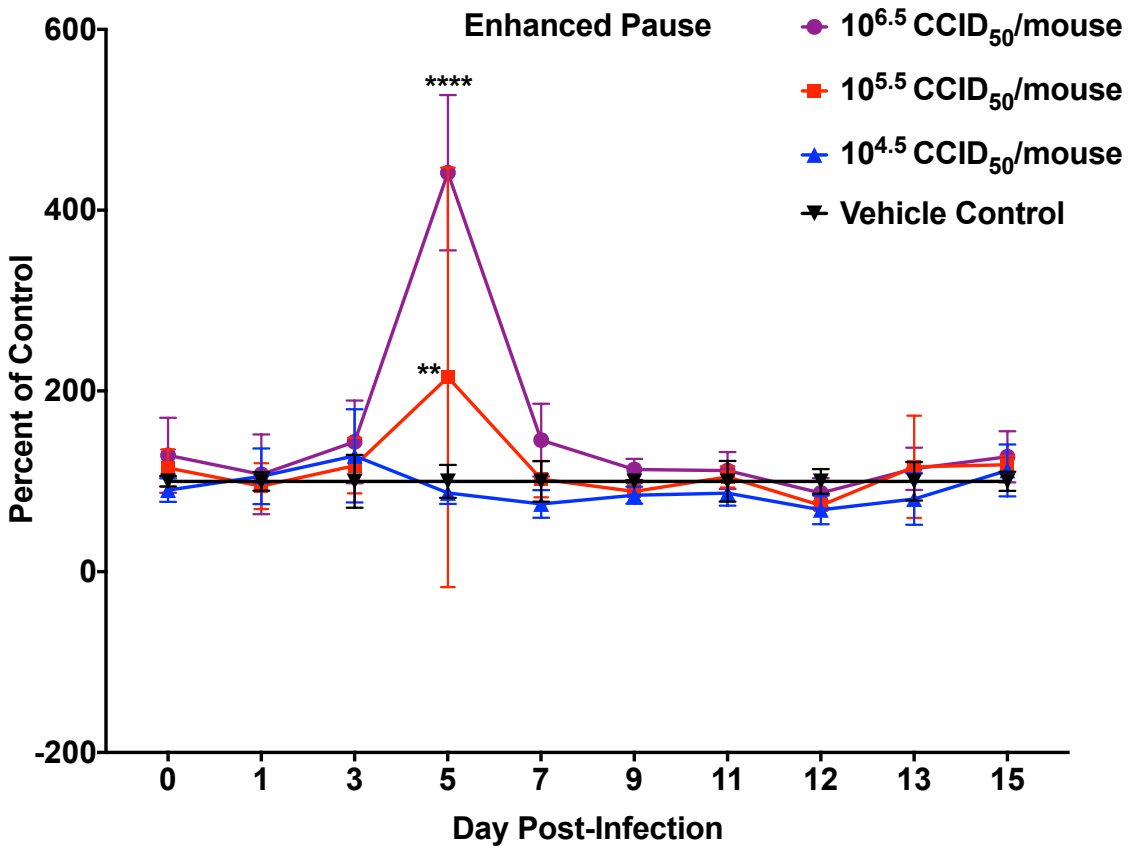

Figure 21 Evaluation of Penh by challenge Dose of EV-D68 MP30pp Under Room Air. A significant difference was observed in mice infected with EV-D68 MP30pp and uninfected mice on day 5 p.i. Data shown is reported as a percentage of the value for uninfected mice. *P <0.05, **P <0.01, ***P <0.001, ****P<0.0001.

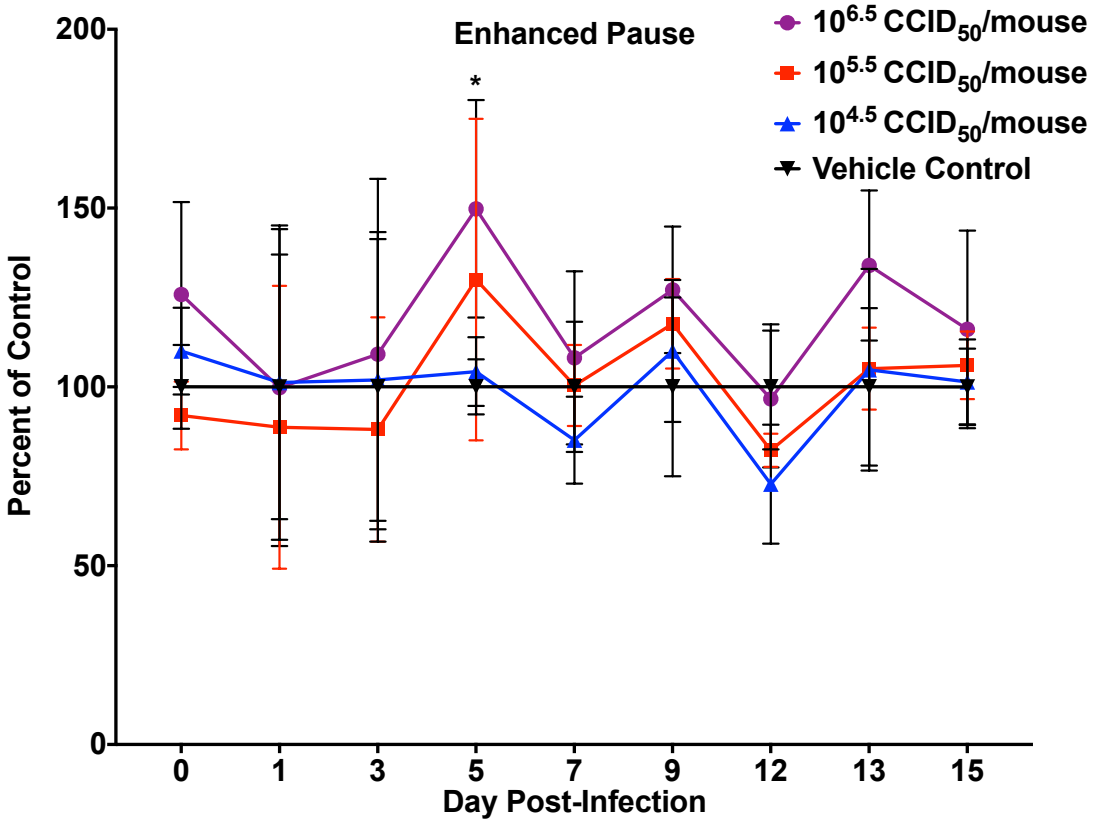

Figure 22 CO_2 plethysmography evaluation of infectious doses of EV-D68 MP30pp against uninfected mice. Statistical difference was observed in mice that were infected with EV-D68 MP30pp and uninfected mice on day 5 p.i. Data shown is a comparison to the control mice and reported as a percentage. *P <0.05, **P <0.01, ***P <0.001, ****P<0.0001.

Plethysmography was used as a tool to measure morbidity and can help determine if antiviral compounds can reduce morbidity. The benefit of this method is that it does not require sacrifice of mice for evaluation. It also allows us to compare overall lung function in mice after infection by EV-D68. Enhanced pause with either a room air or a CO_2 stress appears to be the best parameter to evaluate. Day 5 p.i. showed the greatest difference between EV-D68 MP30pp and uninfected mice.

Several issues were noted with regard to use of plethysmography for evaluation of lung function. The protocol used for plethysmography measurements takes twenty minutes per mouse to complete, so this method is time-consuming. This shortcoming will need to be re-visited when used in evaluation of experimental antivirals. In addition, there can be a lot of variation among measurements. Enhanced pause showed the best consistency between studies, and other parameters showed much more variability. Further evaluation needs to be done for plethysmography to be used as a viable tool.

CHAPTER VI

USE OF THE MOUSE MODEL OF EV-D68 INFECTION FOR EVALUATION OF ANTIVIRAL THERAPEUTICS

Once the mouse model of EV-D68 infection was developed and a basic understanding of the pathogenesis in mice was obtained, the next step was to evaluate potential treatment strategies using this model. A number of antiviral compounds have been evaluated in cell culture against EV-D68. However, until now, there has not been an animal model available for evaluation of antiviral therapies. Therefore, we evaluated several antiviral compounds in mice to determine if our model could be used for evaluation of experimental drugs.

Ideally, experimental compounds selected for evaluation would be effective antivirals for EV-D68 and potentially, rhinoviruses. The antiviral compounds evaluated included rupintrivir, enviroxime, pleconaril, ribavirin and guanidine. These compounds were shown to be effective inhibitors of both EV-D68 and rhinovirus infection in vitro as described in the literature review and the publication manuscript. In addition, ribavirin has been shown to be efficacious against EV-D68 by D. F. Smee, et al. (15), and also against rhinovirus by J. H. Song, et al. (112). From initial *in vitro* screening, the most promising compound identified for evaluation in our mouse model was rupintrivir. This compound showed the highest activity against EV-D68 and HRV-14 of those tested in chapter IV. So Rupintrivir was used as the pilot antiviral compound in this new model.

Evaluation of Rupintrivir as Treatment for an EV-D68 Infection in Mice

Rupintrivir was used as treatment for an EV-71 infection in 2-day-old mouse pups at 0.1mg/kg/day and 1mg/kg/day, and provided 90.9% survivability at the lower dose (113). Because our model for EV-D68 infection is nonlethal, we determined therapeutic efficacy by reduction in virus titer in mouse tissues. Three different concentrations of rupintrivir: 10mg/kg/day, 3mg/kg/day, 1mg/kg/day treated intra-peritoneally (i.p.), were evaluated and compared to a placebo control group. Each treatment dose was evaluated against two challenge doses, $10^{6.5}$ $CCID_{50}$/mouse and $10^{5.5}$ $CCID_{50}$/mouse. Seven mice per treatment group were infected with 90 μL of virus. Two time points were selected for euthanasia of mice and collection of tissues: day 2 p.i. and day 5 p.i. Four mice per group were euthanized on day 2 and three mice per group were euthanized on day 5. Five different tissues were collected from each of the mice including: lungs, whole blood, liver, kidney and spleen. Virus titers in the lung for the placebo group were $10^{7.0}$ $CCID_{50}$/mL on day 2 and $10^{5.3}$ $CCID_{50}$/mL on day 5 after challenge with the $10^{6.5}$ $CCID_{50}$/mouse dose. All three treatment groups had similar virus titers as the placebo group with an average titer of $10^{7.3}$ $CCID_{50}$/mL on day 2 and $10^{5.3}$ $CCID_{50}$/mL on day 5 (Figure 23). The failure of rupintrivir to show efficacy against EV-D68 in the mouse model at the doses evaluated in this study may be due to the i.p. route of administration. Rupintrivir is hydrolyzed in the liver (114, 115), therefore the i.p. route may have affected the rate of metabolism of the compound. Therefore, we evaluated rupintrivir by the intranasal(i.n.) route at the same doses as i.p. treatment. This i.n. treatment yielded the same results as the i.p. treatment (data not shown) suggesting that rupintrivir is not active against EV-D68 infection in the mouse model.

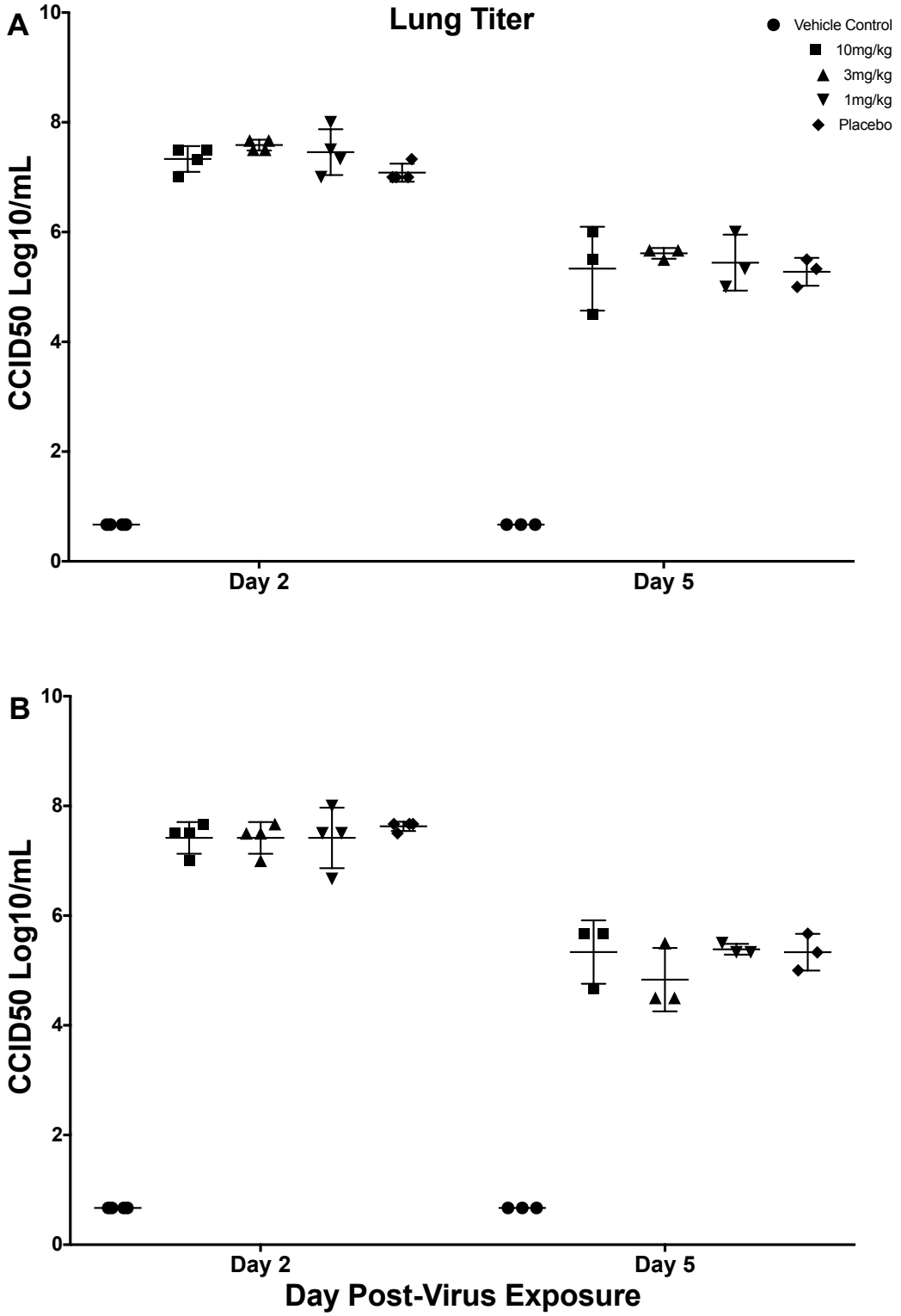

Figure 23 Evaluation of Rupintrivir as treatment of an EV-D68 Infection in Mice. Panel A shows lung virus titers from mice infected with 10^6 $CCID_{50}$/mL virus. Panel B shows lung virus titers from mice infected with 10^5 $CCID_{50}$/mL virus. No virus reduction was observed on either day 2 or day 5 p.i.

Evaluation of Ribavirin, Pleconaril, Guanidine, and Enviroxime as Treatment for an EV-D68 Infection in Mice

We observed rapid replication of EV-D68 after intranasal challenge, producing high titers in the lungs of mice by day 1 post-virus exposure. Therefore, in additional studies using four experimental antiviral compounds, we used a single infectious dose of $10^{5.5}$ $CCID_{50}$/mL EV-D68 MP30pp and treated mice on only a single occasion. On day 1 post-virus exposure, the mice were euthanized and lung tissue and whole blood was collected for virus titration. Using this study design, two concentrations of ribavirin, 500mg/kg/day and 300mg/kg/day p.o., and single concentrations of pleconaril at 10mg/kg/day p.o., guanidine at 200mg/kg/day i.p. and enviroxime at 200mg/kg/day i.p. were evaluated. Each treatment group consisted of four mice.

The results following treatment with ribavirin, pleconaril, and enviroxime were similar to those observed following rupintrivir treatment, with virus titers from lung and whole blood being similar to the placebo group. However, mice treated with guanidine significantly reduced lung virus titers (Figure 24). The virus titers in the placebo group averaged $10^{7.6}$ $CCID_{50}$/mL, while guanidine treated mice showed about a 1000-fold reduction in lung virus titers and whole blood titers. Blood titers for the placebo group were $10^{3.4}$ $CCID_{50}$/mL, while virus titers in the blood of the guanidine treated mice were undetectable.

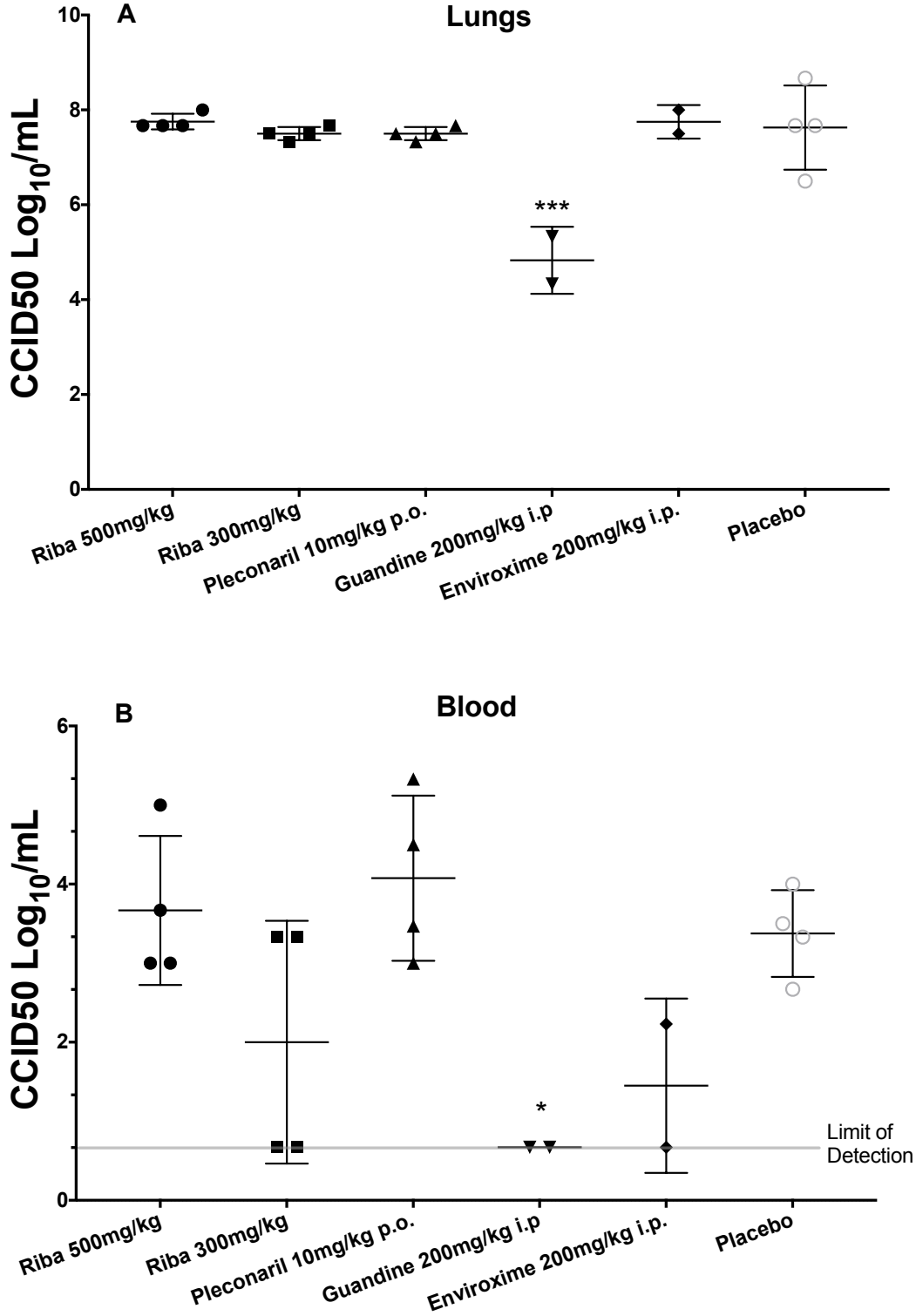

Figure 24 Virus titers in lung and blood following antiviral treatment of EV-D68 infected mice. Guanidine treated mice had significantly lower virus titers in both lung and blood samples. *P <0.05, **P <0.01, ***P <0.001, ****P<0.0001.

Maximum Tolerated Dose of Guanidine

To determine the dose range for use in the antiviral efficacy study, a maximum tolerated dose study evaluating four doses of guanidine was completed in 4-week old AG129 mice (Figure 25). The four concentrations evaluated included 50mg/kg/day, 100mg/kg/day, 200mg/kg/day and 400mg/kg/day and all where i.p. treatments. Treatments were administered twice per day for five days. Mice were evaluated based on individual weights and mortality for eight days. In all of the treatment groups, mice did not lose weight, indicative of low toxicity from the drug.

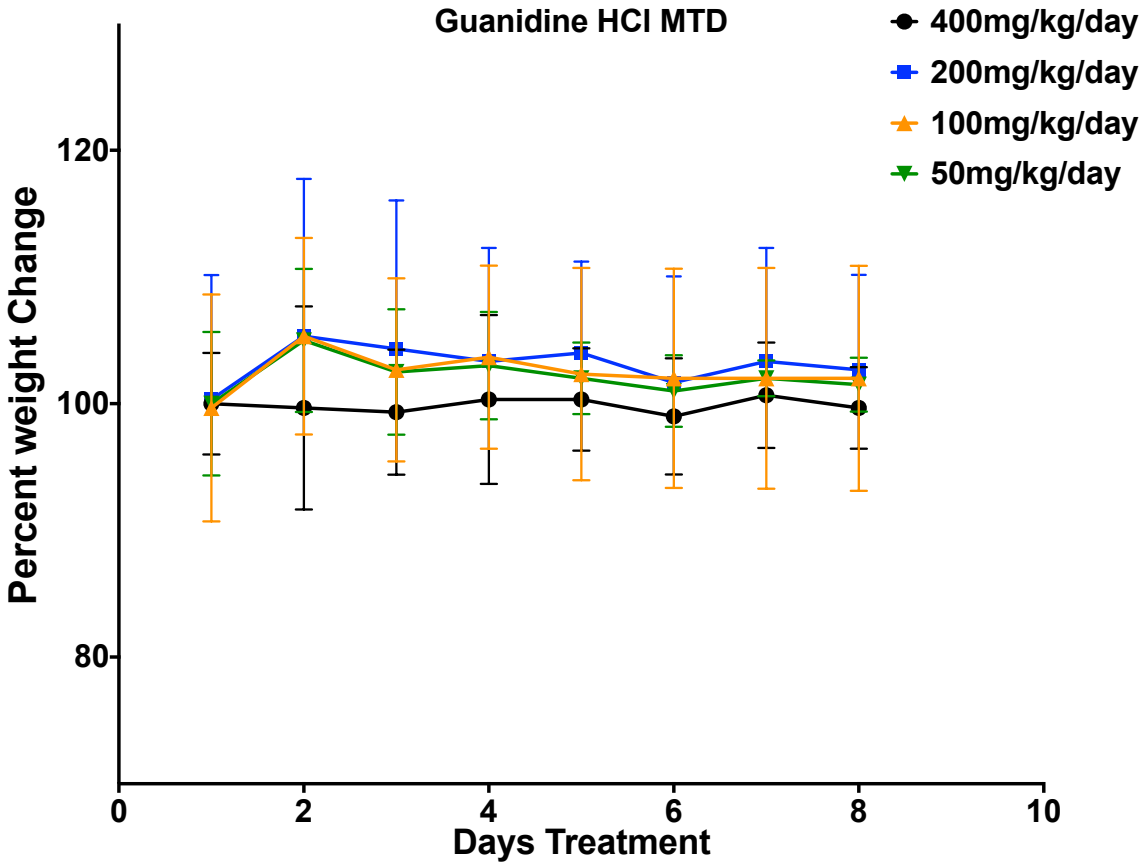

Figure 25 Guanidine maximum tolerated dose. All doses tested appear to be safe as none of the treatments caused a loss in weight, although mice receiving the highest dose did not gain weight.

Dose Response Evaluation of Guanidine as Treatment for an EV-D68 Infection in Mice

Figure 26 shows the results of a dose response study completed to verify the efficacy of guanidine as an antiviral treatment for the AG129 mouse adapted model of EV-D68. Four groups of mice per dose of guanidine were evaluated including 200, 100, and 50 mg/kg/day. Mice were infected with $10^{4.5}$ $CCID_{50}$/mouse EV-D68 i.n., as this lower challenge dose was shown to provide similar results as higher inocula. Treatment was started at the time of infection by the i.p. route. Each treatment was administered twice per day for 1 day. On day 1 post-virus exposure, mice were euthanized and lung and blood samples collected.

Placebo mice had an average lung virus titer of $10^{6.8}$ $CCID_{50}$/mL and an average blood titer of $10^{2.3}$ $CCID_{50}$/mL. Mice treated with 50mg/kg/day, had an average lung titer of $10^{6.2}$ $CCID_{50}$/mL. One mouse in the group had a blood titer of $10^{1.7}$ $CCID_{50}$/mL and in the other three mice the titers were undetectable. Mice treated with 100mg/kg/day i.p. and 200mg/kg/day i.p., also had undetectable blood virus titers. Mice treated at 100mg/kg/day i.p. had an average lung titer of $10^{5.8}$ $CCID_{50}$/mL, a 10-fold reduction from the placebo treated mice. Mice treated at 200mg/kg/day i.p. yielded an average lung titer of $10^{4.5}$ $CCID_{50}$/mL, about a 320-fold reduction from the placebo treated mice. Mice treated with guanidine exhibited lower blood virus titers at all three drug doses then placebo treated mice, demonstrating that guanidine was able to reduce and/or eliminate the viremia. for one day.

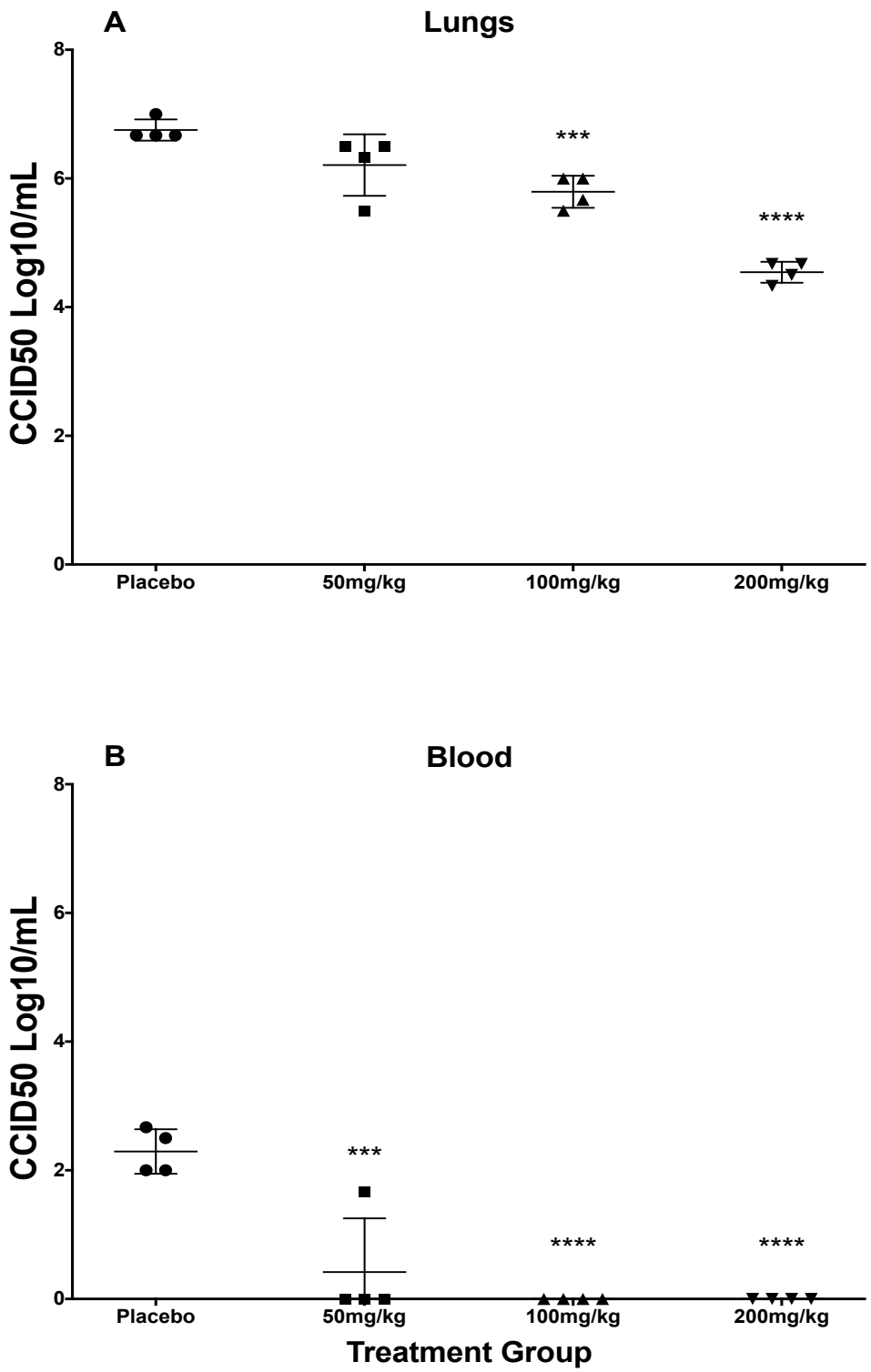

Figure 26 Dose Response of Guanidine as Treatment of EV-D68 Infection in Mice. Dose response of guanidine treatment on virus titers in the lungs and blood. Both 100 and 200 mg/kg/day doses showed significant reduction in virus titers in the lungs (Panel A), while all three doses showed significant reduction in viremia (Panel B). *P <0.05, **P <0.01, ***P <0.001, ****P<0.0001.

CHAPTER VII

SUMMARY

As EV-D68 was passaged in 4-week old AG129 mice, the virus slowly adapted over 30 passages, as indicated by increasing virus titers in the lungs from MP0 to MP30. In addition to an increase in lung virus titers, EV-D68 caused viremia and increased levels of virus in other tissues, including liver, kidney and spleen as virus passage increased. In addition, mouse adapted EV-D68 caused increased levels of the pro-inflammatory chemokines MCP-1 and RANTES. Finally, as EV-D68 adapted to 4-week old AG129 mice, the virus increased in capacity to cause histological legions in lung tissues all shown in Table 12.

Table 13 shows the ability of EV-D68 to replicate within mouse tissues was determined by virus titration of homogenized tissues. In addition, histological lesions in 4-week old AG129 mice was evaluated in multiple tissues, but lesions were only observed in the lungs. Challenge doses of $10^{6.5}$, $10^{5.5}$ and $10^{4.5}$ $CCID_{50}$/mouse were evaluated for EV-D68 infection. By day 3 post-virus exposure, titers in lung, liver and spleen tissues for all challenge doses were similar. For all challenge doses, the mice began clearing virus by day 4 or 5 p.i. and virus was undetectable in all tissues by day 9 p.i. EV-D68 infection by the i.n. route caused a viremia, which occurred rapidly with a peak in virus titers on day 1, which was eventually cleared by day 5 p.i. Guanidine was shown to be an effective treatment for EV-D68 infection in mice by reducing virus titers in the lung at 200 mg/kg/day and reducing viremia at 50, 100 and 200 mg/kg/day

concentrations. We do not propose the use of guanidine as a therapeutic treatment for EV-D68 infections, although these results indicate that guanidine can be used successfully as a positive control in future antiviral studies in our model.

Table 12 Virus Passage Comparison Summarizing Virus Titer, Histological lesions and Chemokines from Lungs in Mice on Day 3 P.I.

Mouse Passage		**MP0**	**MP10**	**MP20**	**MP30**	**MP30pp**
Virus Titer	**Lungs**	5.8	7.1	7.2	7.2	7.3
	Blood	<0.67	1.33	2.2	2.4	2.0
Histological Lesions (Interstitial Pneumonia)		1(-), 2(+), 1(++)	All (++)	All (++ to +++)	1(++), 3(+++)	2(++), 2(++ to +++)
Chemokines	**MCP-1**	1.9	8.6	9.2	14.3	15.8
	RANTES	0.9	1.4	1.4	2.3	1.7

Virus Titers: Value shown represents a log CCID50/100 uL of lungs homogenized in 1 mL of MEM solution.
Histopathology: Scores were obtained from four mice per mouse passage.
Chemokines are expressed as fold changes compared to the baseline or uninfected mice.

Table 13 Summary of Virus Titers, Histological lesions and Chemokines for Mice Infected with EV-D68 MP30pp at $10^{6.5}$, $10^{5.5}$ or $10^{4.5}$ $CCID_{50}$/mouse.

Day Post-Virus Exposure		8hr	Day 1	Day 3	Day 5	Day 7	Day 9
10^6.5 Infection							
Virus Titer	**Lungs**	7.7	8.3	8.0	5.3	3.33	<0.67
	Viremia	1.0	5.4	3.4	<0.67	<0.67	<0.67
Histological lesions (Interstitial Pneumonia)		Not Tested	1(+++), 1(++), 1(+++/++++)	2(++/+++), 2(+++)	2(++), 2(++/+++)	3(++), 1(+++/++++)	2(+), 2(++)
Chemokines	**MCP-1**	2.6	47.6	5	10.7	1.9	0.8
	RANTES	2.4	7.8	1.6	1.6	1.4	1.1

10^5.5 Infection

Virus Titer	**Lungs**	6.9	7.8	8.0	5.75	3.3	<0.67
	Viremia	Not Tested	Not Tested	Not Tested	Not Tested	Not Tested	Not Tested
Histological lesions (Interstitial Pneumonia)		Not Tested	Not Tested	3(++/+++)	1(++), 3(++/+++)	2(++), 2(++/+++)	All(+)
Chemokines	**MCP-1**	2.0	21.6	5.4	9.5	1.3	1.0
	RANTES	2.7	3.3	1.6	1.3	1.4	1.0

10^4.5 infection

Virus Titer	**Lungs**	6.0	7.2	7.7	6.2	4.1	<0.67
	Viremia	<0.67	3	3.39	<0.67	<0.67	<0.67
Histological lesions (Interstitial Pneumonia)		Not Tested	Not Tested	3(++/+++), 1(+++)	3(++), 1(+++)	2(++), 2(++/+++)	3(++), 1(+)
Chemokines	**MCP-1**	2.1	2.1	5.1	9.6	0.9	1.2
	RANTES	2.5	1.3	1.5	1.7	1.2	1.0

Virus Titers: Value shown represents a log value.
Histological lesions: Scores were obtained from four mice per mouse passage.
Chemokines are expressed as fold changes compared to the baseline or uninfected mice.

Future Studies

There are a number of questions pertaining to EV-D68 pathogenesis that can be addressed using this mouse model:

1. How is the virus carried in the blood, and is there a specific cell type associated with viremia?
2. Does intranasal infection of younger mice lead to a lethal model?
3. What is the timing and route for transmission of virus from the lungs to the CNS, and are histological lesions within the CNS produced.
4. During virus adaptation, when does the ability to infect the CNS develop, and can the mutation associated with that ability be identified?
5. What additional antiviral compounds can be evaluated for efficacy in the mouse model of infection?
6. Does guanidine treatment reduce virus titers, cytokines and histopathology in mice at day 3 and 5 p.i. in EV-D68 MP30pp infected mice?
7. Does guanidine treatment reduce enhanced pause for in EV-D68 MP30pp infected mice?

CHAPTER VII

REFERENCES

1. **Khetsuriani N, Lamonte-Fowlkes A, Oberst S, Pallansch MA, Centers for Disease C, Prevention.** 2006. Enterovirus surveillance--United States, 1970-2005. MMWR Surveill Summ **55:**1-20.
2. **Schieble JH, Fox VL, Lennette EH.** 1967. A probable new human picornavirus associated with respiratory diseases. Am J Epidemiol **85:**297-310.
3. **Foster CB, Friedman N, Carl J, Piedimonte G.** 2015. Enterovirus D68: a clinically important respiratory enterovirus. Cleve Clin J Med **82:**26-31.
4. **Martin G, Li R, Cook VE, Carwana M, Tilley P, Sauve L, Tang P, Kapur A, Yang CL.** 2016. Respiratory Presentation of Pediatric Patients in the 2014 Enterovirus D68 Outbreak. Can Respir J **2016:**8302179.
5. **Centers for Disease C.** July 19, 2016 2016. Enterovirus D68. https://www.cdc.gov/non-polio-enterovirus/about/ev-d68.html. Accessed Febuary 21.
6. **Centers for Disease C, Prevention.** 2011. Clusters of acute respiratory illness associated with human enterovirus 68--Asia, Europe, and United States, 2008-2010. MMWR Morb Mortal Wkly Rep **60:**1301-1304.
7. **Kaida A, Kubo H, Sekiguchi J, Kohdera U, Togawa M, Shiomi M, Nishigaki T, Iritani N.** 2011. Enterovirus 68 in children with acute respiratory tract infections, Osaka, Japan. Emerg Infect Dis **17:**1494-1497.
8. **Xiang Z, Gonzalez R, Wang Z, Ren L, Xiao Y, Li J, Li Y, Vernet G, Paranhos-Baccala G, Jin Q, Wang J.** 2012. Coxsackievirus A21, enterovirus 68, and acute respiratory tract infection, China. Emerg Infect Dis **18:**821-824.
9. **Hasegawa S, Hirano R, Okamoto-Nakagawa R, Ichiyama T, Shirabe K.** 2011. Enterovirus 68 infection in children with asthma attacks: virus-induced asthma in Japanese children. Allergy **66:**1618-1620.
10. **Imamura T, Oshitani H.** 2015. Erratum: Global reemergence of enterovirus D68 as an important pathogen for acute respiratory infections. Rev Med Virol **25:**268.
11. **Knoester M, Scholvinck EH, Poelman R, Smit S, Vermont CL, Niesters HG, Van Leer-Buter CC.** 2017. Upsurge of Enterovirus D68, the Netherlands, 2016. Emerg Infect Dis **23:**140-143.
12. **Centers for Disease C.** March 1, 2017 2017. AFM in the United States. https://www.cdc.gov/acute-flaccid-myelitis/afm-surveillance.html. Accessed March 6.
13. **Wylie TN, Wylie KM, Buller RS, Cannella M, Storch GA.** 2015. Development and Evaluation of an Enterovirus D68 Real-Time Reverse Transcriptase PCR Assay. J Clin Microbiol **53:**2641-2647.

14. **Liu Y, Sheng J, Fokine A, Meng G, Shin WH, Long F, Kuhn RJ, Kihara D, Rossmann MG.** 2015. Structure and inhibition of EV-D68, a virus that causes respiratory illness in children. Science **347:**71-74.
15. **Smee DF, Evans WJ, Nicolaou KC, Tarbet EB, Day CW.** 2016. Susceptibilities of enterovirus D68, enterovirus 71, and rhinovirus 87 strains to various antiviral compounds. Antiviral Res **131:**61-65.
16. **Patel MC, Wang W, Pletneva LM, Rajagopala SV, Tan Y, Hartert TV, Boukhvalova MS, Vogel SN, Das SR, Blanco JC.** 2016. Enterovirus D-68 Infection, Prophylaxis, and Vaccination in a Novel Permissive Animal Model, the Cotton Rat (Sigmodon hispidus). PLoS One **11:**e0166336.
17. **Hixon AM, Yu G, Leser JS, Yagi S, Clarke P, Chiu CY, Tyler KL.** 2017. A mouse model of paralytic myelitis caused by enterovirus D68. PLoS Pathog **13:**e1006199.
18. **David M. Knipe PMH (ed).** 2013. Fields Virology. Wolters Kluwer/Lipincott William and Wilkins,
19. **Tan Y, Hassan F, Schuster JE, Simenauer A, Selvarangan R, Halpin RA, Lin X, Fedorova N, Stockwell TB, Lam TT, Chappell JD, Hartert TV, Holmes EC, Das SR.** 2015. Molecular Evolution and Intraclade Recombination of Enterovirus D68 during the 2014 Outbreak in the United States. J Virol **90:**1997-2007.
20. **Blomqvist S, Savolainen C, Raman L, Roivainen M, Hovi T.** 2002. Human rhinovirus 87 and enterovirus 68 represent a unique serotype with rhinovirus and enterovirus features. J Clin Microbiol **40:**4218-4223.
21. **Centers for Disease C.** 2016. Non-polio Enterovirus Home page. https://www.cdc.gov/non-polio-enterovirus/index.html. Accessed August 26.
22. **Oberste MS, Maher K, Schnurr D, Flemister MR, Lovchik JC, Peters H, Sessions W, Kirk C, Chatterjee N, Fuller S, Hanauer JM, Pallansch MA.** 2004. Enterovirus 68 is associated with respiratory illness and shares biological features with both the enteroviruses and the rhinoviruses. J Gen Virol **85:**2577-2584.
23. **Meijer A, van der Sanden S, Snijders BE, Jaramillo-Gutierrez G, Bont L, van der Ent CK, Overduin P, Jenny SL, Jusic E, van der Avoort HG, Smith GJ, Donker GA, Koopmans MP.** 2012. Emergence and epidemic occurrence of enterovirus 68 respiratory infections in The Netherlands in 2010. Virology **423:**49-57.
24. **Stephenson J.** 2014. CDC tracking enterovirus D-68 outbreak causing severe respiratory illness in children in the Midwest. JAMA **312:**1290.
25. **Midgley CM, Watson JT, Nix WA, Curns AT, Rogers SL, Brown BA, Conover C, Dominguez SR, Feikin DR, Gray S, Hassan F, Hoferka S, Jackson MA, Johnson D, Leshem E, Miller L, Nichols JB, Nyquist AC, Obringer E, Patel A, Patel M, Rha B, Schneider E, Schuster JE, Selvarangan R, Seward JF, Turabelidze G, Oberste MS, Pallansch MA, Gerber SI, Group E-DW.** 2015. Severe respiratory illness associated with a nationwide outbreak of enterovirus D68 in the USA (2014): a descriptive epidemiological investigation. Lancet Respir Med **3:**879-887.

26. **Midgley CM, Jackson MA, Selvarangan R, Turabelidze G, Obringer E, Johnson D, Giles BL, Patel A, Echols F, Oberste MS, Nix WA, Watson JT, Gerber SI.** 2014. Severe respiratory illness associated with enterovirus D68 - Missouri and Illinois, 2014. MMWR Morb Mortal Wkly Rep **63:**798-799.
27. **Piralla A, Girello A, Grignani M, Gozalo-Marguello M, Marchi A, Marseglia G, Baldanti F.** 2014. Phylogenetic characterization of enterovirus 68 strains in patients with respiratory syndromes in Italy. J Med Virol **86:**1590-1593.
28. **Diseases NCCfI.** January 15 2015 2015. Enterovirus D68. https://nccid.ca/debrief/ev-d68/. Accessed March 3.
29. **Imamura T, Fuji N, Suzuki A, Tamaki R, Saito M, Aniceto R, Galang H, Sombrero L, Lupisan S, Oshitani H.** 2011. Enterovirus 68 among children with severe acute respiratory infection, the Philippines. Emerg Infect Dis **17:**1430-1435.
30. **Tokarz R, Firth C, Madhi SA, Howie SR, Wu W, Sall AA, Haq S, Briese T, Lipkin WI.** 2012. Worldwide emergence of multiple clades of enterovirus 68. J Gen Virol **93:**1952-1958.
31. **Messacar K, Abzug MJ, Dominguez SR.** 2016. 2014 outbreak of enterovirus D68 in North America. J Med Virol **88:**739-745.
32. **Kreuter JD, Barnes A, McCarthy JE, Schwartzman JD, Oberste MS, Rhodes CH, Modlin JF, Wright PF.** 2011. A fatal central nervous system enterovirus 68 infection. Arch Pathol Lab Med **135:**793-796.
33. **Imamura T, Suzuki A, Lupisan S, Okamoto M, Aniceto R, Egos RJ, Daya EE, Tamaki R, Saito M, Fuji N, Roy CN, Opinion JM, Santo AV, Macalalad NG, Tandoc A, 3rd, Sombrero L, Olveda R, Oshitani H.** 2013. Molecular evolution of enterovirus 68 detected in the Philippines. PLoS One **8:**e74221.
34. **Lauinger IL, Bible JM, Halligan EP, Aarons EJ, MacMahon E, Tong CY.** 2012. Lineages, sub-lineages and variants of enterovirus 68 in recent outbreaks. PLoS One **7:**e36005.
35. **Linsuwanon P, Puenpa J, Suwannakarn K, Auksornkitti V, Vichiwattana P, Korkong S, Theamboonlers A, Poovorawan Y.** 2012. Molecular epidemiology and evolution of human enterovirus serotype 68 in Thailand, 2006-2011. PLoS One **7:**e35190.
36. **Matsumoto M, Awano H, Ogi M, Tomioka K, Unzaki A, Nishiyama M, Toyoshima D, Taniguchi-Ikeda M, Ishida A, Nagase H, Morioka I, Iijima K.** 2016. A pediatric patient with interstitial pneumonia due to enterovirus D68. J Infect Chemother **22:**712-715.
37. **Pevear DC, Tull TM, Seipel ME, Groarke JM.** 1999. Activity of pleconaril against enteroviruses. Antimicrob Agents Chemother **43:**2109-2115.
38. **Greninger AL, Naccache SN, Messacar K, Clayton A, Yu G, Somasekar S, Federman S, Stryke D, Anderson C, Yagi S, Messenger S, Wadford D, Xia D, Watt JP, Van Haren K, Dominguez SR, Glaser C, Aldrovandi G, Chiu CY.** 2015. A novel outbreak enterovirus D68 strain associated with acute flaccid myelitis cases in the USA (2012-14): a retrospective cohort study. Lancet Infect Dis **15:**671-682.
39. **Messacar K, Schreiner TL, Maloney JA, Wallace A, Ludke J, Oberste MS, Nix WA, Robinson CC, Glode MP, Abzug MJ, Dominguez SR.** 2015. A

cluster of acute flaccid paralysis and cranial nerve dysfunction temporally associated with an outbreak of enterovirus D68 in children in Colorado, USA. Lancet **385:**1662-1671.

40. **Smura T, Ylipaasto P, Klemola P, Kaijalainen S, Kyllonen L, Sordi V, Piemonti L, Roivainen M.** 2010. Cellular tropism of human enterovirus D species serotypes EV-94, EV-70, and EV-68 in vitro: implications for pathogenesis. J Med Virol **82:**1940-1949.
41. **Chatterjee S, Quarcoopome CO, Apenteng A.** 1970. Unusual type of epidemic conjunctivitis in Ghana. Br J Ophthalmol **54:**628-630.
42. **Smura TP, Junttila N, Blomqvist S, Norder H, Kaijalainen S, Paananen A, Magnius LO, Hovi T, Roivainen M.** 2007. Enterovirus 94, a proposed new serotype in human enterovirus species D. J Gen Virol **88:**849-858.
43. **Oberste MS, Maher K, Kilpatrick DR, Pallansch MA.** 1999. Molecular evolution of the human enteroviruses: correlation of serotype with VP1 sequence and application to picornavirus classification. J Virol **73:**1941-1948.
44. **Imamura T, Okamoto M, Nakakita S, Suzuki A, Saito M, Tamaki R, Lupisan S, Roy CN, Hiramatsu H, Sugawara KE, Mizuta K, Matsuzaki Y, Suzuki Y, Oshitani H.** 2014. Antigenic and receptor binding properties of enterovirus 68. J Virol **88:**2374-2384.
45. **Loens K, Goossens H, de Laat C, Foolen H, Oudshoorn P, Pattyn S, Sillekens P, Ieven M.** 2006. Detection of rhinoviruses by tissue culture and two independent amplification techniques, nucleic acid sequence-based amplification and reverse transcription-PCR, in children with acute respiratory infections during a winter season. J Clin Microbiol **44:**166-171.
46. **Carlsen KH, Orstavik I, Leegaard J, Hoeg H.** 1984. Respiratory virus infections and aeroallergens in acute bronchial asthma. Arch Dis Child **59:**310-315.
47. **Mertz D, Alawfi A, Pernica JM, Rutherford C, Luinstra K, Smieja M.** 2015. Clinical severity of pediatric respiratory illness with enterovirus D68 compared with rhinovirus or other enterovirus genotypes. CMAJ **187:**1279-1284.
48. **Tapparel C, Sobo K, Constant S, Huang S, Van Belle S, Kaiser L.** 2013. Growth and characterization of different human rhinovirus C types in three-dimensional human airway epithelia reconstituted in vitro. Virology **446:**1-8.
49. **Ishiko H, Miura R, Shimada Y, Hayashi A, Nakajima H, Yamazaki S, Takeda N.** 2002. Human rhinovirus 87 identified as human enterovirus 68 by VP4-based molecular diagnosis. Intervirology **45:**136-141.
50. **Palmenberg AC, Gern JE.** 2015. Classification and evolution of human rhinoviruses. Methods Mol Biol **1221:**1-10.
51. **Liu Y, Sheng J, Baggen J, Meng G, Xiao C, Thibaut HJ, van Kuppeveld FJ, Rossmann MG.** 2015. Sialic acid-dependent cell entry of human enterovirus D68. Nat Commun **6:**8865.
52. **Oberste MS, Maher K, Kilpatrick DR, Flemister MR, Brown BA, Pallansch MA.** 1999. Typing of human enteroviruses by partial sequencing of VP1. J Clin Microbiol **37:**1288-1293.
53. **Gong YN, Yang SL, Shih SR, Huang YC, Chang PY, Huang CG, Kao KC, Hu HC, Liu YC, Tsao KC.** 2016. Molecular evolution and the global

reemergence of enterovirus D68 by genome-wide analysis. Medicine (Baltimore) **95:**e4416.

54. **Huang W, Wang G, Zhuge J, Nolan SM, Dimitrova N, Fallon JT.** 2015. Whole-Genome Sequence Analysis Reveals the Enterovirus D68 Isolates during the United States 2014 Outbreak Mainly Belong to a Novel Clade. Sci Rep **5:**15223.
55. **Piralla A, Girello A, Premoli M, Baldanti F.** 2015. A new real-time reverse transcription-PCR assay for detection of human enterovirus 68 in respiratory samples. J Clin Microbiol **53:**1725-1726.
56. **Xiang Z, Xie Z, Liu L, Ren L, Xiao Y, Paranhos-Baccala G, Wang J.** 2016. Genetic divergence of enterovirus D68 in China and the United States. Sci Rep **6:**27800.
57. **Casasnovas JM, Springer TA.** 1995. Kinetics and thermodynamics of virus binding to receptor. Studies with rhinovirus, intercellular adhesion molecule-1 (ICAM-1), and surface plasmon resonance. J Biol Chem **270:**13216-13224.
58. **McDermott BM, Jr., Rux AH, Eisenberg RJ, Cohen GH, Racaniello VR.** 2000. Two distinct binding affinities of poliovirus for its cellular receptor. J Biol Chem **275:**23089-23096.
59. **Alexander DA, Dimock K.** 2002. Sialic acid functions in enterovirus 70 binding and infection. J Virol **76:**11265-11272.
60. **Nokhbeh MR, Hazra S, Alexander DA, Khan A, McAllister M, Suuronen EJ, Griffith M, Dimock K.** 2005. Enterovirus 70 binds to different glycoconjugates containing alpha2,3-linked sialic acid on different cell lines. J Virol **79:**7087-7094.
61. **Wilks S, de Graaf M, Smith DJ, Burke DF.** 2012. A review of influenza haemagglutinin receptor binding as it relates to pandemic properties. Vaccine **30:**4369-4376.
62. **Shinya K, Ebina M, Yamada S, Ono M, Kasai N, Kawaoka Y.** 2006. Avian flu: influenza virus receptors in the human airway. Nature **440:**435-436.
63. **Schuster JE, Miller JO, Selvarangan R, Weddle G, Thompson MT, Hassan F, Rogers SL, Oberste MS, Nix WA, Jackson MA.** 2015. Severe enterovirus 68 respiratory illness in children requiring intensive care management. J Clin Virol **70:**77-82.
64. **Dragovich PS, Prins TJ, Zhou R, Webber SE, Marakovits JT, Fuhrman SA, Patick AK, Matthews DA, Lee CA, Ford CE, Burke BJ, Rejto PA, Hendrickson TF, Tuntland T, Brown EL, Meador JW, 3rd, Ferre RA, Harr JE, Kosa MB, Worland ST.** 1999. Structure-based design, synthesis, and biological evaluation of irreversible human rhinovirus 3C protease inhibitors. 4. Incorporation of P1 lactam moieties as L-glutamine replacements. J Med Chem **42:**1213-1224.
65. **Matthews DA, Dragovich PS, Webber SE, Fuhrman SA, Patick AK, Zalman LS, Hendrickson TF, Love RA, Prins TJ, Marakovits JT, Zhou R, Tikhe J, Ford CE, Meador JW, Ferre RA, Brown EL, Binford SL, Brothers MA, DeLisle DM, Worland ST.** 1999. Structure-assisted design of mechanism-based irreversible inhibitors of human rhinovirus 3C protease with potent antiviral

activity against multiple rhinovirus serotypes. Proc Natl Acad Sci U S A **96:**11000-11007.

66. **Patick AK, Binford SL, Brothers MA, Jackson RL, Ford CE, Diem MD, Maldonado F, Dragovich PS, Zhou R, Prins TJ, Fuhrman SA, Meador JW, Zalman LS, Matthews DA, Worland ST.** 1999. In vitro antiviral activity of AG7088, a potent inhibitor of human rhinovirus 3C protease. Antimicrob Agents Chemother **43:**2444-2450.
67. **Sun L, Meijer A, Froeyen M, Zhang L, Thibaut HJ, Baggen J, George S, Vernachio J, van Kuppeveld FJ, Leyssen P, Hilgenfeld R, Neyts J, Delang L.** 2015. Antiviral Activity of Broad-Spectrum and Enterovirus-Specific Inhibitors against Clinical Isolates of Enterovirus D68. Antimicrob Agents Chemother **59:**7782-7785.
68. **Rhoden E, Zhang M, Nix WA, Oberste MS.** 2015. In Vitro Efficacy of Antiviral Compounds against Enterovirus D68. Antimicrob Agents Chemother **59:**7779-7781.
69. **Schmidtke M, Hammerschmidt E, Schuler S, Zell R, Birch-Hirschfeld E, Makarov VA, Riabova OB, Wutzler P.** 2005. Susceptibility of coxsackievirus B3 laboratory strains and clinical isolates to the capsid function inhibitor pleconaril: antiviral studies with virus chimeras demonstrate the crucial role of amino acid 1092 in treatment. J Antimicrob Chemother **56:**648-656.
70. **Barnard DL, Hubbard VD, Smee DF, Sidwell RW, Watson KG, Tucker SP, Reece PA.** 2004. In vitro activity of expanded-spectrum pyridazinyl oxime ethers related to pirodavir: novel capsid-binding inhibitors with potent antipicornavirus activity. Antimicrob Agents Chemother **48:**1766-1772.
71. **Kaiser L, Crump CE, Hayden FG.** 2000. In vitro activity of pleconaril and AG7088 against selected serotypes and clinical isolates of human rhinoviruses. Antiviral Res **47:**215-220.
72. **Filman DJ, Syed R, Chow M, Macadam AJ, Minor PD, Hogle JM.** 1989. Structural factors that control conformational transitions and serotype specificity in type 3 poliovirus. EMBO J **8:**1567-1579.
73. **Smith TJ, Kremer MJ, Luo M, Vriend G, Arnold E, Kamer G, Rossmann MG, McKinlay MA, Diana GD, Otto MJ.** 1986. The site of attachment in human rhinovirus 14 for antiviral agents that inhibit uncoating. Science **233:**1286-1293.
74. **Smyth M, Pettitt T, Symonds A, Martin J.** 2003. Identification of the pocket factors in a picornavirus. Arch Virol **148:**1225-1233.
75. **Rossmann MG, He Y, Kuhn RJ.** 2002. Picornavirus-receptor interactions. Trends Microbiol **10:**324-331.
76. **Zhang G, Zhou F, Gu B, Ding C, Feng D, Xie F, Wang J, Zhang C, Cao Q, Deng Y, Hu W, Yao K.** 2012. In vitro and in vivo evaluation of ribavirin and pleconaril antiviral activity against enterovirus 71 infection. Arch Virol **157:**669-679.
77. **Hayden FG, Herrington DT, Coats TL, Kim K, Cooper EC, Villano SA, Liu S, Hudson S, Pevear DC, Collett M, McKinlay M, Pleconaril Respiratory Infection Study G.** 2003. Efficacy and safety of oral pleconaril for treatment of

colds due to picornaviruses in adults: results of 2 double-blind, randomized, placebo-controlled trials. Clin Infect Dis **36:**1523-1532.

78. **Kim Y, Kankanamalage AC, Damalanka VC, Weerawarna PM, Groutas WC, Chang KO.** 2016. Potent inhibition of enterovirus D68 and human rhinoviruses by dipeptidyl aldehydes and alpha-ketoamides. Antiviral Res **125:**84-91.
79. **Heinz BA, Vance LM.** 1996. Sequence determinants of 3A-mediated resistance to enviroxime in rhinoviruses and enteroviruses. J Virol **70:**4854-4857.
80. **Heinz BA, Vance LM.** 1995. The antiviral compound enviroxime targets the 3A coding region of rhinovirus and poliovirus. J Virol **69:**4189-4197.
81. **Brown-Augsburger P, Vance LM, Malcolm SK, Hsiung H, Smith DP, Heinz BA.** 1999. Evidence that enviroxime targets multiple components of the rhinovirus 14 replication complex. Arch Virol **144:**1569-1585.
82. **Barton DJ, Flanegan JB.** 1997. Synchronous replication of poliovirus RNA: initiation of negative-strand RNA synthesis requires the guanidine-inhibited activity of protein 2C. J Virol **71:**8482-8489.
83. **Loddo B, Ferrari W, Brotzu G, Spanedda A.** 1962. In vitro inhibition of infectivity of polio viruses by guanidine. Nature **193:**97-98.
84. **Eggers HJ.** 1976. Successful treatment of enterovirus-infected mice by 2-(alpha-hydroxybenzyl)-benzimidazole and guanidine. J Exp Med **143:**1367-1381.
85. **Herrmann EC, Jr., Herrmann JA, Delong DC.** 1982. Prevention of death in mice infected with coxsackievirus A16 using guanidine HCl mixed with substituted benzimidazoles. Antiviral Res **2:**339-346.
86. **Smee DF, Barnard DL.** 2013. Methods for evaluation of antiviral efficacy against influenza virus infections in animal models. Methods Mol Biol **1030:**407-425.
87. **Blanco JC, Pletneva LM, Wan H, Araya Y, Angel M, Oue RO, Sutton TC, Perez DR.** 2013. Receptor characterization and susceptibility of cotton rats to avian and 2009 pandemic influenza virus strains. J Virol **87:**2036-2045.
88. **Sejvar JJ, Lopez AS, Cortese MM, Leshem E, Pastula DM, Miller L, Glaser C, Kambhampati A, Shioda K, Aliabadi N, Fischer M, Gregoricus N, Lanciotti R, Nix WA, Sakthivel SK, Schmid DS, Seward JF, Tong S, Oberste MS, Pallansch M, Feikin D.** 2016. Acute Flaccid Myelitis in the United States, August-December 2014: Results of Nationwide Surveillance. Clin Infect Dis **63:**737-745.
89. **van den Broek MF, Muller U, Huang S, Zinkernagel RM, Aguet M.** 1995. Immune defence in mice lacking type I and/or type II interferon receptors. Immunol Rev **148:**5-18.
90. **van den Broek MF, Muller U, Huang S, Aguet M, Zinkernagel RM.** 1995. Antiviral defense in mice lacking both alpha/beta and gamma interferon receptors. J Virol **69:**4792-4796.
91. **Goodman AG, Zeng H, Proll SC, Peng X, Cilloniz C, Carter VS, Korth MJ, Tumpey TM, Katze MG.** 2010. The alpha/beta interferon receptor provides protection against influenza virus replication but is dispensable for inflammatory response signaling. J Virol **84:**2027-2037.

92. **Biron CA.** 1998. Role of early cytokines, including alpha and beta interferons (IFN-alpha/beta), in innate and adaptive immune responses to viral infections. Semin Immunol **10:**383-390.
93. **Le Page C, Genin P, Baines MG, Hiscott J.** 2000. Interferon activation and innate immunity. Rev Immunogenet **2:**374-386.
94. **Julander JG, Siddharthan V, Evans J, Taylor R, Tolbert K, Apuli C, Stewart J, Collins P, Gebre M, Neilson S, Van Wettere A, Lee YM, Sheridan WP, Morrey JD, Babu YS.** 2017. Efficacy of the broad-spectrum antiviral compound BCX4430 against Zika virus in cell culture and in a mouse model. Antiviral Res **137:**14-22.
95. **Tan GK, Ng JK, Trasti SL, Schul W, Yip G, Alonso S.** 2010. A non mouse-adapted dengue virus strain as a new model of severe dengue infection in AG129 mice. PLoS Negl Trop Dis **4:**e672.
96. **Thibodeaux BA, Garbino NC, Liss NM, Piper J, Schlesinger JJ, Blair CD, Roehrig JT.** 2012. A humanized IgG but not IgM antibody is effective in prophylaxis and therapy of yellow fever infection in an AG129/17D-204 peripheral challenge mouse model. Antiviral Res **94:**1-8.
97. **Calvert AE, Dixon KL, Delorey MJ, Blair CD, Roehrig JT.** 2014. Development of a small animal peripheral challenge model of Japanese encephalitis virus using interferon deficient AG129 mice and the SA14-14-2 vaccine virus strain. Vaccine **32:**258-264.
98. **van den Doel P, Volz A, Roose JM, Sewbalaksing VD, Pijlman GP, van Middelkoop I, Duiverman V, van de Wetering E, Sutter G, Osterhaus AD, Martina BE.** 2014. Recombinant modified vaccinia virus Ankara expressing glycoprotein E2 of Chikungunya virus protects AG129 mice against lethal challenge. PLoS Negl Trop Dis **8:**e3101.
99. **Metz SW, Martina BE, van den Doel P, Geertsema C, Osterhaus AD, Vlak JM, Pijlman GP.** 2013. Chikungunya virus-like particles are more immunogenic in a lethal AG129 mouse model compared to glycoprotein E1 or E2 subunits. Vaccine **31:**6092-6096.
100. **Caine EA, Fuchs J, Das SC, Partidos CD, Osorio JE.** 2015. Efficacy of a Trivalent Hand, Foot, and Mouth Disease Vaccine against Enterovirus 71 and Coxsackieviruses A16 and A6 in Mice. Viruses **7:**5919-5932.
101. **Reed LJ aHM.** 1938. A simple method of estimating fifty percent endpoints. American Journal of tropical medicine and Hygiene **27:**493-197.
102. **Deshmane SL, Kremlev S, Amini S, Sawaya BE.** 2009. Monocyte chemoattractant protein-1 (MCP-1): an overview. J Interferon Cytokine Res **29:**313-326.
103. **Ajuebor MN, Hogaboam CM, Kunkel SL, Proudfoot AE, Wallace JL.** 2001. The chemokine RANTES is a crucial mediator of the progression from acute to chronic colitis in the rat. J Immunol **166:**552-558.
104. **Huang Y, Hogle JM, Chow M.** 2000. Is the 135S poliovirus particle an intermediate during cell entry? J Virol **74:**8757-8761.
105. **Solomon T, Lewthwaite P, Perera D, Cardosa MJ, McMinn P, Ooi MH.** 2010. Virology, epidemiology, pathogenesis, and control of enterovirus 71. Lancet Infect Dis **10:**778-790.

106. **Muller U, Steinhoff U, Reis LF, Hemmi S, Pavlovic J, Zinkernagel RM, Aguet M.** 1994. Functional role of type I and type II interferons in antiviral defense. Science **264:**1918-1921.
107. **National Research Council (U.S.) Committe for the Update of the Guide for the Care and Use of Laboratory Animals IfLARUS, National Academies Press (U.S.).** 2011. Guide for the care and use of Laboratory Animals National Academies Press,
108. **Centers for Disease C.** 2013. Standard Operating Procedure: Enterovirus 71 (EV71) specific real-time (Taqman) RT-PCR assay. Protocol Vietnam 1.
109. **Zheng HW, Sun M, Guo L, Wang JJ, Song J, Li JQ, Li HZ, Ning RT, Yang ZN, Fan HT, He ZL, Liu LD.** 2017. Nasal Infection of Enterovirus D68 Leading to Lower Respiratory Tract Pathogenesis in Ferrets (Mustela putorius furo). Viruses **9**.
110. **Imamura T, Suzuki A, Lupisan S, Kamigaki T, Okamoto M, Roy CN, Olveda R, Oshitani H.** 2014. Detection of enterovirus 68 in serum from pediatric patients with pneumonia and their clinical outcomes. Influenza Other Respir Viruses **8:**21-24.
111. **Schuster JE, Newland JG.** 2015. Management of the 2014 Enterovirus 68 Outbreak at a Pediatric Tertiary Care Center. Clin Ther **37:**2411-2418.
112. **Systems B.** 2017. Full Body Plethysmograph PENH. https://www.biopac.com/application/pulmonary-function/advanced-feature/full-body-plethysmograph-penh/ - tabs. Accessed April 1
113. **Song JH, Choi HJ, Song HH, Hong EH, Lee BR, Oh SR, Choi K, Yeo SG, Lee YP, Cho S, Ko HJ.** 2014. Antiviral activity of ginsenosides against coxsackievirus B3, enterovirus 71, and human rhinovirus 3. J Ginseng Res **38:**173-179.
114. **Zhang XN, Song ZG, Jiang T, Shi BS, Hu YW, Yuan ZH.** 2010. Rupintrivir is a promising candidate for treating severe cases of Enterovirus-71 infection. World J Gastroenterol **16:**201-209.
115. **De Palma AM, Vliegen I, De Clercq E, Neyts J.** 2008. Selective inhibitors of picornavirus replication. Med Res Rev **28:**823-884.
116. **Zhang KE, Hee B, Lee CA, Liang B, Potts BC.** 2001. Liquid chromatography-mass spectrometry and liquid chromatography-NMR characterization of in vitro metabolites of a potent and irreversible peptidomimetic inhibitor of rhinovirus 3C protease. Drug Metab Dispos **29:**729-734.

Appendices

Cycling: Enterovirus 68

Target	Enterovirus 68 Protocol → Enterovirus 68
Normalisation	LinRegPCR
Fluorescence Cutoff	500%
Threshold	0.379 (Automatic) starting at cycle 1

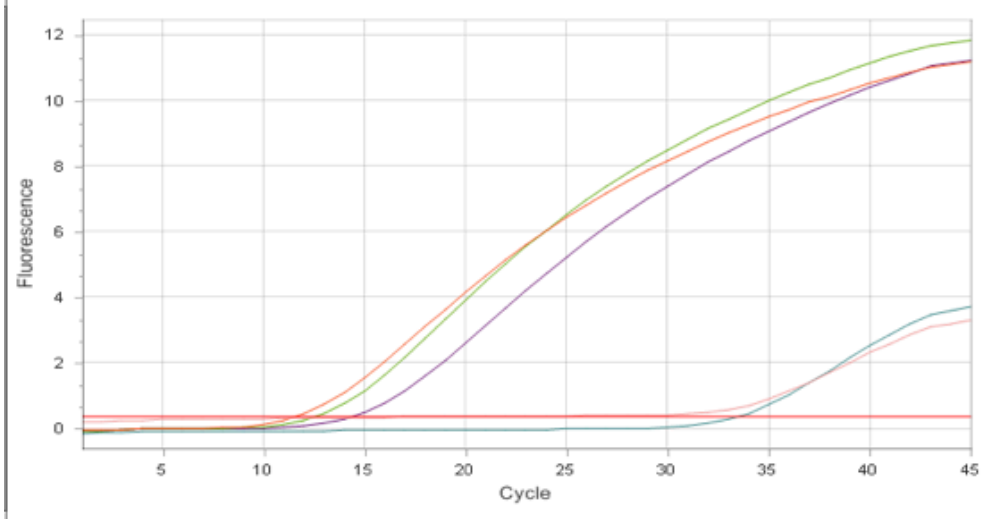

Well	Sample Name	Cq	Efficiency	Efficiency R^2	Result	
1	EV68 MO MP0	14.34	0.71	1.00	Success	Purple
2	EV68 MO 30M	12.55	0.81	1.00	Success	Green
3	EV68 MO 30Mpp	11.60	0.76	1.00	Success	Orange
4	EV71 MP4	33.47	0.68	1.00	Success	Blue
5	EV71 MP10	-1.00	-1.00	-1.00	Excluded	Light Red
6	EV71 MP10pp	17.92	0.02	0.78	Success	Yellow
7	H2O	-1.00	-1.00	-1.00	Excluded	Red

Figure 27 RT-qPCR of EV-D68 MP0, MP30 and MP30pp. EV-D68 Primers and protocol were used; CACTGAACCAGAAGAAGCCA (forward), CCAAAGCTGCTCTACTGAGAAA (reverse) and TCGCACAGTGATAAATCAGCACGG (probe). EV71 was used as a negative control to verify specificity of primers to EV-D68. All EV-D68 strains were identified by cycle 13.

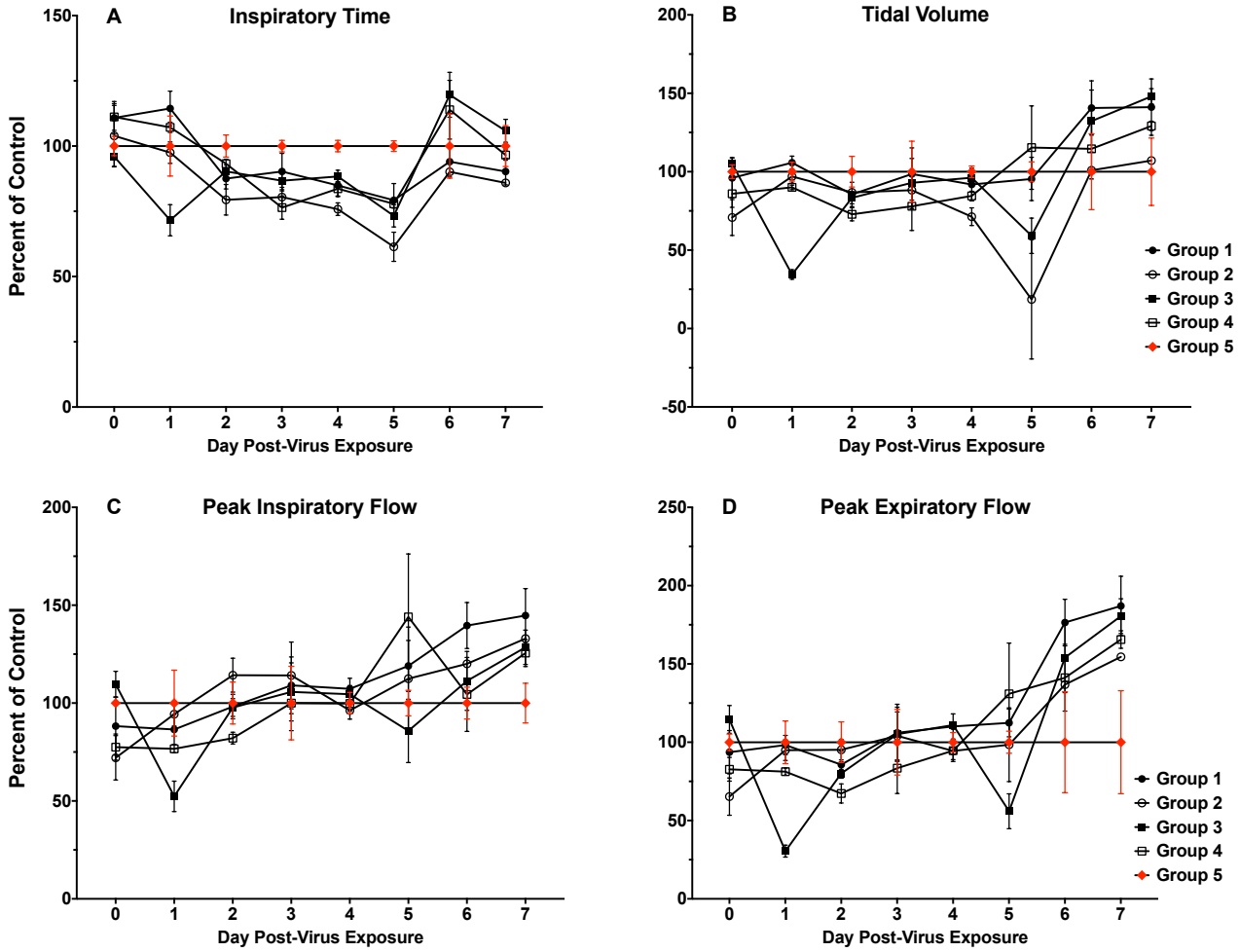

Figure 28 Plethysmography Evaluation of Lung Function in EV-D68 MP30 Infected Mice Compared to Uninfected Mice. Parameters of infected mice were compared to uninfected controls and are reported as percentages, 100% being the baseline. *P <0.05, **P <0.01, ***P <0.001, ****P<0.0001.

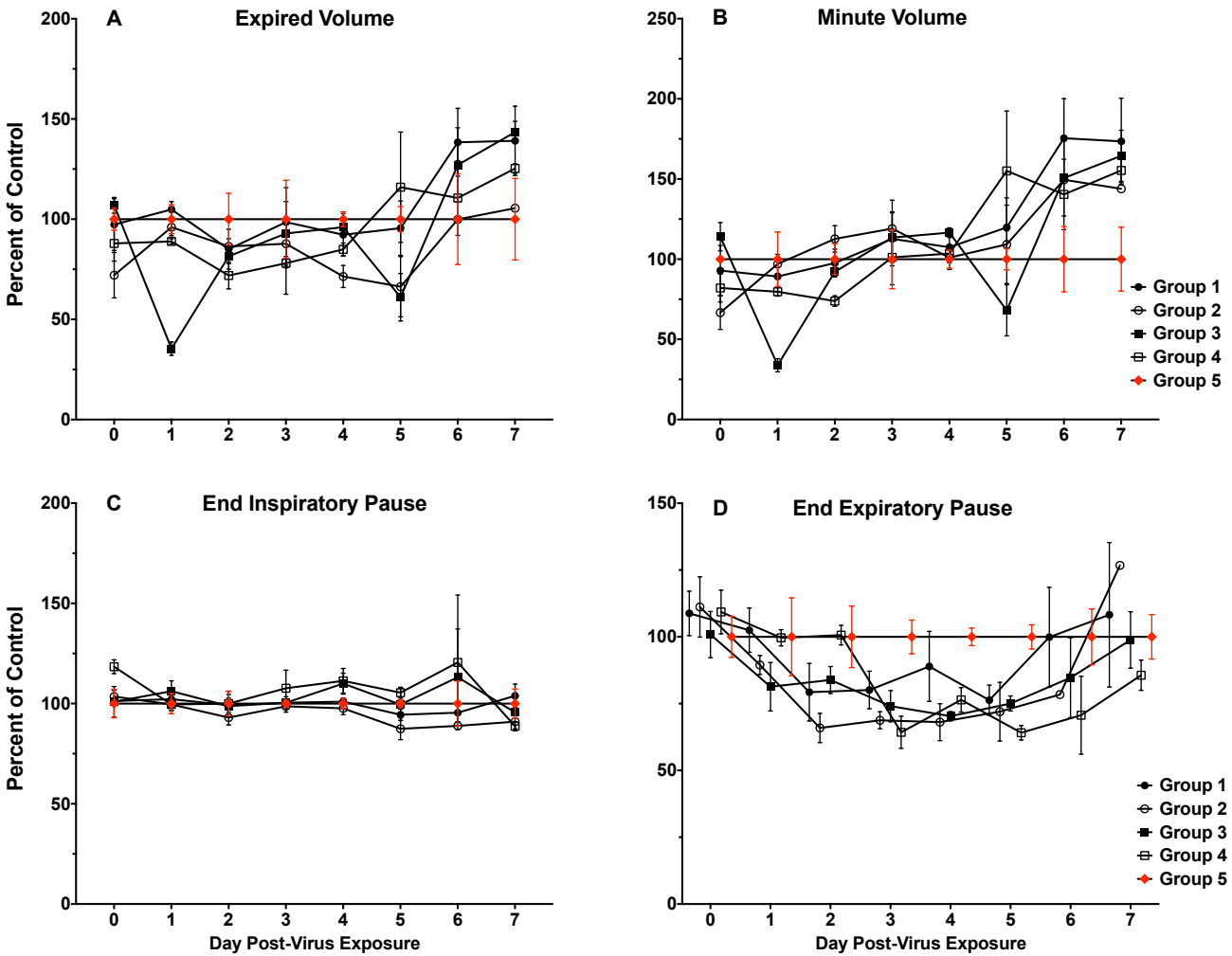

Figure 29 Plethysmography Evaluation of Lung Function in EV-D68 MP30 Infected Mice Compared to Uninfected Mice. Parameters of infected mice were compared to uninfected controls and are reported as percentages, 100% being the baseline. *P <0.05, **P <0.01, ***P <0.001, ****P<0.0001.

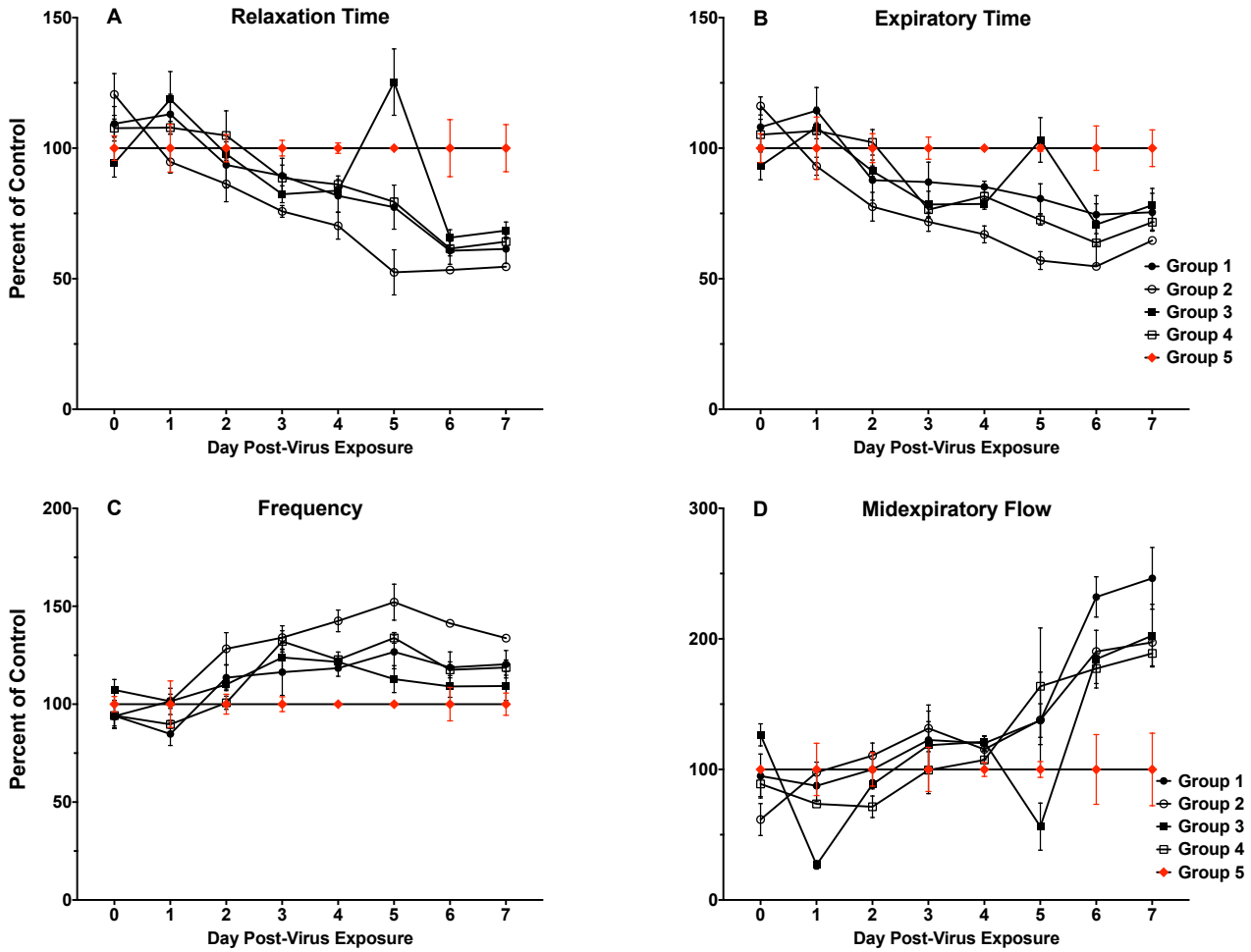

Figure 30 Plethysmography Evaluation of Lung Function in EV-D68 MP30 Infected Mice Compared to Uninfected Mice. Parameters of infected mice were compared to uninfected controls and are reported as percentages, 100% being the baseline. *P <0.05, **P <0.01, ***P <0.001, ****P<0.0001..

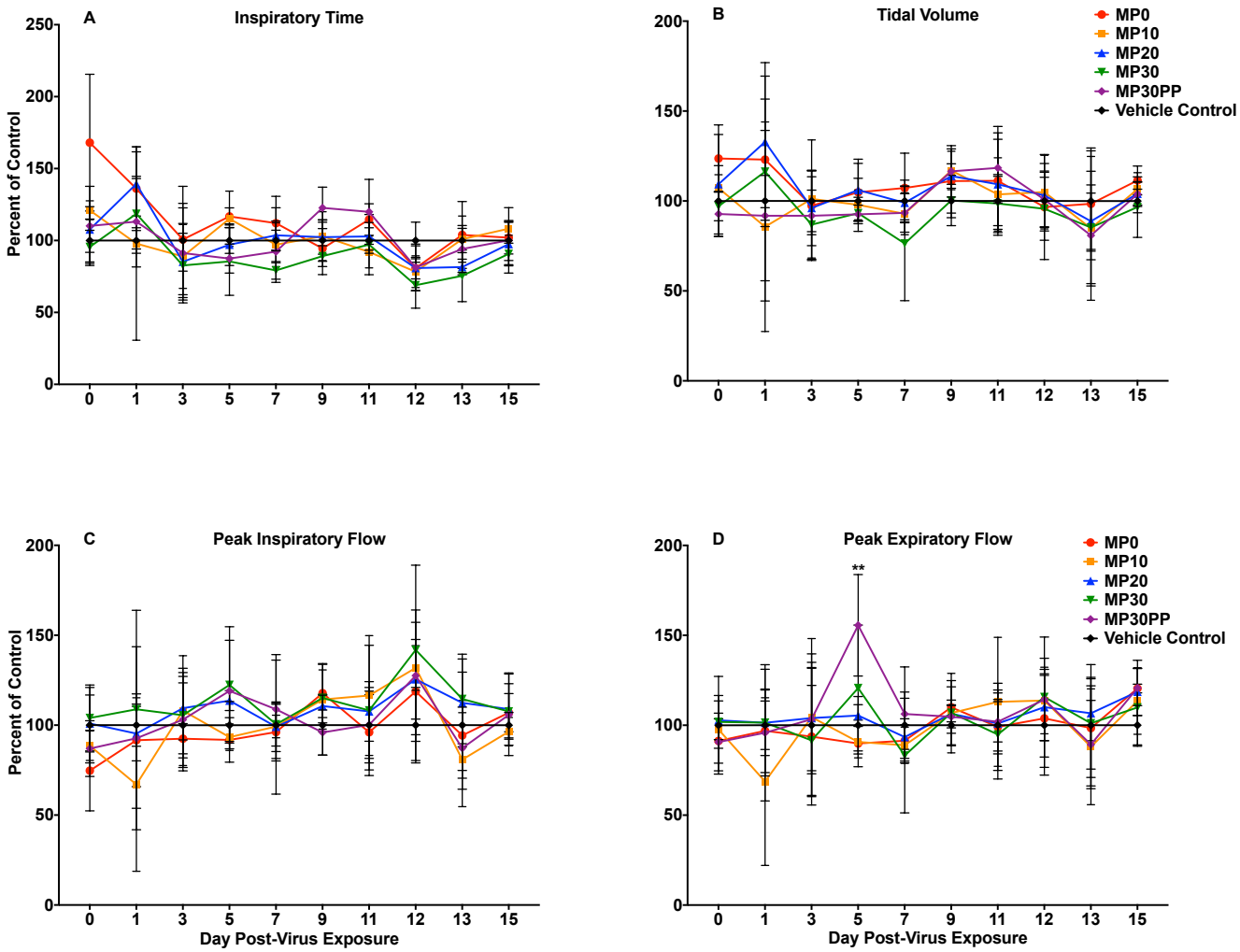

Figure 31 Plethysmography (Room Air) Evaluation of EV-D68 Mouse Passages MP0, MP10, MP20, MP30, MP30pp to Uninfected Mice. Parameters of infected mice were compared to uninfected controls and are reported as percentages, 100% being the baseline. *P <0.05, **P <0.01, ***P <0.001, ****P<0.0001.

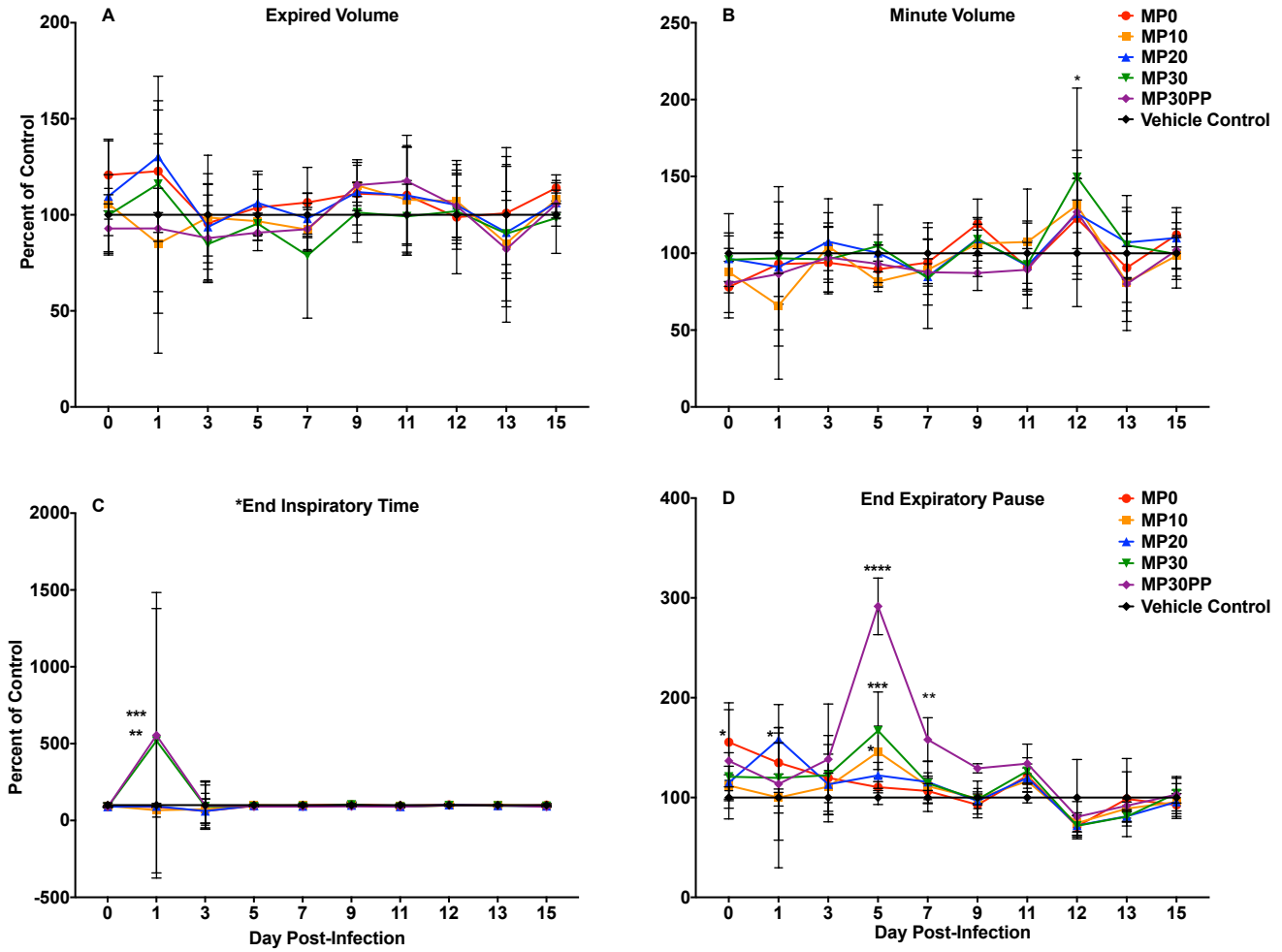

Figure 32 Plethysmography (Room Air) Evaluation of EV-D68 Mouse Passages MP0, MP10, MP20, MP30, MP30pp to Uninfected Mice. Parameters of infected mice were compared to uninfected controls and are reported as percentages, 100% being the baseline. *P <0.05, **P <0.01, ***P <0.001, ****P<0.0001.

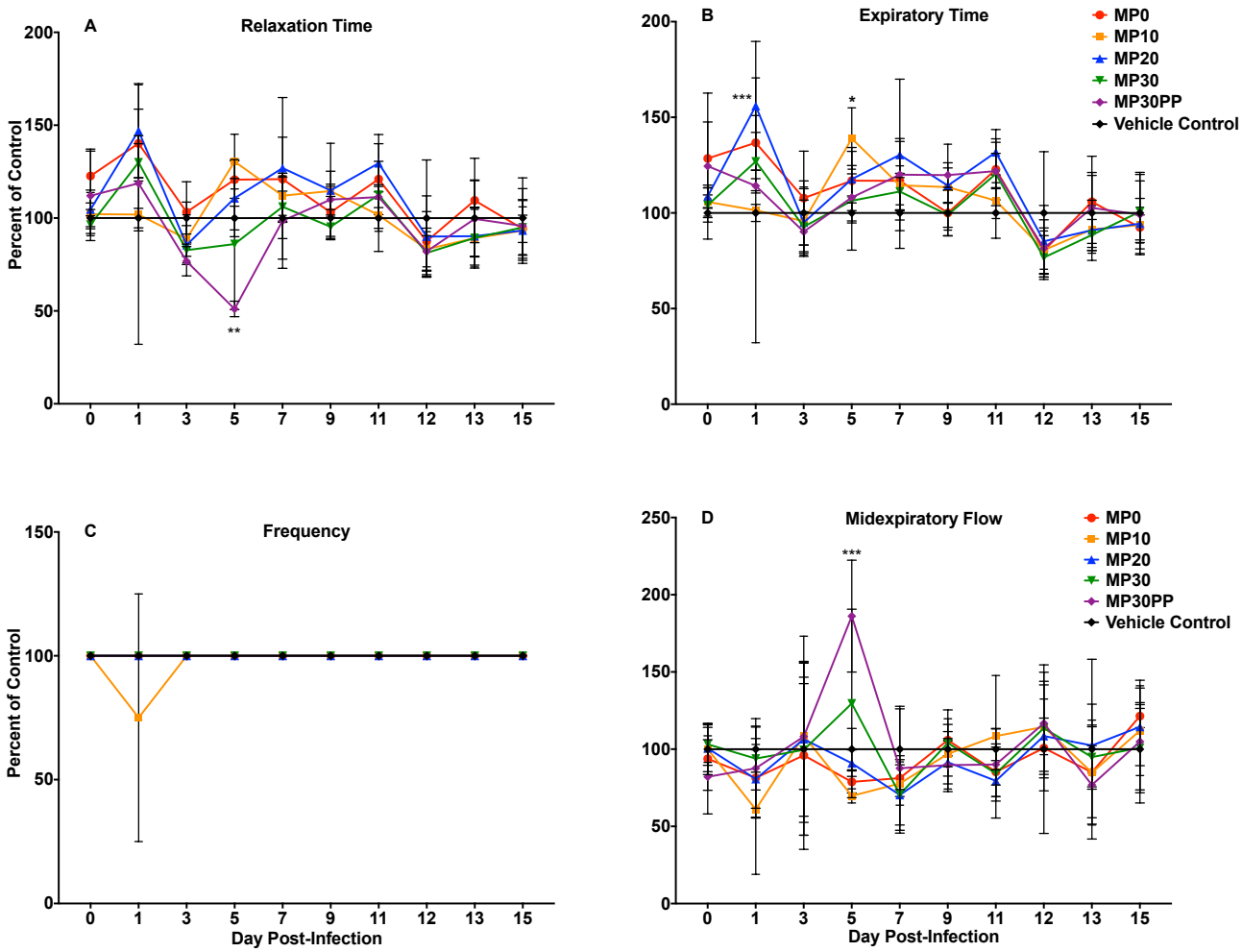

Figure 33 Plethysmography (Room Air) Evaluation of EV-D68 Mouse Passages MP0, MP10, MP20, MP30, MP30pp to Uninfected Mice. Parameters of infected mice were compared to uninfected controls and are reported as percentages, 100% being the baseline. *P <0.05, **P <0.01, ***P <0.001, ****P<0.0001.

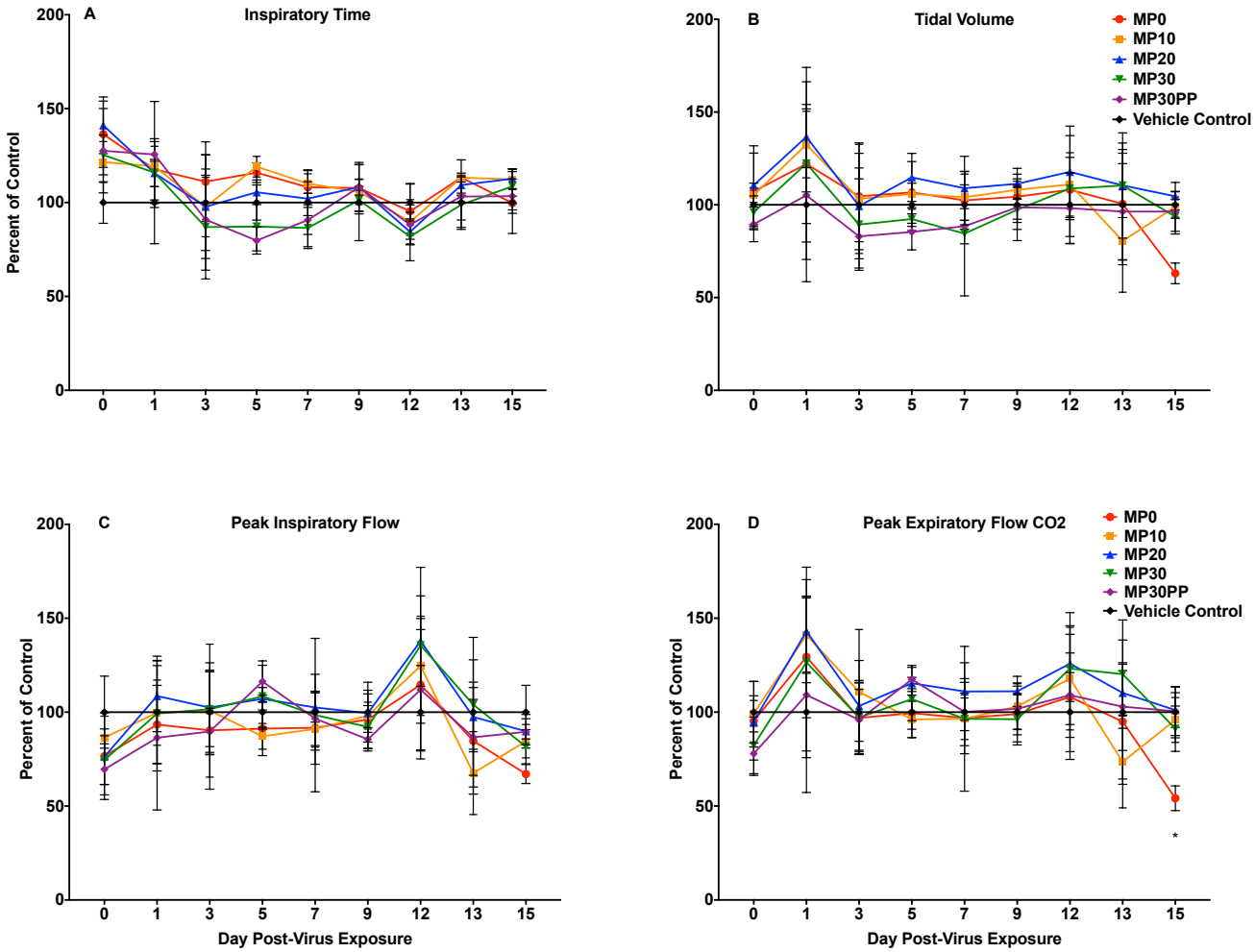

Figure 34 Plethysmography (CO_2) Evaluation of EV-D68 Mouse Passages MP0, MP10, MP20, MP30, MP30pp to Uninfected Mice. Parameters of infected mice were compared to uninfected controls and are reported as percentages, 100% being the baseline. *P <0.05, **P <0.01, ***P <0.001, ****P<0.0001.

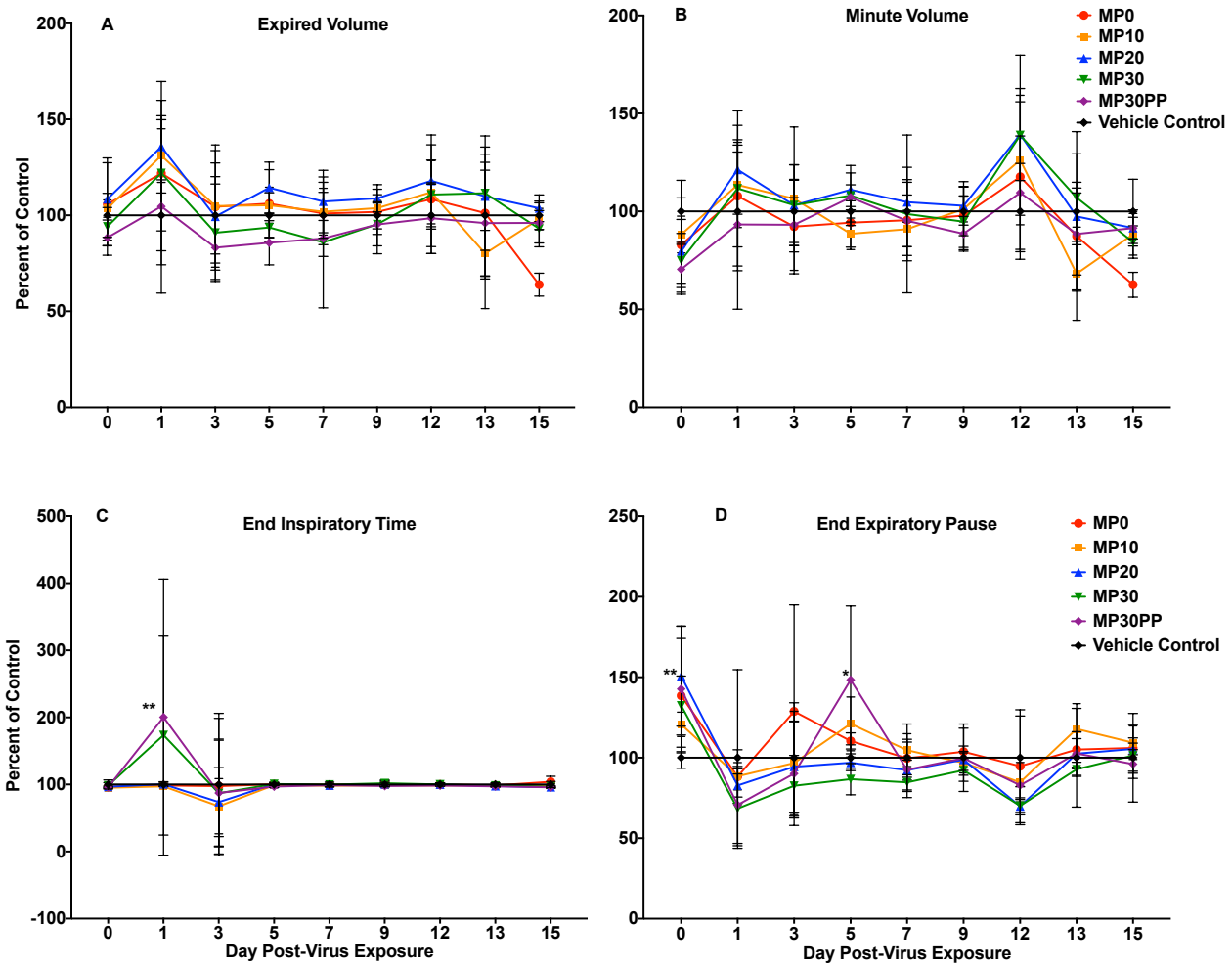

Figure 35 Plethysmography (CO_2) Evaluation of EV-D68 Mouse Passages MP0, MP10, MP20, MP30, MP30pp to Uninfected Mice. Parameters of infected mice were compared to uninfected controls and are reported as percentages, 100% being the baseline. *P <0.05, **P <0.01, ***P <0.001, ****P<0.0001.

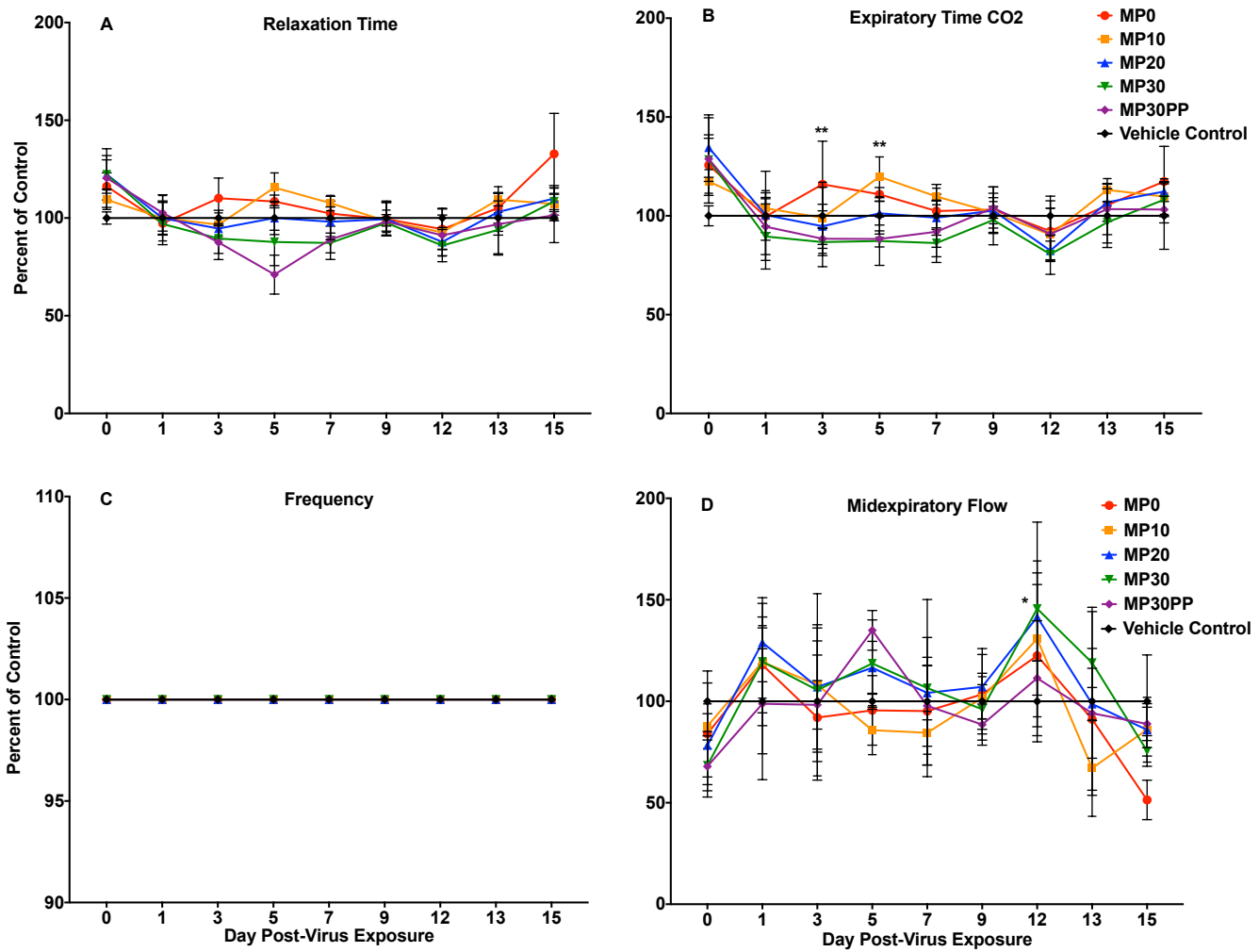

Figure 36 Plethysmography (CO_2) Evaluation of EV-D68 Mouse Passages MP0, MP10, MP20, MP30, MP30pp to Uninfected Mice. Parameters of infected mice were compared to uninfected controls and are reported as percentages, 100% being the baseline. *P <0.05, **P <0.01, ***P <0.001, ****P<0.0001.

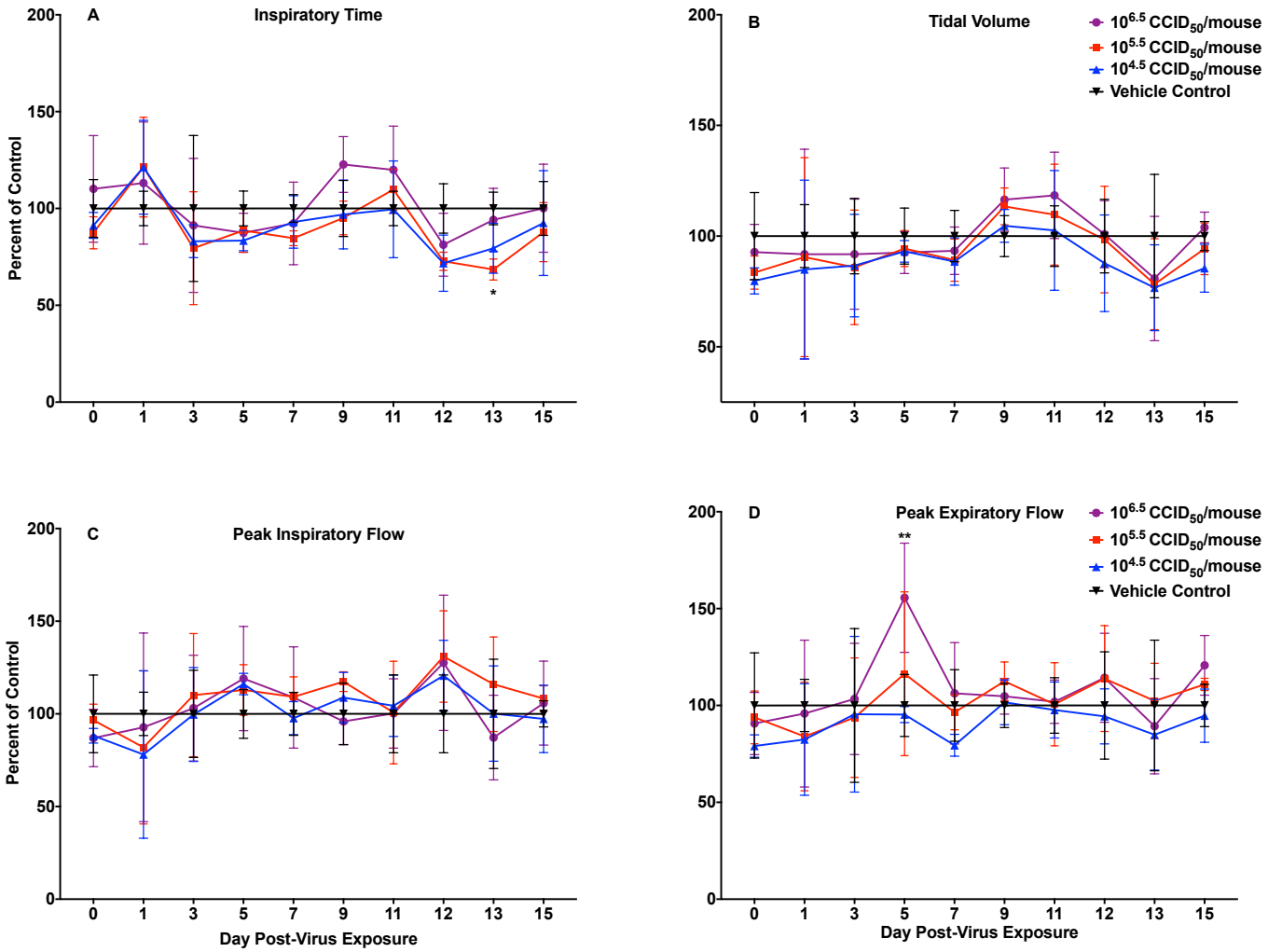

Figure 37 Plethysmography (Room Air) Evaluation of EV-D68 Infectious Doses of MP30pp and Uninfected Mice Evaluation.
Parameters of infected mice were compared to uninfected controls and are reported as percentages, 100% being the baseline.
*P <0.05, **P <0.01, ***P <0.001, ****P<0.0001.

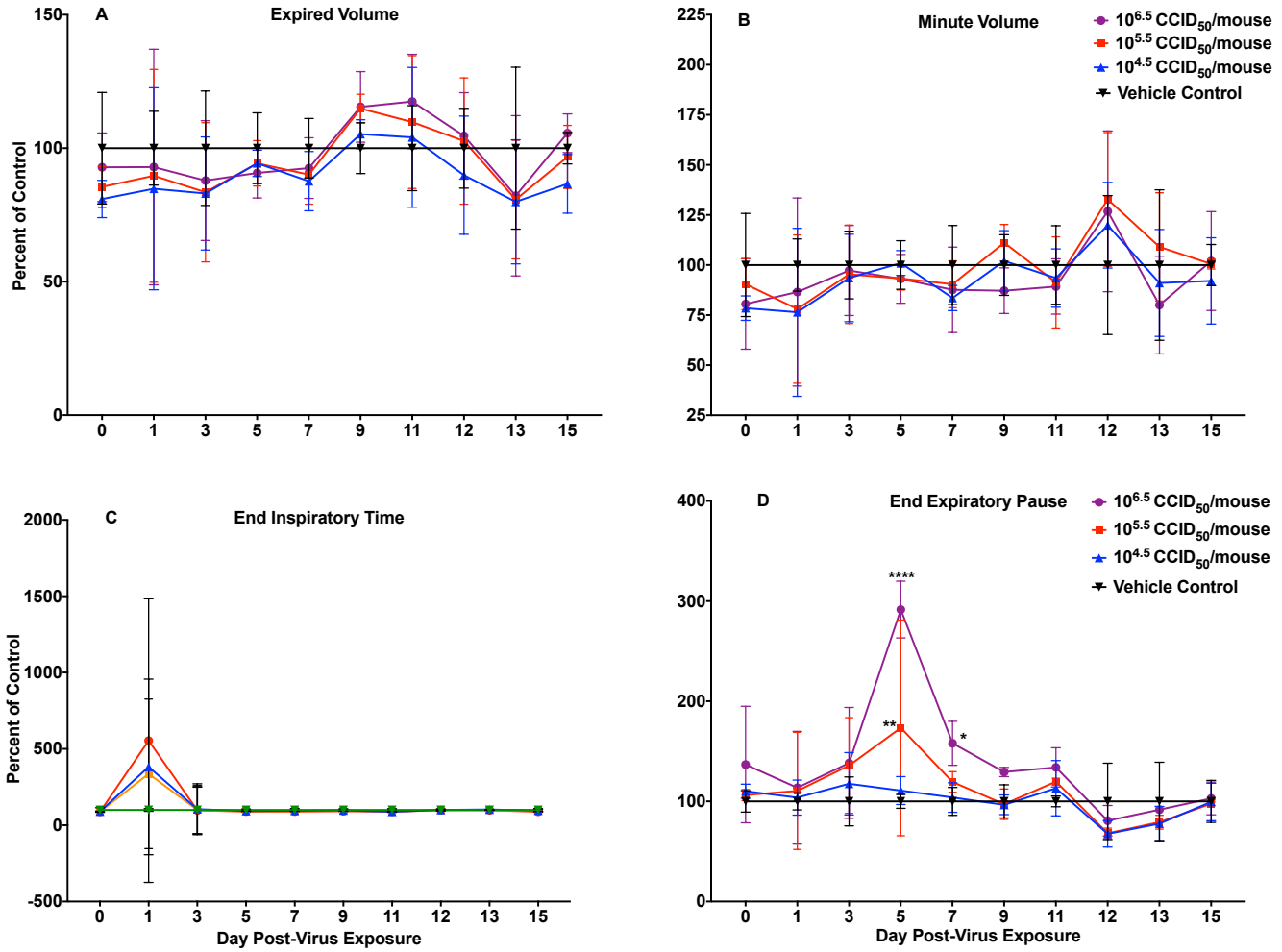

Figure 38 Plethysmography (Room Air) Evaluation of EV-D68 Infectious Doses of MP30pp and Uninfected Mice Evaluation. Parameters of infected mice were compared to uninfected controls and are reported as percentages, 100% being the baseline. *P <0.05, **P <0.01, ***P <0.001, ****P<0.0001.

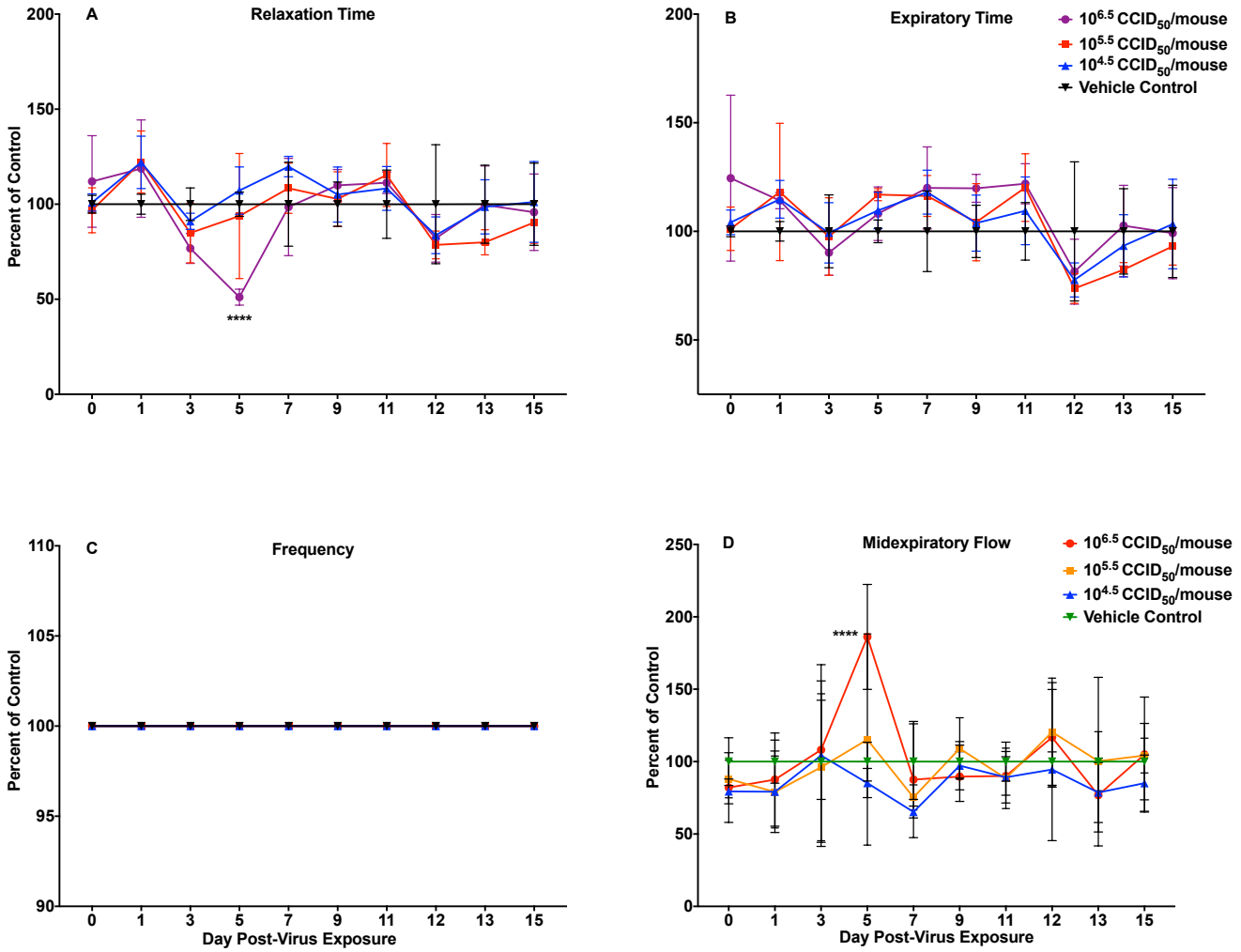

Figure 39 Plethysmography (Room Air) Evaluation of EV-D68 Infectious Doses of MP30pp and Uninfected Mice Evaluation. Parameters of infected mice were compared to uninfected controls and are reported as percentages, 100% being the baseline. *P <0.05, **P <0.01, ***P <0.001, ****P<0.0001.

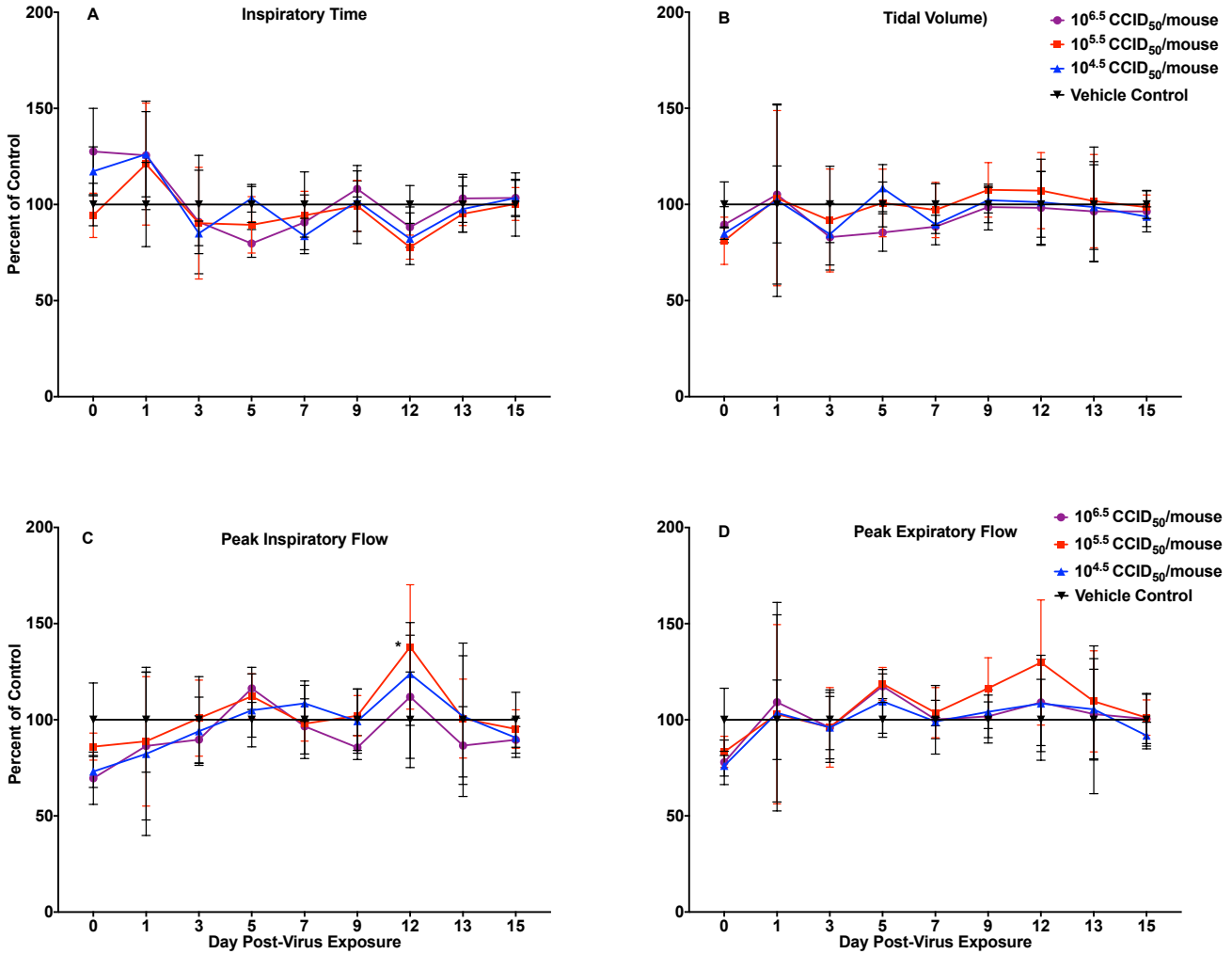

Figure 40 Plethysmography (CO_2) Evaluation of EV-D68 Infectious Doses of MP30pp and Uninfected Mice Evaluation. Parameters of infected mice were compared to uninfected controls and are reported as percentages, 100% being the baseline. *P <0.05, **P <0.01, ***P <0.001, ****P<0.0001.

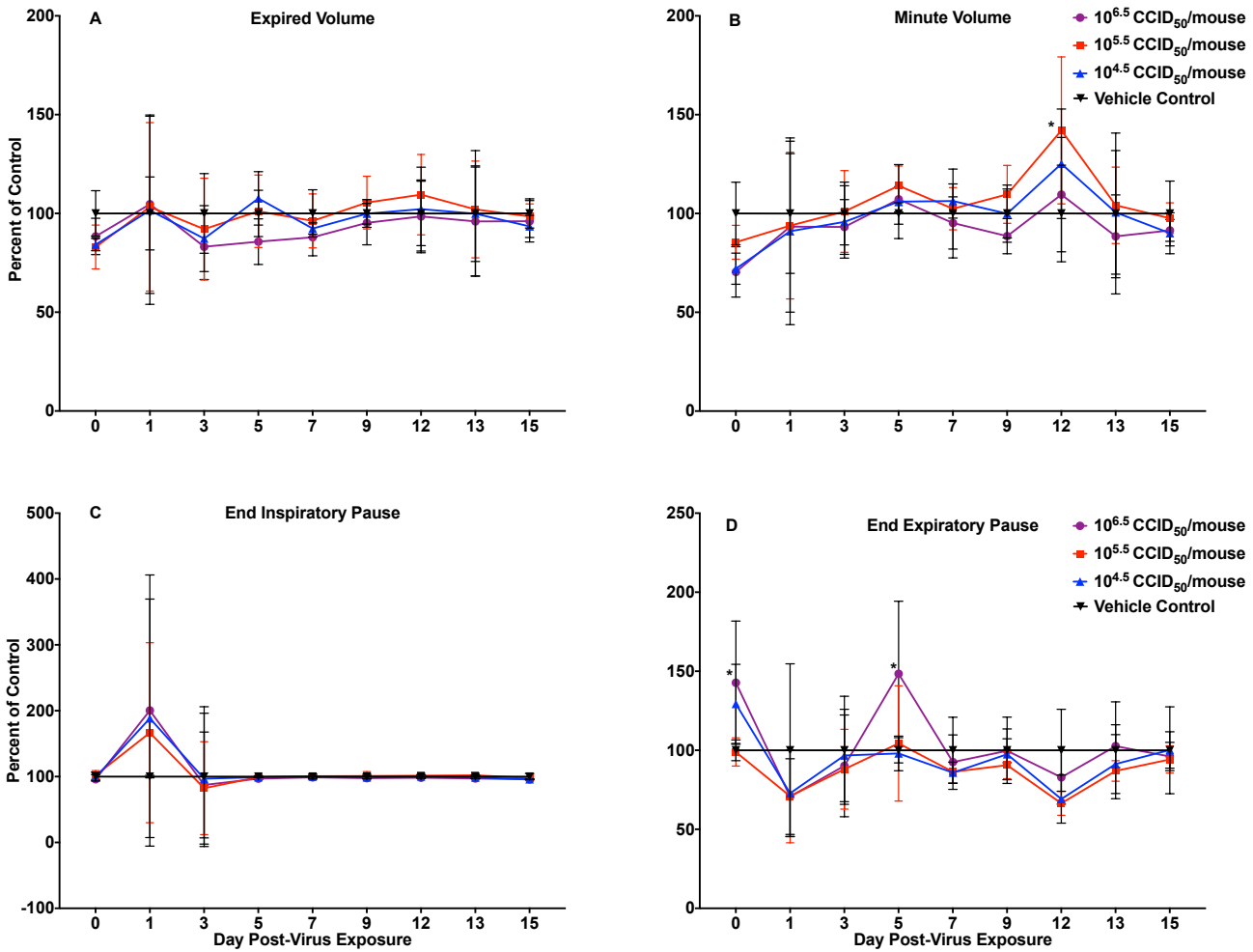

Figure 41 Plethysmography (CO_2) Evaluation of EV-D68 Infectious Doses of MP30pp and Uninfected Mice Evaluation. Parameters of infected mice were compared to uninfected controls and are reported as percentages, 100% being the baseline. *P <0.05, **P <0.01, ***P <0.001, ****P<0.0001.

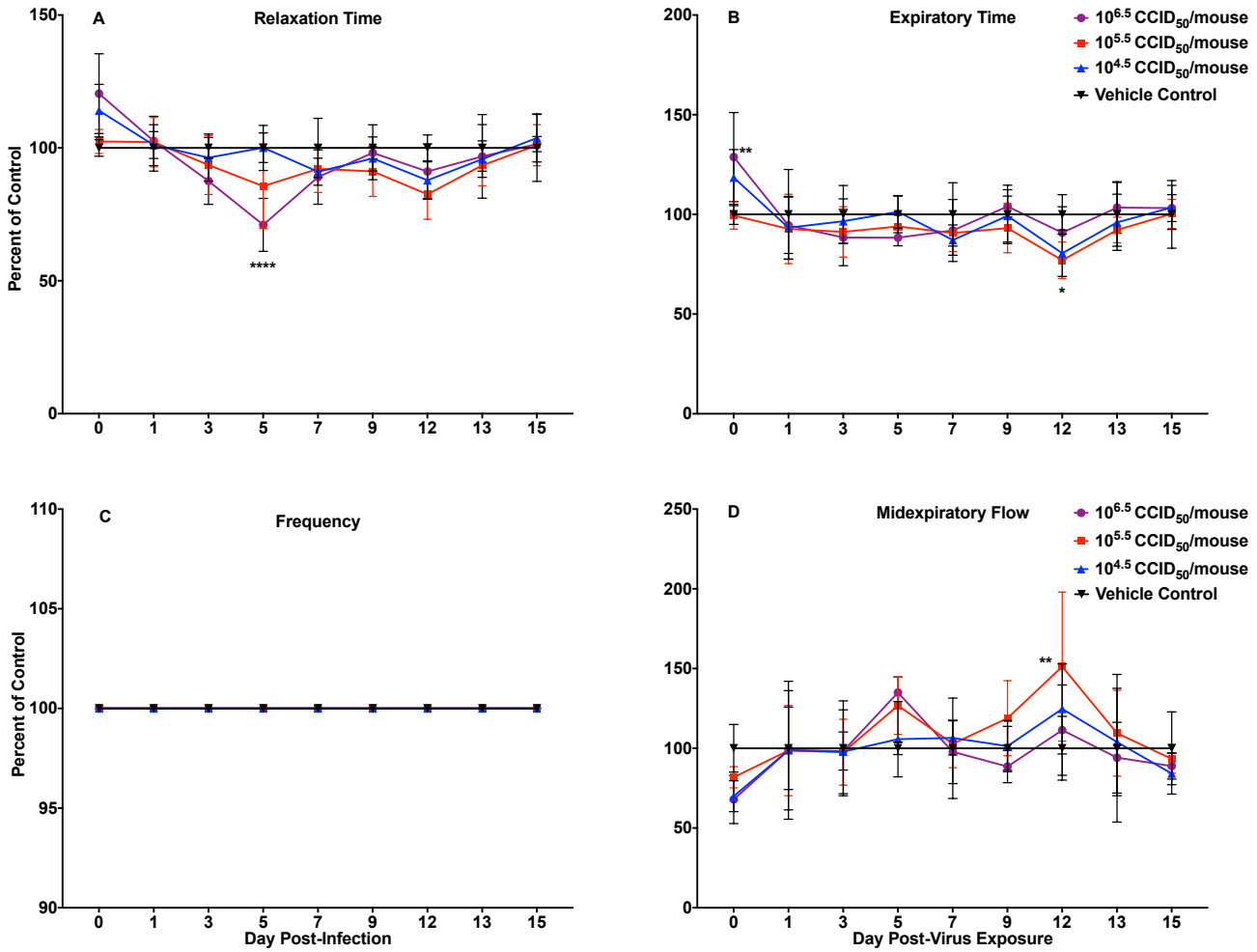

Figure 42 Plethysmography (CO_2) Evaluation of EV-D68 Infectious Doses of MP30pp and Uninfected Mice Evaluation. Parameters of infected mice were compared to uninfected controls and are reported as percentages, 100% being the baseline. *P <0.05, **P <0.01, ***P <0.001, ****P<0.0001.